In vitro toxicity testing of phthalocyanines on different cell lines using a continuous laser source

Submitted in fulfilment of the requirements of the degree of Master of Technology: Biotechnology in the Faculty of Applied Sciences at the Durban University of Technology

Kaminee Maduray

SEPTEMBER 2010

Promoter: Professor Bharti Odhav

Co – Promoter: Aletta Karsten

DURBAN UNIVERSITY of TECHNOLOGY

DECLARATION

I, Kaminee Maduray hereby declare that the thesis herewith submitted for the M. tech: Biotechnology at the Durban University of Technology has not been previously submitted for a degree at any other university.

_____

Kaminee Maduray (Miss)

Approved for final submission

_____	_____
Professor B Odhav (Ph.D.)	Aletta Karsten (Mrs)
Supervisor	Co - Supervisor

ABSTRACT

Photodynamic therapy is a promising treatment for cancer. It involves the combination of a photosensitizer and light of an appropriate wavelength (laser source) to cause the destruction of cancer cells. Phthalocynanines are second–generation photosensitizers with enhanced photophysical and photochemical properties.

In this *in vitro* study the effect of aluminium (AlTSPc) or zinc (ZnTSPc) tetrasulfophthalocyanines in its inactive and active state (laser induced) on melanoma (skin cancer cells), fibroblast (healthy normal skin cells) and keratinocyte (healthy normal skin cells) cells was evaluated. For each of the cell lines approximately 3×10^4 cells/ml were seeded onto 24-well cell culture plates and allowed to attach overnight, after which cells were treated with different concentrations of AlTSPc or ZnTSPc. The photosensitizers were synthesized at Rhodes University. After 2 hrs, cells were irradiated with a diode laser at a wavelength of 672 nm and a beam diameter of 1 cm. The laser power varied between 20-30 mW and the irradiation time was calculated to deliver a light dose of 4.5 J/cm^2. Post-irradiated cells were incubated for 24 hrs before cell viability was measured using the CellTiter-Blue™ Viability Assay.

Also, the efficacy of the light dose and laser source used for the killing of approximately 50% of the melanoma cancer cells were investigated. AlTSPc and ZnTSPc decreased cell viability of melanoma cancer cells to approximately 50% with photosensitizer concentrations of 40 µg/ml and 50 µg/ml respectively. These photosensitizer concentrations caused a slight decrease in the percentage cell viability of fibroblast and keratinocyte cells. Results for the dark toxicity assay showed that

both photosensitizers in the presence of high concentrations (60 µg/ml – 100 µg/ml) showed cytotoxicity effects on melanoma cancer cells in their inactive state. This was not observed in fibroblast and keratinocyte cells treated under the same experimental conditions. The optimal AlTSPc and ZnTSPc concentrations in combination with the light dose of 4.5 J/cm^2 was the most efficient in killing the melanoma cancer cells with reduced killing effects on healthy normal fibroblast and keratinocyte cells when compared to other light doses (2.5 J/cm^2, 7.5 J/cm^2 and 10 J/cm^2).

The irradiation of cells photosensitized with the optimal photosensitizer concentrations with a femtosecond laser using similar laser parameters to continuous wave laser experiments resulted in a reduction in the cell viability of healthy normal fibroblast and keratinocyte cells compared to melanoma cancer cells. The presence of DNA degradation on agarose gel, morphological changes like blebbing and ultrastructural changes like nucleus condensation indicated that photodynamic therapy treated melanoma cancer cells with the optimal concentrations of AlTSPc and ZnTSPc induced cell death via apoptosis. This concludes that low concentrations of AlTSPc and ZnTSPc activated with an appropriate laser source can be used to induce cell death in melanoma cancer cells. Both AlTSPc and ZnTSPc exhibit the potential to be used as a photosensitizer in photodynamic therapy for the treatment of melanoma cancer with the occurrence of minimal damage to surrounding healthy tissue.

DEDICATION

I dedicate this work to:

My mother Mrs S Maduray and father Mr Y Maduray for their continuous support and motivation. I am truly blessed to have you as parents.

My late uncle (Mr George Govender) and dear friend (Itumeleng Tshoke) for their inspiration and guidance.

To God, who had given me the strength together with an abundance of courage to overcome my obstacles and go bravely forward to complete my degree.

ACKNOWLEDGEMENTS

I would like to express my gratitude and thanks to my supervisors Prof Odhav and Aletta Karsten for his guidance, supervision, assistance, patience and above all encouragement throughout my undergraduate study.

I am indebted to the CSIR for giving me the opportunity to study and conduct my Master Degree research project at the National Laser Centre, Biophotonics Group. My special appreciation is for Dr Ndumiso Cingo (The Centre Manger) and Dr Lourens Botha (Competency Area Manager) for their on-going support. I strongly feel that my potential as a professional researcher has increased multifold because of the National Laser Centre, CSIR association. I would like to also thank the Femtosecond group (Dr Anton Du Plessis, Dr Ted Roberts, Dr Alina Stefan and Saturnin Ombinda-Lemboumba) at National Laser Centre for their assistance during my femtosecond laser experimental work.

A special thanks to Prof Tebello Nyokong and her students from the University of Rhodes, Department of Chemistry for synthesizing the phthalocynanines (drug) and giving me the opportunity to test the photodynamic effects of this magnificent drug on melanoma cancer cells.

I wish to extend my sincere appreciation to Dr Lester from the University of Cape Town, Department of Human Biology for kindly providing me with Keratinocyte cells for my experiments. Also, I would like to thank two staff members from Biosciences at CSIR. Firstly, Natasha Kolesnikova for kindly providing me with the melanoma cancer cells for my experiments. Secondly, Olona Gqwaka for your willingness to help me conduct my agarose gel experiments at your molecular

laboratory in Biosciences. I would like to acknowledge Dr Alan Hall from the University of Pretoria (laboratory for microscopy and microanalysis) for your assistance with the Transmission Electron Microscopy.

I am tremendously grateful to my family (Sally Maduray, Roy Maduray, Shaun Maduray, Ravina Maduray and Calvin Pillay) for their support, blessings and prayers. I have successfully completed this degree with their constant encouragement and faith in me.

TABLE OF CONTENTS

LIST OF FIGURES

LIST OF TABLES

ABBREVATIONS

AIF	Apoptosis Inducing Factor
Apaf-1	Apoptotic Protease-activating factor 1
Al	Aluminum
AlTSPc	Aluminum tetrasulfonatedphthalocyanine
Atg	Autophagy-related gene
ATP	Adenosine-5'-triphosphate
BP	Base pairs
BPD	MA-Benzoporphyrin derivative monoacid ring A
CANSA	The Cancer Association of South Africa
Co	Cobalt
COOH	Carboxyl group
CV	Cell Viability
CW	Continuous Wave
DNA	Deoxyribonucleic acid
DED	Death Effector Domain
DISC	Death Inducing Signaling Complex
DR-4	Death Receptor 4
DR-5	Death Receptor 5
EMEM	Eagles Minimum Essential Media
Endo G	Endonuclease G
ER	Endoplasmic reticulum
FADD	Fas Associated protein with Death Domain
FBS	Foetal Bovine Serum

Ga	Gallium
GTP	Guanosine-5'-triphosphate
Hb	Hemoglobin
HbO_2	Oxyhemoglobin
HBSS	Hank’s Balanced Salt Solution
HDLs	High density lipoproteins
IMS	Inter-Mitochondrial membrane Space
IR	Infrared
JNK	c-JunN-terminal Kinase
KZN	KwaZulu–Natal
LDH	Lactate dehydrogenase
LDLs	Low density lipoproteins
LLLT	Low-level laser therapy
MMP	Mitochondrial Membrane Permeabilization
NEAA	Non Essential Amino Acids
Omi/HtrA2	Omi stress-regulated endoprotease/High temperature requirement protein A 2
OMM	Outer Mitochondrial Membrane
$^3O_2$	Molecular oxygen
$^1O_2$	Singlet oxygen
PARP-1	Poly ADP-Ribose Polymerase-1
PBS	Phosphate Buffered Saline
PDT	Photodynamic Therapy
Pl3K	Phosphatidylinositol 3 kinase
PS	Photosensitizer

R	Radius
RIP1	Receptor Interacting Protein 1
ROS	Reactive oxygen species
RPM	Revolutions per minute
RPMI-1640	Roswell Park Memorial Institute
RT	Room Temperature
Si	Silicon
Smac	Second mitochondria derived activator of caspase
DIABLO	Direct IAP Binding protein with a Low PI
tBid	Truncated Bid
TNF	Tumor Necrosis Factor
TNFR	Tumor Necrosis Factor Receptor
TRADD	TNFR-Associated protein with Death Domain
TRAIL	Tumor necrosis factor Related Apoptosis Inducing Ligand
UACC	University of Arizona Cancer Centre
UV	Ultraviolet
VDAC	Voltage-Dependent Anion Channel
V	Volts
Zn	Zinc
ZnTSPc	Zinc tetrasulfophthalocyanine

10^{-9} sec	nanosecond
10^{-15} sec	femtosecond

CHAPTER 1

BACKGROUND AND AIM OF STUDY

Cancer is one of the major health problems in South Africa. Figure 1.1 shows the expected incidence of cancers in South Africa in 2009. Data collected by the Cancer Association of South Africa (CANSA) have revealed that one in six South African men and one in seven South African women will get cancer during their lives (McLeod, 2009).

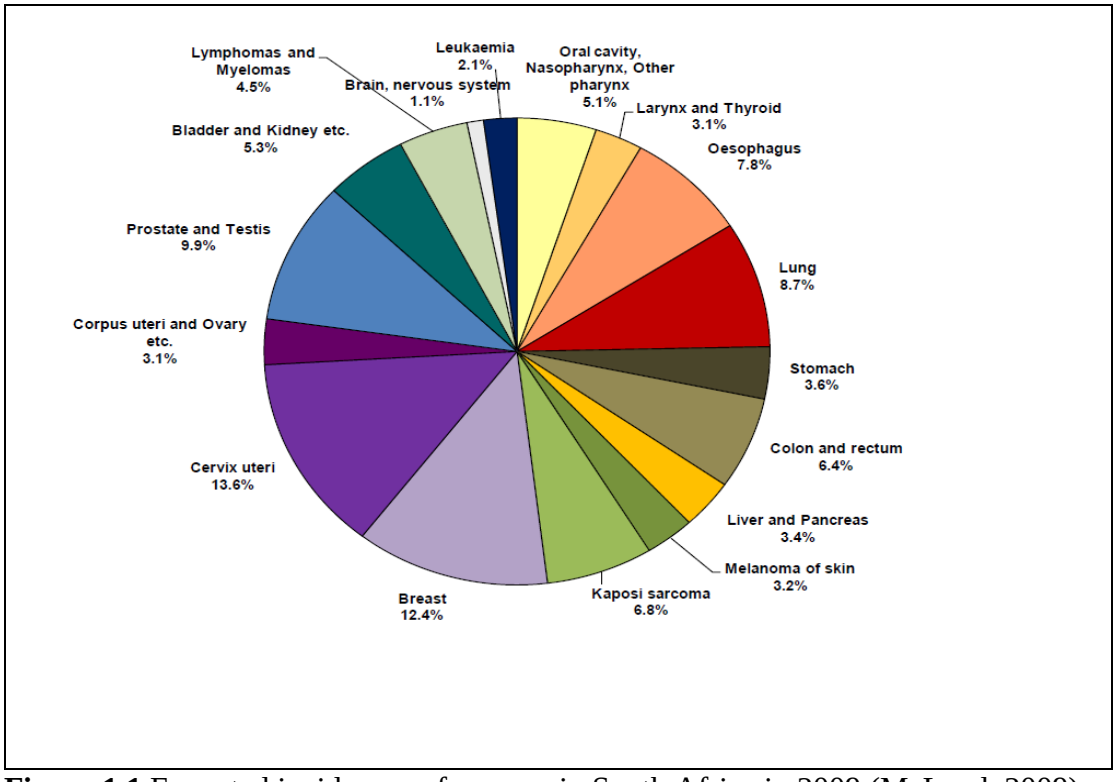

Figure 1.1 Expected incidences of cancers in South Africa in 2009 (McLeod, 2009).

In the South African Health Review 2008, Day and Gray provided some information on the death rates caused from cancer in the different provinces in South Africa. The information indicated that the Western Cape had the highest cancer death rates followed by Gauteng, the Northern Cape and the Eastern Cape Provinces. The lowest rates were found in KwaZulu–Natal (KZN), Limpopo and Mpumalanga. The type of cancer also differed enormously across the provinces which may be related to levels of wealth and development, population group differences, demographic features of the provinces, geographical differences, environmental exposures and access to health services or other basic services (McLeod, 2009).

Current treatment in oncology is based on chemotherapy or large doses of ionizing radiation. This is dependent on host tolerance and the type of cancer which limits the extent to which these modalities can be applied. Therefore, skilled use of effective but non-selective modalities is the present basis of oncology (Calin and Parasca, 2006).

Photodynamic therapy (PDT) is an innovative cancer treatment which has received much attention recently. PDT is a very simple principle which requires three essential components: a photosensitizer (PS), visible light (laser source) and tissue oxygen. The combination of these components can result in the destruction of tumor cells (Banfi *et al*., 2007). This oncology treatment is non- invasive in comparison to conventional surgical, excision, radiotherapy and chemotherapy, because the effect of PDT can be localized by applying the laser light to the affected site only. It is considered to be an inexpensive treatment that can be repeated if necessary (Kömerik, 2002).

An important consideration for PDT is whether the cancer cells are more susceptible to PDT-induced cell death than healthy normal cells (Ketabchi *et al*., 1998). Hence, the fundamental prerequisite for optimal response to photosensitization is a sufficient amount of PS localized in the target tissue. Thus, an understanding of the mechanistic and phototoxicity of PDT is essential to determine the appropriate dose for successful PDT treatment of cancer (Wyld, Reed and Brown, 2001).

The aim of the study was to determine the *in vitro* cytotoxic effect of aluminum tetrasulfonatedphthalocyanine (AlTSPc) and zinc tetrasulfophthalocyanine (ZnTSPc) activated with continuous wave laser at a wavelength of 672 nm and the (femtosecond) pulsed laser for the destruction of melanoma cancer cells.

In order to achieve this aim, the following objectives were set out:

- To determine the optimum concentration of AlTSPc and ZnTSPc activated with a continuous wave laser (CW) at a wavelength of 672 nm to kill approximately 50% of melanoma cancer cells and the concentration required for minimal toxicity for healthy normal fibroblast and keratinocyte cells
- To verify the light dose and exposure time of the CW laser by photosensitizing the melanoma cancer, fibroblast and keratinocyte cells with the optimal AlTSPc and ZnTSPc concentrations
- To compare the efficacy of CW laser with the femtosecond laser using the optimum AlTSPc and ZnTSPc concentrations
- To evaluate the mechanism of cell death using the optimum treatment parameters

The rationale for this research project is that research on the photodynamic effect of AlTSPc and ZnTSPc on melanoma cancer cells, healthy normal skin fibroblast and keratinocytes have not been studied previously. These drugs are produced and provided by Professor Nyokong from Rhodes University, South Africa. Therefore, the photodynamic effect together with the cell death mechanism of AlTSPc and ZnTSPc would be studied in this project using melanoma cancer cells. The toxic effects would be investigated using healthy normal fibroblast and keratinocyte cells. Also, this study design may prove useful in determining the safety and value of PDT as an oncology treatment for skin cancers. The limitation of this study is that it was carried out *in vitro* and therefore the results have to be investigated *in vivo* for an "ideal PS" dose evaluation.

CHAPTER 2

LITERATURE REVIEW

2.1 History of Phototherapy

Light has been used for therapy for more than three thousand years. Ancient Egyptian, Indian and Chinese civilizations used light to treat various diseases, including psoriasis, rickets, vitiligo and skin cancer. At the end of the nineteenth century, Niels Finsen further developed “phototherapy” or the use of light to treat diseases in Denmark. He discovered that red–light exposure prevents the production and discharge of smallpox pustules. Niels Finsen also used ultraviolet light from the sun to treat cutaneous tuberculosis and this was the beginning of the modern light therapy. In 1903, Finsen was awarded a Nobel Prize for his work on phototherapy (Dolmans, Fukumura and Jain, 2003).

More than 100 years ago, researchers also observed that light combined with specific chemicals could induce cell death. In 1903 Herman Von Trappeiner and A. Jesionek used topically applied eosin and white light to treat tumors of the skin. They used the term “photodynamic action” to introduce this phenomenon. Experiments to investigate the effect of combinations of reagents and light led to the discovery of modern photodynamic therapy (PDT). In modern PDT two individual non-toxic components (light and photosensitive molecule) interact to induce cellular and tissue effects in an oxygen-dependent manner for the destruction of the tumors (Dolmans, Fukumura and Jain, 2003).

2.2 Basic Principles on Photodynamic Therapy (PDT)

PDT consists of two simple procedures Figure 2.1:

- The administration of inactive drug known as the photosensitizer (PS)
- Illumination/ irradiation of the tumor to activate the drug (Triesscheijn *et al.*, 2006).

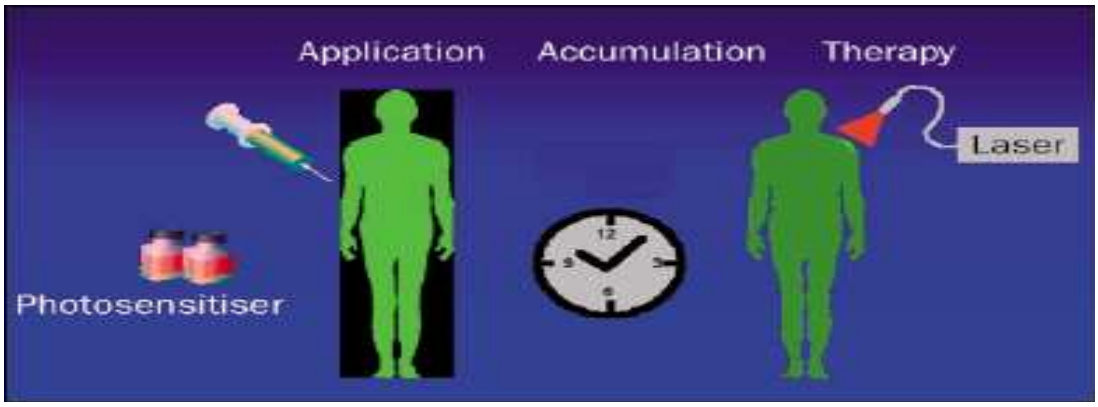

Figure 2.1 The basic principles of PDT. The photosensitizer is injected into the patient and the photosensitizer is given some time to accumulate at the cancer site before the photosensitizer is activated by light from a laser source to selectively destroy the cancerous cells (Hopper, 2000).

The PS is activated by the light and interacts with molecular oxygen present in the tissue. The interaction between the PS and the molecular oxygen results in the formation of an excited state-reactive singlet oxygen. This singlet oxygen is highly cytotoxic and contributes to the destruction of the tumor cells. There is normal healing and re-epithelisation of the healthy tissue surrounding the treated site (Hopper, 2000). Most PS are administrated systemically via bloodstream or applied topically for the treatment of skin cancer. The PS is allowed to accumulate in the tumor cells before light of an appropriate wavelength is directed onto the tumor (Figure 2.1). The depth of effect that can be achieved is highly dependent on the PS and tissue type, because human tissue transmits light most effectively in the red part of the visible spectrum

(Figure 2.2). Therefore, second-generation PS having a strong absorption band in the region of (630 nm and above) can be activated at a depth up to 1 cm. Treatment times vary. The treatment time is related to the absorption of light by the PS and the efficiency of transfer of light energy to oxygen present in the tissue. First-generation PS required treatment times that were 1000 seconds whereas second-generation PS can induce effective cell killing with the treatment time of 200 seconds using a low-power laser light. Laser light is coherent, monochromatic and can be directed along fibre optic cables, allowing light to be introduced into hollow organs as well as deep-seated tumors (Hopper, 2000).

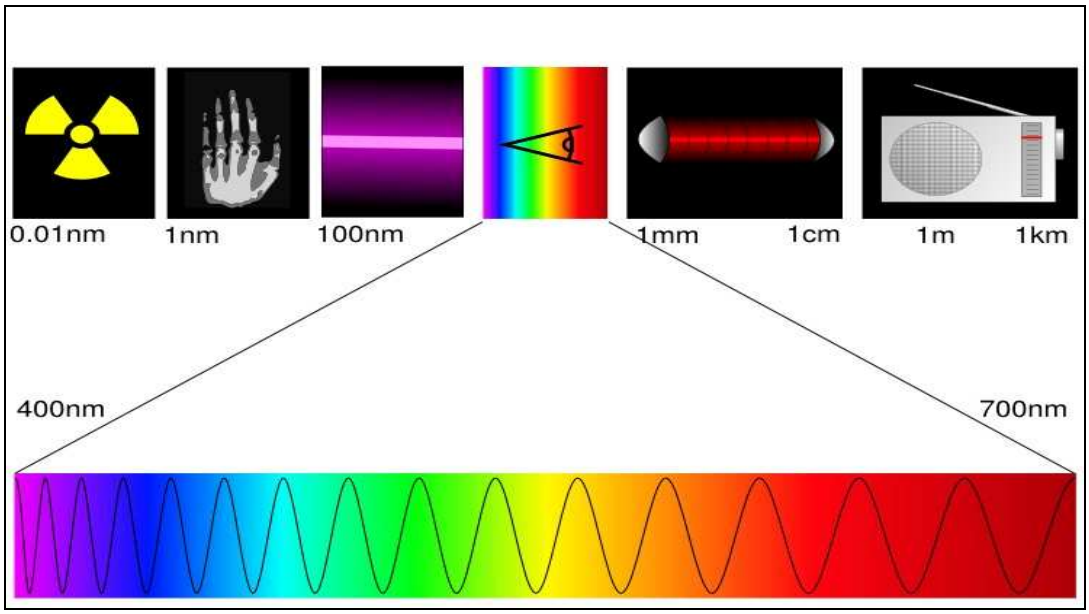

Figure 2.2 An illustration of the optical visible spectrum or light (from the violet to the red region) of the electromagnetic radiation and the wavelength is between 400-700 nm (Jones, 2008).

2.3 Photosensitizers (PS)

A photosensitizer is a non – toxic, inactive or photosensitive drug that accumulates preferentially in abnormal tissue (e.g. tumor) and is capable of absorbing light (laser)

at a specific wavelength. An ideal photosensitizer for PDT would have the following characteristics (Sharman, CM Allen and Lier, 1999):

- Be chemically pure
- Composition is known and constant
- Should have minimal cytotoxicity in the absence of light and only be cytotoxic in the presence of light
- Preferentially retained by the target tissue (e.g. cancerous tissue)
- Rapidly excreted from the body
- High photochemical reactivity
- Produce singlet oxygen and reactive oxygen species
- Longer wavelengths (e.g. in the red region) for deeper skin penetration
- Strong absorbance peak at wavelengths around 600 – 800 nm
- No skin photosensitivity

Many of the existing photosensitizers used for the different types of cancers are summarized by Dolmans, Fukumura and Jain (2003) in Table 2.1.

2.3.1 First – Generation Photosensitizers

Porfimer sodium was the first PS to receive approval (Table 2.1). It is now licensed for the use in the oesophagus, lung, stomach, cervix and bladder treatments. A light wavelength of 630 nm is needed for the activation of porfimer sodium and the absorption band at this wavelength is weak. The efficiency of energy transfer from light to cytotoxic products is moderate and tissue penetration is limited. It could not be used to treat deep-seated or larger tumors (Hopper, 2000). The therapeutic dose of

porfimer sodium resulted in skin photosensitivity which persisted for many weeks (Hopper, 2000).

Table 2.1 Registered and developing photosensitizers with their activation wavelength for different types of cancers (Dolmans, Fukumura and Jain, 2003).

Sensitizer	Trade name	Potential indications	Activation wavelength
HPD (partially purified), porfimer sodium	Photofrin	Cervical*, endobronchial*, oesophageal*, bladder* and gastric cancers*, and brain tumours	630 nm
BPD-MA	Verteporfin	Basal-cell carcinoma	689 nm
m-THPC	Foscan	Head and neck tumours*, prostate and pancreatic tumours	652 nm
5-ALA	Levulan	Basal-cell carcinoma, head and neck, and gynaecological tumours Diagnosis of brain, head and neck, and bladder tumours	635 nm 375–400 nm
5-ALA-methylesther	Metvix	Basal-cell carcinoma*	635 nm
5-ALA benzylesther	Benzvix	Gastrointestinal cancer	635 nm
5-ALA hexylesther	Hexvix	Diagnosis of bladder tumours	375–400 nm
SnET2	Purlytin	Cutaneous metastatic breast cancer, basal-cell carcinoma, Kaposi's sarcoma, prostate cancer	664 nm
Boronated protoporphyrin	BOPP	Brain tumours	630 nm
HPPH	Photochlor	Basal-cell carcinoma	665 nm
Lutetium texaphyrin	Lutex	Cervical, prostate and brain tumours	732 nm
Phthalocyanine-4	Pc 4	Cutaneous/subcutaneous lesions from diverse solid tumour origins	670 nm
Taporfin sodium	Talaporfin	Solid tumours from diverse origins	664 nm

*Indications that are registered in one or more countries (all other indications are in development). 5-ALA, 5-aminolevulinic acid; BPD-MA, benzoporphyrin derivative-monoacid ring A; HPD, haematoporphyrin derivative; HPPH, 2-(1-hexyloxyethyl)-2-devinyl pyropheophorbide-alpha; mTHPC, meta-tetrahydroxyphenylchlorin; SnET2, tin ethyl etiopurpurin.

The other most extensively studied first-generation PS is porphyrins, which was identified in the mid-nineteenth century (Dolmans, Fukumura and Jain, 2003). They are a group of naturally occurring and intensely coloured compounds (Josefsen and Boyle, 2008). These compounds contain a porphin structure with four pyrrole rings connected by methine bridges in a cyclic configuration along with a side chain that is usually metallic. For example, the combination of iron with a porphin structure forms haem (Dolmans, Fukumura and Jain, 2003). Hausmann (1911) conducted the first studies with this PS and he reported skin reactions in mice that were exposed to this

PS. Friedrich Meyer-Bertz was the first to perform *in vivo* experiments by treating himself with porphyrins. He observed swelling and pain especially in light exposed areas (Dolmans, Fukumura and Jain, 2003). These disadvantages (swelling, photosensitivity and pain) associated with the first-generation PS have not prevented the search for second-generation PS (Josefsen and Boyle, 2008).

2.3.2 Second-Generation Photosensitizers (PS)

First-generation photosensitizers encouraged the search for novel, chemically well-defined photosensitizers with improved biological properties generally referred to as "second generation photosensitizers" (Banfi *et al*., 2007). The second-generation PS, benzoporphyrin derivative monoacid ring A (BPD – MA) has been developed by QLT Phototherapeutics (Canada) under the trade name Visudyne (Verteporfin, injection). The chromophore of BPD-MA has long-wavelength absorption maxima at approximately 690 nm. Tissue penetration by light at this wavelength is 50% greater than that achieved for first-generation PS like porfimer sodium (wavelength at 630 nm). Verteporfin has further advantages over the first-generation PS as it is rapidly excreted from the body within 1 – 2 days, minimizing patient photosensitivity. It is also rapidly absorbed by the cancerous tissue at 30 minutes as compared to healthy tissue at 150 minutes post-intravenous injection (Josefsen and Boyle, 2008).

Another commercially available PS is Lutetium Texaphyrin, marketed under the trade name Lutex and Lutrin (Pharmacyclics, USA). This PS is a modification of the first-generation PS porphyrins (Josefsen and Boyle, 2008). The modification of the pent–aza core of the porphyrin resulted in Lutetium Texaphyrin having a strong absorption at a wavelength of 730 nm – 770 nm of the electromagnetic spectrum. At this range

tissue transparency is optimal. As a result, Lutex has the potential to be used in PDT with the advantage that it can effectively treat larger tumors and deep-seated tumors (Josefsen and Boyle, 2008).

Among the more promising second-generation PS are phthalocyanines (Decreau *et al*., 1999). Phthalocyanines are chemically pure compounds (Decreau *et al*., 1999). They also contain azaporphyrin derivatives which have stronger absorbance at longer wavelengths. Phthalocyanines have characteristic absorption spectra with a strong Soret absorption peak at approximately 350 nm, a weak maximum around 600 nm and a narrow, very strong, absorption peak in the far-red region of the visible spectra around 680 nm, where tissue penetration by visible light is greater (Allen, Sharman and Van Lier, 2001).

An attractive feature of phthalocyanines is that its properties can be changed using different central metal ions (e.g. zinc or aluminum) in the phthalocyanine core. This advantage can be used to enhance phototoxic activity. A ring substitution in phthalocyanines (Figure 2.3) with sulphonated groups will render them water soluble (Kolarova *et al*., 2007). The most common water-soluble complexes are the sulfonated metallophthalocyanine. The solubility of PS in water is an essential characteristic because blood is water-based. Water soluble phthalocyanines are desirable photosensitizers for PDT because phthalocyanines can be easily absorbed by blood, when administrated intravenously (Nyokong, 2007).

Additionally, the PS will have to transverse lipid membranes for cellular uptake so it should also be lipophilic (Nyokong, 2007). Literature states that the less sulphonated

phthalocyanines are more lipophilic. It is known that cellular uptake by cancerous cells and targeting subcellular organelles occur more efficiently with lipophilic PS, due to better diffusion through the cell membrane. Therefore, the high tumor to normal tissue ratio after 1 - 3 h is 1:8 (Kolarova *et al*., 2007). Studies have shown that tumor selectivity can be increased further by using a biologically compatible drug delivery system or drug carrier like liposomes (Allen, Sharman and Van Lier, 2001).

The parameters affecting the localization of PS in tumors do not only depend on the lipophilic character of the PS, but also whether the PS is hydrophobic or hydrophilic in nature. It is well accepted that the selectivity increases with the lipophilic character of the PS (Ochsner, 1997). The administration of hydrophobic PS generally binds to high density lipoproteins (HDLs) and low density lipoproteins (LDHs) distributed within the blood system and transported to the malignant tissue with a distinct selectivity (Ochsner, 1997). *In vivo* and *in vitro* studies have indicated that lipophilic PS such as zinc (II) phthalocyanine have a tendency to be taken up directly by tumor cells expressing a particularly large number of membrane receptors e.g. LDLs (Fabris, 2006). Following receptor-mediated endocytosis the PS molecules preferentially accumulates in the lipophilic compartments of tumor cells including plasma, mitochondrial, endoplasmic reticulum, nuclear and lysosomal membrane for direct cell killing. Microscopic measurements revealed that hydrophilic PS or water-soluble phthalocyanines which are largely carried by albumin and other serum proteins preferentially accumulate within the interstitial space and vascular stroma of the tumor tissue (Fabris, 2006). Due to the PS hydrophilic character its ability to diffuse across the plasma membrane into the cytoplasm is limited (Fabris, 2006). Therefore the cytotoxic potential of membrane-associated lipophilic PS is higher than that of

hydrophilic PS. The primary localization of the PS strongly depends on the lipophilic or hydrophilic character of the PS considered. Fabris (2006) has shown that topical formulation of phthalocyanines can penetrate sufficiently into the epidermal layers. This makes phthalocyanine an ideal photosensitizer for the treatment of skin diseases or cancers. The use of phthalocyanines in PDT for the treatment of cutaneous cancers needs to be explored in more detail (Fabris, 2006).

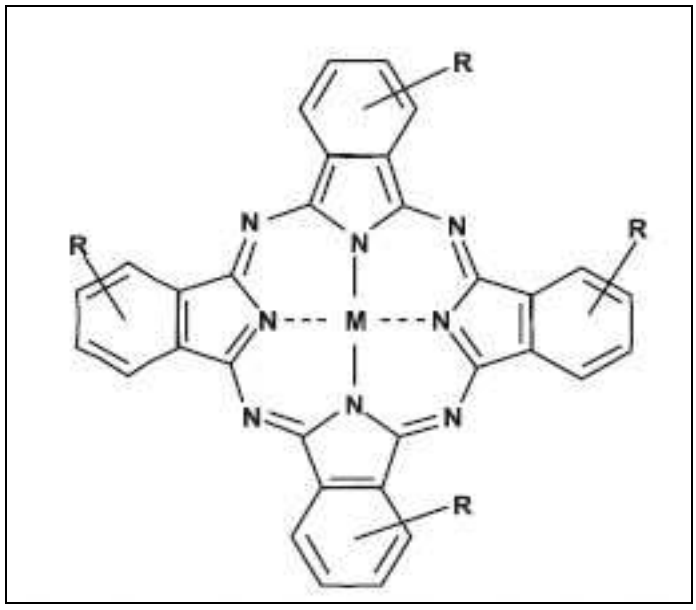

Figure 2.3 General phthalocyanine structure where M is the central metal atom (Al, Zn, Co, Ga or Si) and R represents a multitude of possible ring substituent including COOH, F or SO_3H (Allen, Sharman and Van Lier, 2001).

2.4 Light Source - Laser

The term "laser" is an acronym for **l**ight **a**mplification by **s**timulated **e**mission of **r**adiation. A laser is constructed using three major principles as illustrated in Figure 2.4:

- An energy source (pumps or pump source)
- A gain medium or laser medium (e.g. crystal, dye, gas)
- Two or more mirrors that form an optical resonator

The pump source is the energy provider for the laser system. The type of pump source depends on the gain medium (Paschotta, 2008). The gain medium is the major determining factor of the wavelength of operation and other properties of the laser. There are numerous different types of gain medium e.g. liquid, gases, solids, semiconductors. The optical resonator or optical cavity is two parallel mirrors placed outside the gain medium which provide feedback of the light. The mirrors are given optical coatings which determine their reflective properties (Paschotta, 2008). One mirror will be a high reflector and the other partial reflector. The latter is known as the output coupler because it allows some of the light to leave the cavity to produce an output laser beam. The light produced by spontaneous emission from the medium is reflected by the mirrors back into the medium, where the light may be amplified by stimulated emission (Paschotta, 2008). Thereafter, the light may reflect from the mirrors and thus pass through the gain medium numerous times before exciting the cavity. The design and alignment of the mirrors with respect to the gain medium is important for the determination of the exact operating wavelength, laser output power and other attributes of the laser system. Other optical devices such as modulators, filters and absorbers may be placed within the optical resonator to produce a variety of effects on the laser output such as altering the output power, or size of laser beam (Paschotta, 2008).

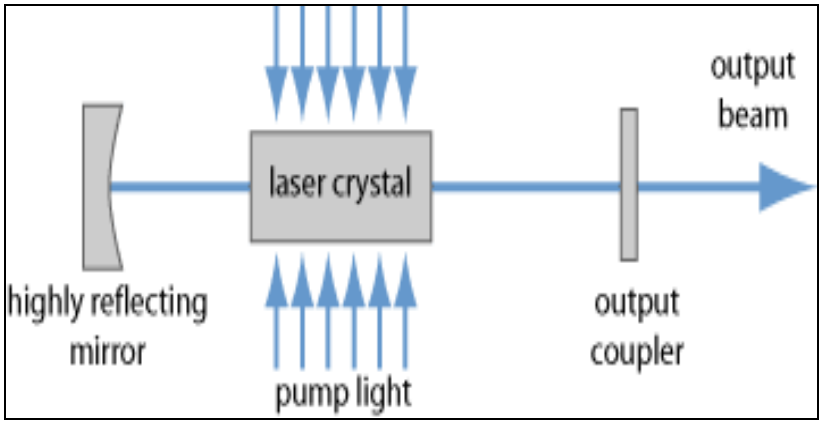

Figure 2.4 Set-up of a simple optically pumped laser. The cavity between the highly reflecting mirror and the output coupler is known as the laser resonator, which extracts some of the circulating laser light as the output beam. Laser crystals are the gain medium (Paschotta, 2008).

Also, lasers are operated in a continuous or pulsed mode (Paschotta, 2008). A continuous wave (CW laser) operation of a laser means that the laser is continuously pumped and continuously emits light. A pulsed laser emits pulses with durations of microseconds, nanoseconds, picoseconds or femtoseconds (ultrashort pulses from mode-locked lasers). There are a number of methods for pulse generation with pulsed lasers (e.g. femtosecond laser). The laser resonator contains either an active element (an optical modulator) or a non-linear passive element (a saturable absorber), which causes the production of an ultrashort pulse circulating in the laser resonator (Paschotta, 2008).

2.4.1 Lasers in PDT

The choice of light sources for PDT is determined by the following factors (Alexiades-Armenakas, 2006):

- The optimal wavelength for the maximum absorption of the PS
- Adequate power to deliver the requested fluence rate and light dose to drive the PDT reaction illustrated in Figure 2.5 (A)

- The penetration depth of the light through the tissue to reach the tumor as illustrated in Figure 2.5 (B)

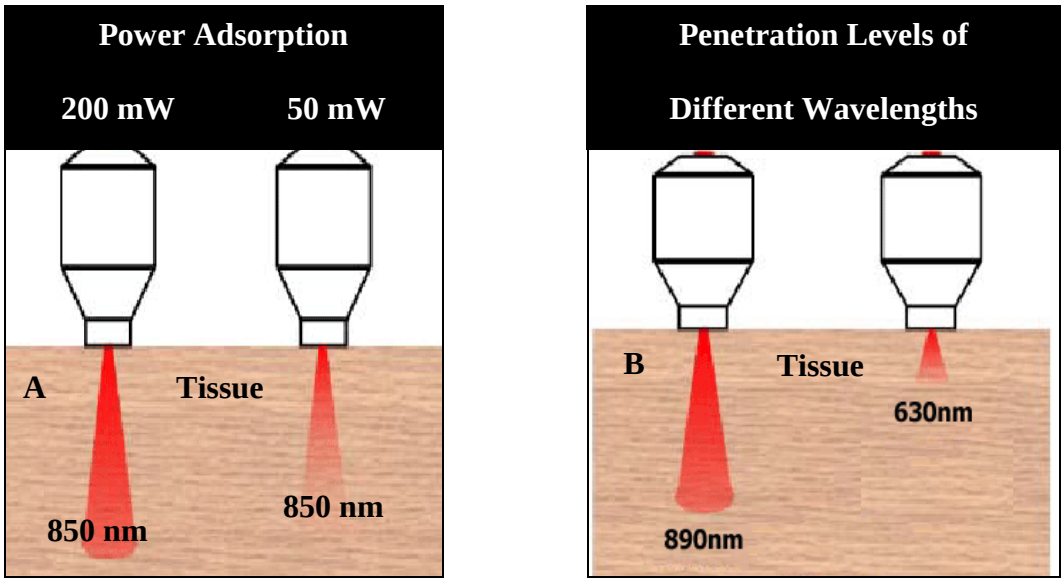

Figure 2.5 Fluence Rate (A) and penetration depth increases in relation to wavelength across the visible spectrum (B) (Satino and Markou, 2003).

Lasers are frequently used in PDT as a light source because lasers are:

- Monochromatic (one colour or wavelength)
- A highly directional beam with low divergence
- Capable of being focused into a very small spot
- Uniquely capable of producing ultra-short pulses (in 10^{-9} - 10^{-15} sec i.e. nanoseconds to femtoseconds) and a coherent light beam (Mitton and Ackroyd, 2008)

Lasers are used in many medical applications like PDT because of their availability and convenience. Recent developments in laser technology have produced highly compact and energy–efficient solid state lasers which can readily be integrated with

efficient delivery systems (such as optical fibres) to tissues or internal tumors that are deep-seated in the body. In case of a superficial skin cancer, a direct illumination method can be used (Mitton and Ackroyd, 2008).

In 2000 Diomed Incorporation (Andover, MA) gained FDA approval for their 630 nm diode laser to be used for the activation of Photofrin® in the treatment of oesophageal and lung malignancies. These lasers represented a new generation of laser devices entering the medical field and a remarkable breakthrough in laser technology for PDT (Mang, 2004). Diode lasers can be used in continuous wave mode or pulsed (picosecond to millisecond) making them very versatile. The power supply is also compact and diode lasers are generally air–cooled. They are easy to operate and portable making this device ideal for laboratory or clinical settings. Diode lasers have been used in the treatment of various skin lesions, oral cavity and age–related macular degeneration of the eye. At present diode lasers can offer only a single output wavelength (Brancaleon and Moseley, 2002). However diode laser systems are being developed that will contain multiple wavelengths and allow selectivity of wavelength according to treatment requirements (Brancaleon and Moseley, 2002).

In the past few years the development of femtosecond lasers has advanced to a stage where their use in phototherapy (and PDT in particular) is possible. A femtosecond laser emits optical pulses with duration well below one picosecond or ultrashort pulses (one femtosecond = 10^{-15} seconds). The advantage of this laser is that it offers multiple excitation wavelengths and the incident irradiation is in the near infrared region, and as a result penetration into tissue would be much greater. This is an

attractive feature especially for the treatment of less superficial lesions (Brancaleon and Moseley, 2002).

New laser technology and laser development is continuously improving laser therapy. Laser sources like the diode laser will become smaller and more powerful. Developing the laser into a more universal tool will be a large step forward in improving the safety and effectiveness of laser treatment (Steiner, 2006).

2.5 Photochemical and Photophysical Principles of PDT

Molecular oxygen ($^3O_2$) that is present in tissue exists in its ground state containing two unpaired electrons with parallel spins in two degenerate anti-bonding orbitals, which gives it a spin multiplicity of three. Singlet oxygen ($^1O_2$) in its excited singlet state is characterised by paired electrons with opposite spins in the outer orbital (Plaetzer *et al*., 2009).

It is this singlet oxygen that is an essential component in the PDT process as shown in Figure 2.6. The production of $^1O_2$ in PDT involves two important processes:

- Light absorption by the PS at an appropriate wavelength
- PS capable of absorbing the light and energy transfer

This is a simple and controllable method for the production of $^1O_2$ in PDT. The main role of processes mentioned above is to excite molecular oxygen to its singlet state (DeRosa and Crutchley, 2002).

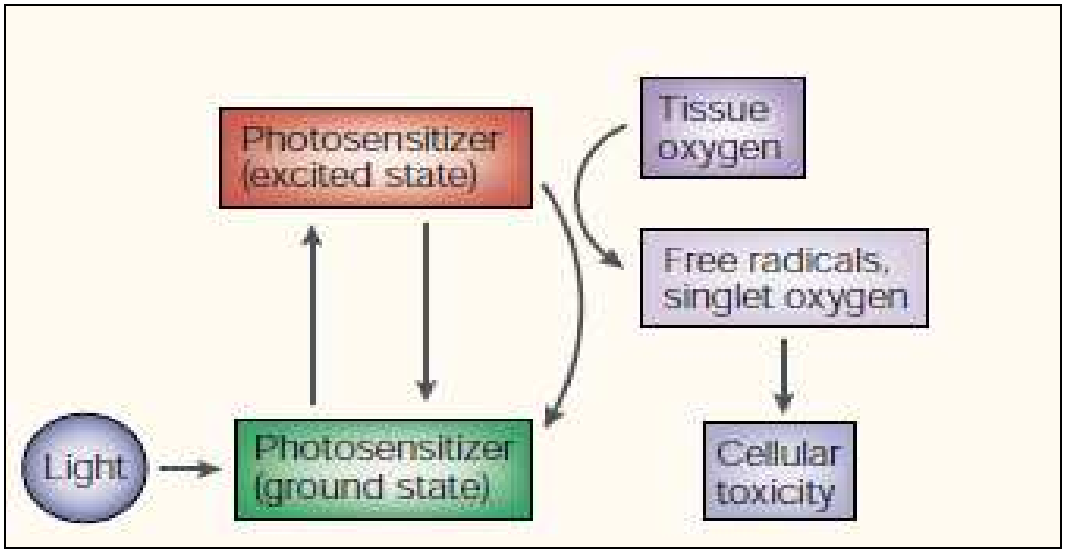

Figure 2.6 Mechanism of action of PDT (Dolmans, Fukumura and Jain, 2003).

During PDT, the ground state PS contains two electrons with opposite spins in a low energy molecular orbital; known as the singlet state. The laser light is absorbed in form of photons by the PS and one of the electrons present in the ground state PS is excited into a high–energy orbit, but keeps its spin from the first excited singlet state. This state is short lived and loses its energy by emitting fluorescence light or by internal heat conversion (Robertson, Evans and Abrahamse, 2009). The excited singlet state PS may also undergo a process whereby the spin of the excited electron inverts to form a relatively long-lived excited triplet-state that has electrons which spin in a parallel conformation. Thereafter, the reaction pathways of the activated PS in that excited triplet state can be characterized as Type I or Type II photoreactions (Figure 2.7) and these reactions are important for the induction of cell death or cell destruction (Robertson, Evans and Abrahamse, 2009).

In Type I reaction the activated PS can directly react with a substrate (e.g. cell membrane or molecule) and transfer a proton or hydrogen atom to form free radicals. These radicals will react with oxygen present in the tissue to produce reactive oxygen

species (ROS). In Type II reaction, the activated PS in its triplet state will transfer its energy directly to molecular oxygen (a triplet form in the ground state), to form an excited state singlet oxygen. This highly reactive form of oxygen will react with many biological molecules (e.g. lipids, proteins or nucleic acid). Type I and Type II reactions can occur simultaneously (Robertson, Evans and Abrahamse, 2009).

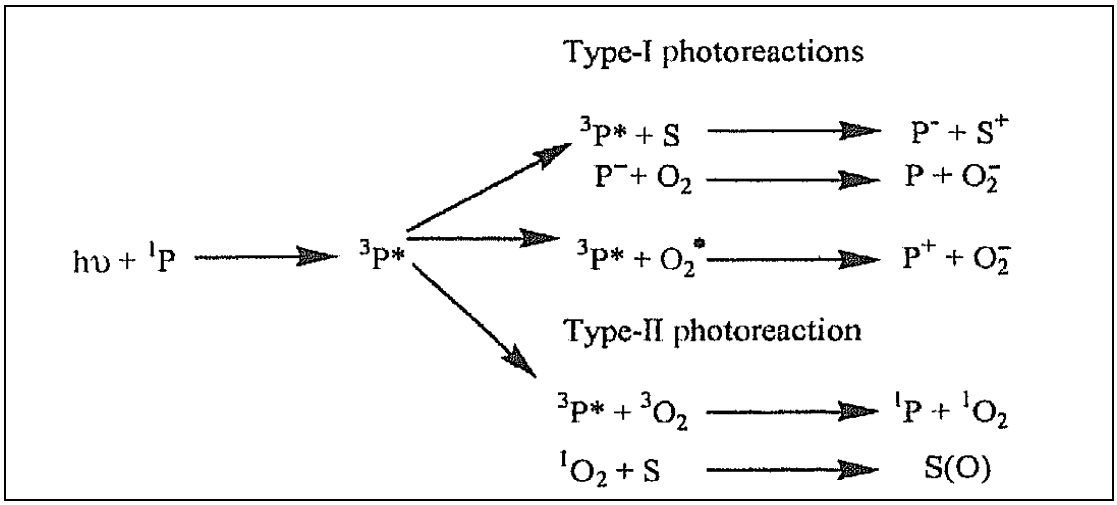

Figure 2.7 Overview of photochemical reactions during PDT. Type I and Type II reactions. ^1P is a PS in ground state, ^3P is a PS in a triplet excited state, S is a substrate molecule, P^- reduced PS molecule, S^+ is an oxidised substrate molecule, O_2 is the superoxide radical. P^+ is the oxidized PS, $^3O_2$ is triplet ground-state oxygen, $^1O_2$ is oxygen in a singlet excited state, and S (O) is oxygen adduct of a substrate (MacDonald and Dougherty, 2001).

The amount of $^1O_2$ produced during each reaction pathway depends on three factors:

- Type of PS used and the dose of PS
- Concentration of substrate available
- Concentration of oxygen present in the tissue (Robertson, Evans and Abrahamse, 2009).

PDT is highly dependent on the above factors and the amount of $^1O_2$ produced, which is the primary cytotoxic agent responsible the destruction of tumor cells (Robertson, Evans and Abrahamse, 2009).

Literature states that phthalocyanines are efficient Type II reaction pathways sensitizers (Rosenthal and Ben–Hur, 1995), which is the heart of photo-initiated cell death (Josefsen and Boyle, 2008). ROS can initiate a large number of reactions with biomolecules, including amino acids residues in proteins and these interactions cause damage and potential destruction to cellular membranes and enzymes resulting in cell death of cancer cells (Josefsen and Boyle, 2008).

Both Type I and Type II reactions are oxygen dependent and in the absence of oxygen the photochemical reactions can not proceed which means cell destruction of cancer cells does not occur (Stewart, Baas and Star, 1998).

2.6 Photobiology Principles in PDT

The increasing recognition of PDT as an efficacious cancer treatment requires the understanding of the interaction of light and biological tissue in order to enhance the destructive action of targeted tissue (Lukšienė, 2003). The first law of photobiology states “for low-power visible light to have any effect on biological system, the photons must be absorbed by electronic absorption bands belonging to some molecular chromophore or photoacceptor (Castano, Demidova and Hamblin, 2004).

Light is either scattered or absorbed when it enters the tissue. The absorption process is due to endogenous tissue chromophores such as hemoglobin (Hb), oxyhemoglobin

(HbO_2), melanin, water and cytochromes. Biological tissue is considered to be inhomogeneous because it contains macromolecules, cell organelles, organized cell structure, interstitial layers etc which makes it turbid (Castano, Demidova and Hamblin, 2004). Multiple scattering of light in tissue will occur within turbid medium resulting in spreading of the light beam and loss of directionality. Scattering is a major limiting factor in the penetration of light into tissue. Both these processes depend on tissue type and laser light wavelength (Castano, Demidova and Hamblin, 2004).

Castano, Demidova and Hamblin (2004) found that the absorption of shorter wavelengths of light by the important tissue chromophores (Hb, HbO_2, and melanin) together with reduced light scattering at longer wavelengths including the occurrence of water absorption at wavelengths greater than 1300 nm has led to the concept of the "optical window" in tissue as illustrated in Figure 2.8. The absorption spectra of these molecules also define the therapeutic window for PDT in tissue. It is important to note that hemoglobin (Hb) and HbO_2 show different absorption features in the range of 600 - 800 nm, which is commonly used in PDT. There might be a reasonable difference *in vivo* in the amount of Hb and HbO_2 between healthy and cancerous tissue due to the possible lower oxygenation and pH of the latter. When using PDT as a treatment for solid tumor the effective penetration depth is of great relevance (Plaetzer *et al*., 2009). Therefore, the effective tissue penetration of light is at its maximal at red and near-IR wavelengths (Figure 2.8). Thus, although blue, green, and yellow light may have significant effects on cells growing in optically transparent culture medium, low-level laser therapy (LLLT) use in animals and patients require red and near-IR light (600 – 1070 nm). In terms of PDT the average effective

penetration depth is about 1 - 3 mm at 630 nm. The increased penetration depth of longer wavelength light is a major incentive for the development of PS like phthalocyanine which has absorbance values at longer wavelengths at about 600 – 800 nm (Castano, Demidova and Hamblin, 2004). The use of PS with absorption peaks at wavelengths greater than 700 nm (or even higher) should double the penetration depth and thus enable treatment of thicker tumor (Plaetzer *et al*., 2009).

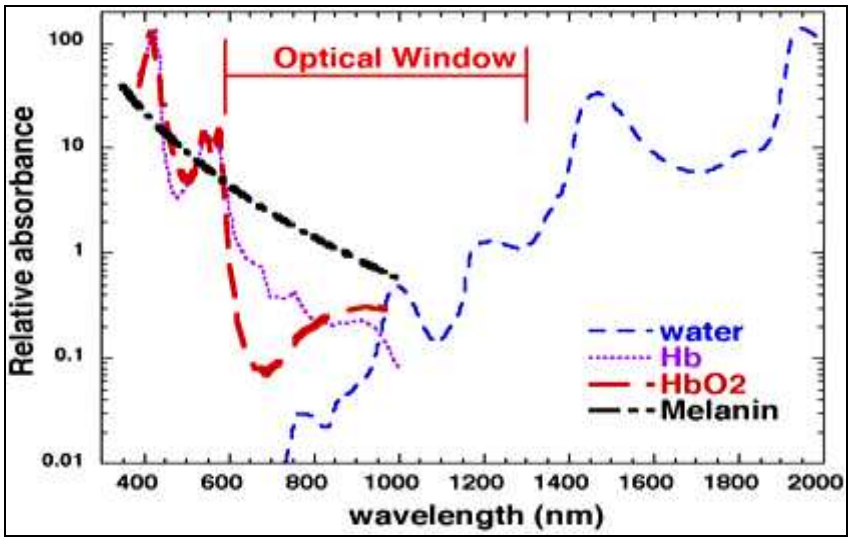

Figure 2.8 The optical window in tissue with absorption spectra of important tissue chromophores plotted on logarithmic scale (Castano, Demidova and Hamblin, 2004).

It is important that the absorption spectrum of the PS corresponds to the optical window where tissue penetration is the deepest and the energy of the triplet state PS is apparently sufficient for singlet oxygen production (Plaetzer *et al*., 2009). Among the cytotoxic substances (ROS & radicals) produced by triplet state PS, singlet oxygen (from Type-II photochemical reactions) predominately represents the most important effector in PDT (Plaetzer *et al*., 2009). In the cellular environment these cytotoxic substances cause cell death or tissue destruction. As a consequence, the intracellular localization of the PS greatly determines the site of cellular damage and cell death mechanism set by PDT (Plaetzer *et al*., 2009). These cytotoxic substances have a

short half–life and act close to the site of generation. The type of photodamage that occurs in cancer cell loaded with PS and irradiated depends on the precise subcellular localization of the PS within the cell.

2.6.1 Subcellular localization of PS

The intracellular distributions or accumulation in cultured cells for a variety of photosensitizers that have differing structures have been determined by Castano, Demidova and Hamblin, 2004. The photosensitizer can localize at the following sites in a cell:

- Lysosome (Kessel, 2006; Castano, Demidova and Hamblin, 2004)
- Mitochondria (Kessel, 2006; Castano, Demidova and Hamblin, 2004)
- Plasma membrane (Kessel, 2006; Castano, Demidova and Hamblin, 2004)
- Endoplasmic reticulum or ER (Kessel, 2006; Castano, Demidova and Hamblin, 2004)
- Golgi apparatus (Castano, Demidova and Hamblin, 2004)

Second-generation photosensitizers are designed to target a certain site within a cell as illustrated in Figure 2.9. This would help in triggering the effective cellular signals needed for expressing the pro-apoptotic factors (e.g. Bax) for the induction of programmed cell death (Kessel, 2006). Plasma membrane monocationic porphyrin (MCP) is designed to localize in the plasma membrane of the photosensitized cells. The cationic PS tin octaethyl-purpurin amadine (SnOPA) and Lysyl chlorine e6 (LCI) can localize in various sites e.g. mitochondria (mito), ER and lysosomes (Kessel, 2006). Photosensitizers like meta-tetrahydroxyphenyl chlorin (mTHPc), 9-capronyoxyter-akismethoxyethyl porphycene (CPO), aluminium phthalocyanine

(AlPc), 2-devinyl-2-I-hexyloxyethyl pyropheophorbide (HPPH), tin etiopurpurin (SnET2), lysyl chlorin p diester (LCP), Lutetium Texaphyrin (LuTex), mono L aspartyl chlorin e6 (NPe6) and dichlorophenol (DCP-0) can localise in the ER, and in lysosomes (Kessel, 2006). Phthalocynanines (Pc 4), photofrin and Benezoporphyrin derivative (BPD) can localise in the mitochondria and the ER. Dicyclopentenyl acrylate (DCPa) can only localise in the mitochondria (Kessel, 2006).

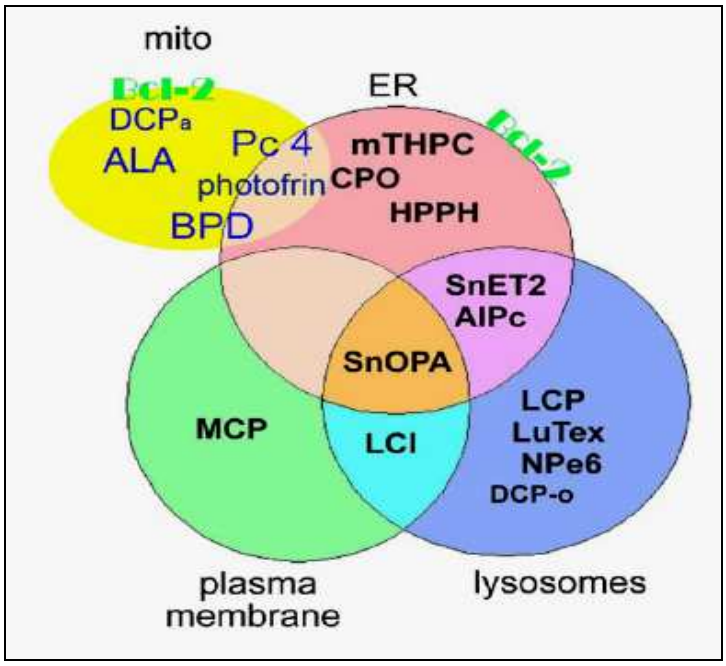

Figure 2.9 Localization sites of a variety of "second generation" PS (Kessel, 2006).

The important structural features of a photosensitizer which play a role in determining the localization site within a cell are (Castano, Demidova and Hamblin, 2004):

- The net ionic charge which can range from -4 (anionic) to +4 (cationic)
- The degree of hydrophobicity
- The degree of asymmetry present in the molecule

The PS which are hydrophobic and contain two or less negative charges can easily diffuse across the plasma membrane to relocate in other intracellular membranes. Also, the *in vitro* cells tend to have a greater uptake of these PS as compared to in *vivo* cells especially when the PS of this nature is present in relatively low concentrations in the medium (< 1 µM). The less hydrophobic PS which contains more than 2 negative charges tends to be too polar to diffuse across the plasma membrane. Therefore, less hydrophobic PS are taken up by a process known as endocytosis (Castano, Demidova and Hamblin, 2004).

Studies have shown that PS localised in the lysosomes can lead to cell death upon irradiation but the efficacy is lower than PS localised in mitochondria or in other organelles (Castano, Demidova and Hamblin, 2004). This could be due to the tendency for PS with greater degrees of aggregation to accumulate in lysosome. PS that possess characteristics like having a net anionic charge of -2 or greater accumulate in the lysosome (Castano, Demidova and Hamblin, 2004). PS that localize in the lysosome induces cell death by activating the apoptosis pathway via two different routes:

- Redistribution of the PS after irradiation to the cytoplasm more specifically, the nucleus, photodynamic permeabilization of the lysosomal membrane allowing the PS to leak out into the cytoplasm (Castano, Demidova and Hamblin, 2004)
- The release of lysosomal enzymes in the mitochondria (Morgan and Oseroff , 2001)

This is a slower initiating process of apoptosis than that induced by mitochondrial based PS. Research indicates that mitochondrial depolarization is an early step leading to cell death and states that the mitochondria is central in effecting death signals from upstream events (Morgan and Oseroff, 2001). Therefore, the localization of the PS in the mitochondria allows for the direct initiation of apoptosis because upon irradiation specific pathways are activated rapidly for the release of cytochrome C from the mitochondria into the cytosol of the PDT treated cells. Cytochrome C release can cause the initiation of a cascade of events leading to the activation of cytotoxic caspases 3 and 9, and subsequently the occurrence of the final stages of apoptosis (Moor, 2000). PS localized to non-mitochondrial organelles and redistribute into the mitochondria after irradiation also cause depolarization of the mitochondria by a common pathway. It should be noted that mitochondrial depolarization also may lead to early steps associated with necrosis (Morgan and Oseroff, 2001).

The functional mitochondria have polarized membranes with the inside being negatively charged relative to the outside. This is due to a combination of a membrane potential and a pH gradient produced by proton pumping at respiratory chain proteins. The polarization together with the presence of specific lipids and proteins in the outer and in inner membranes influence the distribution of the PS. Cationic PS accumulates in the mitochondrion which is also dependent on the PS degree of lipophilicity and the extent of their delocalized charge. In the presence of a series of cationic zinc phthalocyanines the more lipophilic members entered the mitochondria more readily than the less lipophilic molecules, indicating that positively charged PS may need additional characteristics than charge for proper targeting (Morgan and Oseroff, 2001).

The plasma membrane is the preferred site of localization for hydrophobic PS and a number of signaling pathways can be activated from this level (Moor, 2000). Characteristics like plasma disruption and cell swelling were observed immediately after PDT. DNA fragmentation and phosphatidylserine externalization were not detected in the cell death process induced by PDT regime (Castano, Demidova and Hamblin, 2004). It has been hypothesized by that by using photoactivation of PS localized in the ER to stimulate a rapid increase in intracellular levels of calcium is sufficient to trigger cell death as part of a stress response via mitochondrial cell death machinery (Buytaert, Dewaele and Agostinis, 2007). Therefore, PDT leads to destabilization of mitochondria or ER-membranes, thus increasing the concentration of cytosolic calcium which opens the mitochondrial pore to induce apoptosis (Plaetzer *et al*., 2003).

Although PDT can activate many signalling events in cells, the main aim is generally to kill cancerous cells. There is an existence of many pathways whereby mammalian cells can die and some of these pathways or processes can be initiated by PDT. The mode and extent of cell death depends on:

- Concentration of the PS
- Physical and chemical properties of the PS
- Subcellular location of the PS
- Concentration of the oxygen present in biological tissue
- The wavelength
- Intensity of the light and fluence rate
- Cell type specific properties (Castano, Demidova and Hamblin, 2005a)

2.7 Modes and mechanisms of cell death in PDT

Researchers in the field of PDT have looked at the occurrence of apoptosis and necrosis both *in vitro* and *in vivo* because of the intense interest involving cell death mechanisms (Castano, Demidova and Hamblin, 2005a). There are three distinct types of cell death mechanisms:

- Necrosis
- Apoptosis
- Autophagy

2.7.1 Necrosis

Necrosis is known as accidental cell death caused by extreme external physical and chemical damage. It is morphologically characterized by cytoplasm swelling, destruction of organelles and disruption of the plasma membrane, resulting in the release of intracellular contents and inflammation as illustrated in Figure 2.10. Disruption of the plasma membrane occurs due to the ability of the plasma membrane to control the passage of ions and water is interrupted, and the cell contents leak out leading to an inflammation of surrounding tissues (Buytaert, Dewaele and Agostinis, 2007).

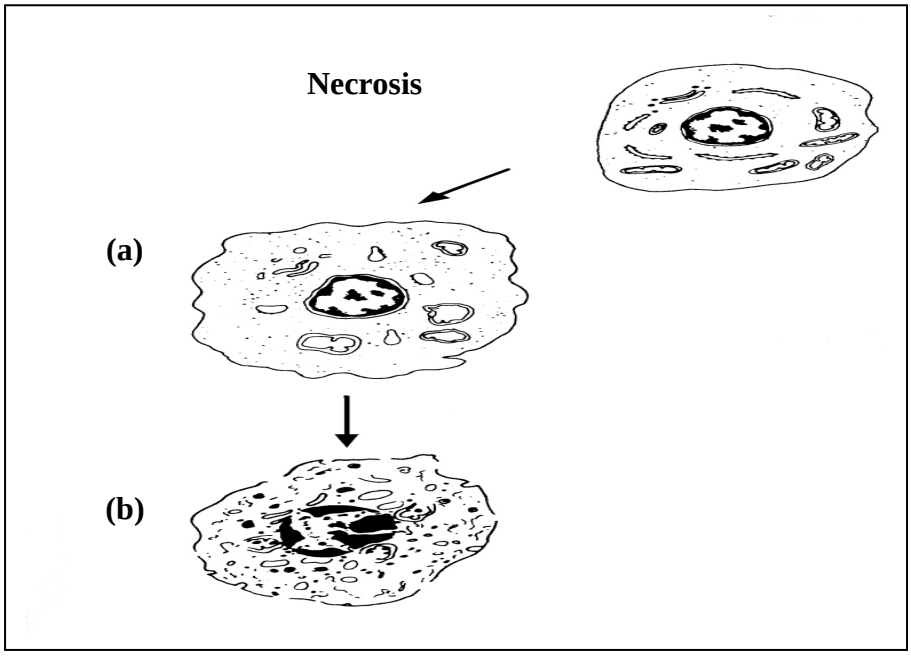

Figure 2.10 Morphology of dying cells via necrosis (a) destruction of organelles and disruption of the plasma membrane (b) release of intracellular contents and inflammation (Blom, 2000).

Necrosis is a passive and unorganized way in which cells die. Recent evidence shows that necrotic death can be propagated as part of a signal transduction pathway activated by switching on gene transcription (Figure 2.11). The signal transduction pathway which occurs in certain cell lines involves the engagement of TNF (Tumor Necrosis Factor) and Fas receptors triggering necrosis through the activation of RIP1 (receptor interacting protein 1) kinase, under the inhibition of caspase . RIP1 is the main element for the JNK (c – JunN – terminal Kinase) - mediated necrotic cascade activated by poly (ADP-ribose) polymerase-1 (PARP-1) following oxidative stress injury (Buytaert, Dewaele and Agostinis, 2007).

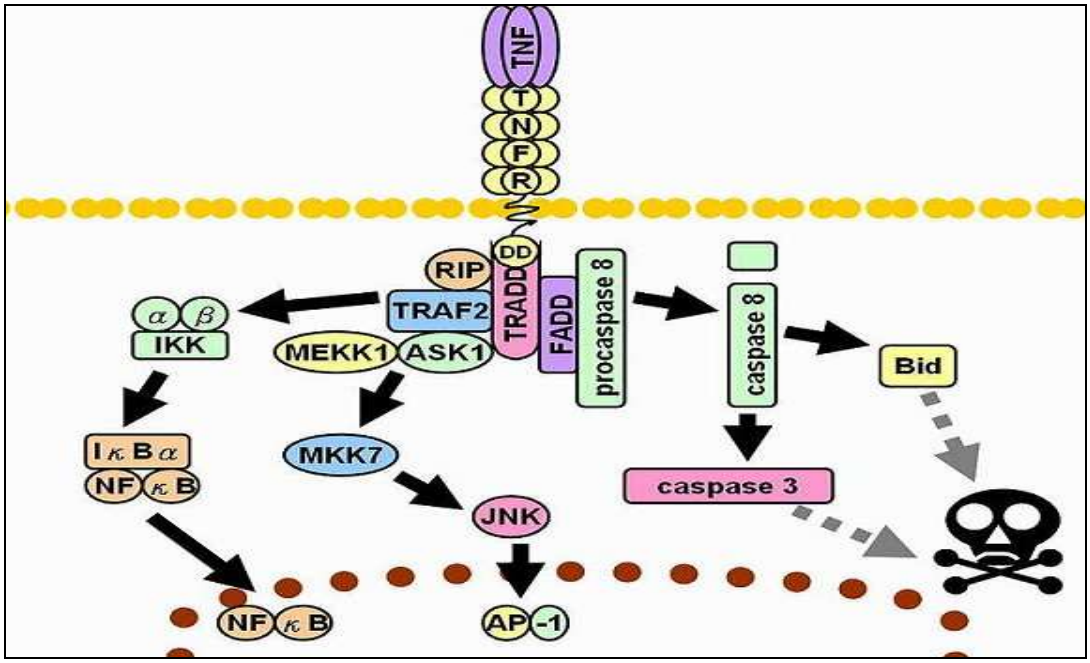

Figure 2.11 Necrosis pathway (Chen and Goeddal, 2002).

In PDT, a shift from apoptotic to necrotic cell death using a specific PS can usually be initiated by (Plaetzer *et al*., 2003):

- high fluences (light dose)
- high PS concentrations
- lipophilic and anionic dyes localize in membrane systems

The intensity of the PDT dose creates a massive induction of ROS leading to an immediate bioenergetic catastrophe such as a decrease in ATP levels and general metabolic inhibition (inhibition of mitochondrial enzymes). Also, the PS which localize in membrane systems act on the membrane cholesterol and other unsaturated phospholipids causing their peroxidation (Plaetzer *et al*., 2003). This result in changes occurring in the cell e.g. membrane permeability, loss of fluidity, cross–linking of amino lipids, cross–linking of polypeptides, inactivation of membrane associated enzyme systems and receptors. This causes a loss of membrane integrity and ion homeostasis and might be the prime reason for the occurrence of necrosis in PDT treated cells (Plaetzer *et al*., 2003).

2.7.2 Apoptosis

Apoptosis is one of the best-studied cell death mechanisms as it is considered to have the most wide spread physiological, pathological and therapeutic role (Kerr, Wyllie and Currie, 1972). The execution of apoptosis disrupts the balance between cell proliferation and cell death, eliciting a spectrum of diseases including cancer. It is morphologically characterized by blebbing membrane, cell shrinkage, chromatin condensation, cleavage of chromosomal DNA into internucleosomal fragments, formation of apoptotic bodies (apoptosome) without plasma membrane breakdown and phagocytosis by neighbouring cells as illustrated in Figure 2.12 (Buytaert, Dewaele and Agostinis, 2007).

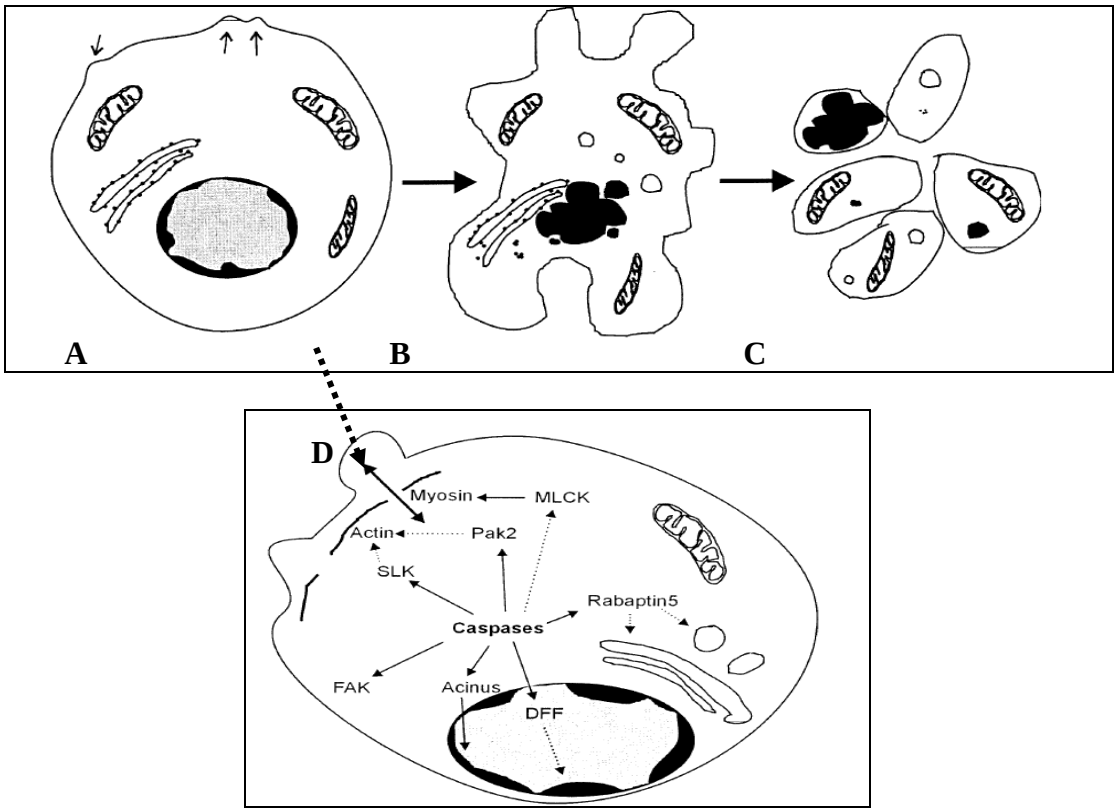

Figure 2.12 A schematic representation of the morphological changes that occur in dying apoptotic cell at various stages of apoptosis. (A) Blebbing (B) Nucleus condenses completely (C) Formation of apoptotic bodies (D) The morphologically changes require the activation of specific apoptosis biochemical pathways (Häcker, 2000).

Apoptosis in contrast to necrosis is an ATP or energy-requiring process. The apoptosis depends on energy equivalents in the form of ATP or GTP. Thus, the formation of apoptotic bodies as well as morphological changes requires ATP or equivalents (Plaetzer *et al*., 2003).

Apoptosis or "programmed cell suicide" can be mediated via two major apoptotic pathways namely:

- Death receptor mediated or extrinsic pathway
- Mitochondria-mediated or intrinsic pathway (Almeida *et al.,* 2004)

The extrinsic pathway (Figure 2.13) is mediated by the activation of death receptors. Death receptors belong to the tumor necrosis factor receptor (TNFR) gene family and include TNFR-1, Fas/CD95 and TRAIL (TNF–Related Apoptosis-Inducing Ligand) receptors e.g. DR-4 (Death Receptor 4) and DR-5 (Death Receptor 5). These death receptors which are cell surface receptors are transmitters of apoptotic signals after ligation with specific ligands. The adaptor molecules like FADD (Fas-Associated protein with Death Domain) or TRADD (TNF Receptor-Associated protein with Death Domain) contain their own DDs by which they are recruited to the DDs of the activated death receptor. This leads to the formation of the death inducing signalling complex (DISC). Also, the adaptor FADD has a death effector domain (DED) which through homotypic DED-DED interaction sequesters procaspase-8 to the DISC. This will trigger the release of active caspase-8 and initiation of effector caspases (caspase-3, caspase-7 and caspase-6) for the execution of apoptosis (Denault and Salvesen, 2002).

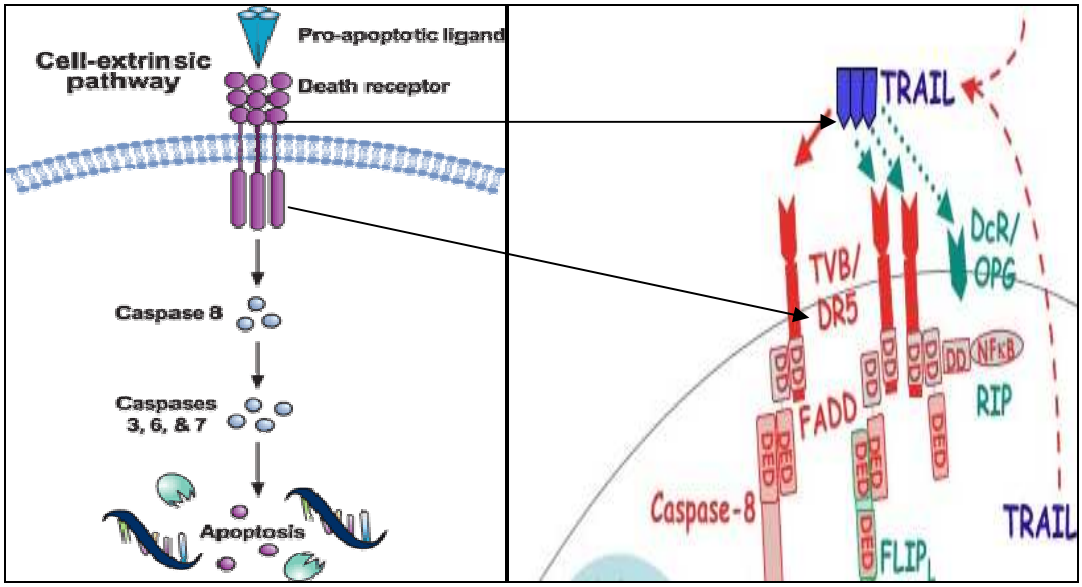

Figure 2.13 The extrinsic pathway starts outside the cell through the activation of specific pro-apoptotic ligand and receptors (death receptors) on the cell surface. Ligands (e.g. TRAIL) bind to receptors (e.g. DR5) for the triggering of apoptosis imitators (e.g. caspase 8) within the cell for the execution of apoptosis (Ashkenazi, 2002; Johnson, 2009).

In the intrinsic pathway the mitochondria plays a central role (Figure 2.14). The permeabilization of the mitochondrial membranes results in the release of several apoptosis proteins. The mitochondrial membrane permeabilization (MMP) depends on two mechanisms (Buytaert, Dewaele and Agostinis, 2007):

- Favoured mitochondrial Ca^{2+} uptake and by the exposure of mitochondria to damaging ROS
- Formation of proteinaceous channels in the outer mitochondrial membrane (OMM) through the process involving oligomerization of pro–apoptotic Bcl_2 members or interaction between Bcl-2 proteins and voltage-dependent anion channel (VDAC)

During the permeability of mitochondrial membrane apoptosis proteins which are stored in the inter-mitochondrial membrane space (IMS) are released into the cytosol

(Buytaert, Dewaele and Agostinis, 2007). IMS apoptosis proteins such as cytochrome C, Omi/HtrA2 (Omi stress-regulated endoprotease/ High temperature requirement protein A 2) and Smac/DIABLO (Second Mitochondria-Derived Activator of caspase / Direct IAP Binding protein with a low pI), including apoptosis-inducing factor (AIF) and endonuclease G (Endo G) are activators of caspases (Buytaert, Dewaele and Agostinis, 2007). When cytochrome C is released into the cytosol it immediately binds to Apaf – 1 (apoptotic protease-activating factor 1) forming a complex called apoptosome in the presence of ATP or dATP and this results in the activation of procaspase-9. Caspases activation is promoted by Omi/HtrA2 and Smac/Diablo antagonizing the activity of inhibitors of caspases (IAPs). AIF and EndoG translocate to the nucleus to mediate chromatin condensation and DNA fragmentation, independently from caspase signaling (Buytaert, Dewaele and Agostinis, 2007).

The Bcl-2 protein family contains 20 members comprising one of four Bcl-2 domains (BH1 to BH4). The anti-apoptotic Bcl-2 proteins (e.g. Bcl-2, Bcl-X_L, Bcl-w) contain all four residues and are located at the cytoplasmic side of the cellular membranes of the mitochondria, ER and nucleus. The pro-apoptotic Bcl-2 proteins contain BH123 multidomain (e.g. Bax, Bak) and BH3 only proteins (e.g. Bid, Bad). Therefore, the molecular cross-talk between the intrinsic and extrinsic pathway is granted by the caspase-8 mediated cleavage of the cytosolic protein Bid as truncated Bid (tBid) , which translocates to the mitochondria to facilitate the release of cytochrome C into the cytosol (Buytaert, Dewaele and Agostinis, 2007).

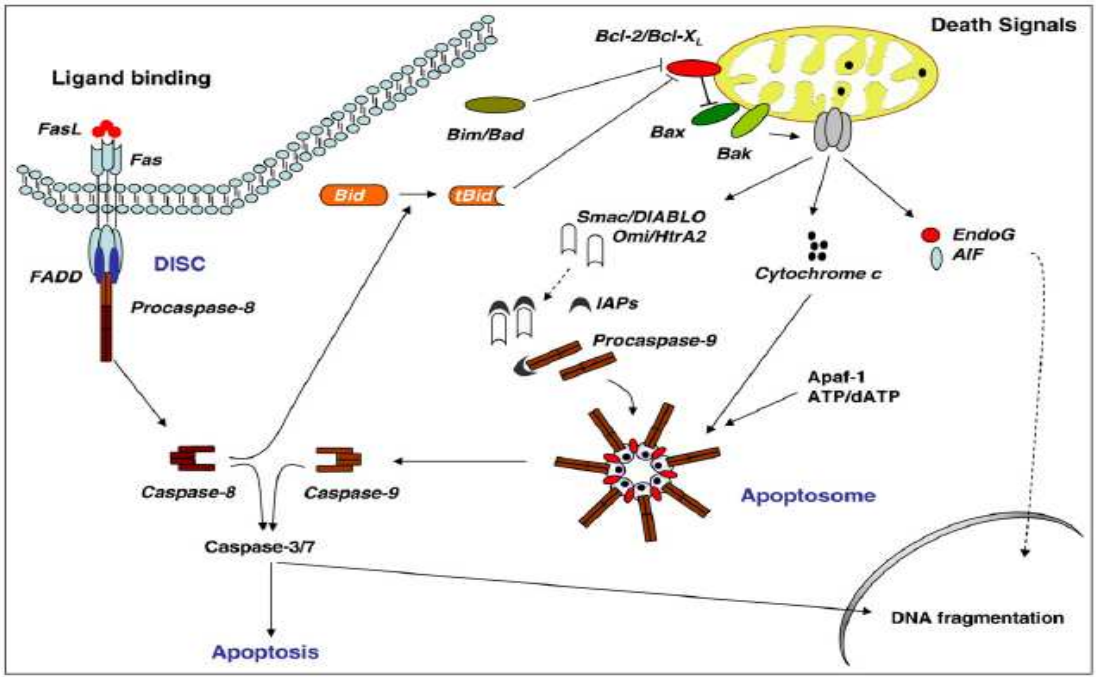

Figure 2.14 The intrinsic or the mitochondrial pathway is initiated by the release of apoptogenic factors (e.g. cytochrome c) from the intermembrane space of the mitochondria into the cytosol for the activation of apoptosis initiators known as caspases (Buytaert, Dewaele and Agostinis, 2007).

In PDT, the critical role of apoptosis in photosensitized cells has been largely documented. Figure 2.15 illustrates some of the cellular and molecular signalling pathways leading to apoptosis that have been found to occur in cells treated with PDT. It has been observed that during PDT–mediated apoptosis mitochondrial transmembrane potential progressively collapses, intracellular ATP levels steadily decrease and damage to the mitochondria becomes irreversible cell death. This is largely true for PS that locates in the mitochondria. This includes porphyogenic sensitizers and phthalocyanine-related compounds which upon irradiation swiftly mediate MMP.

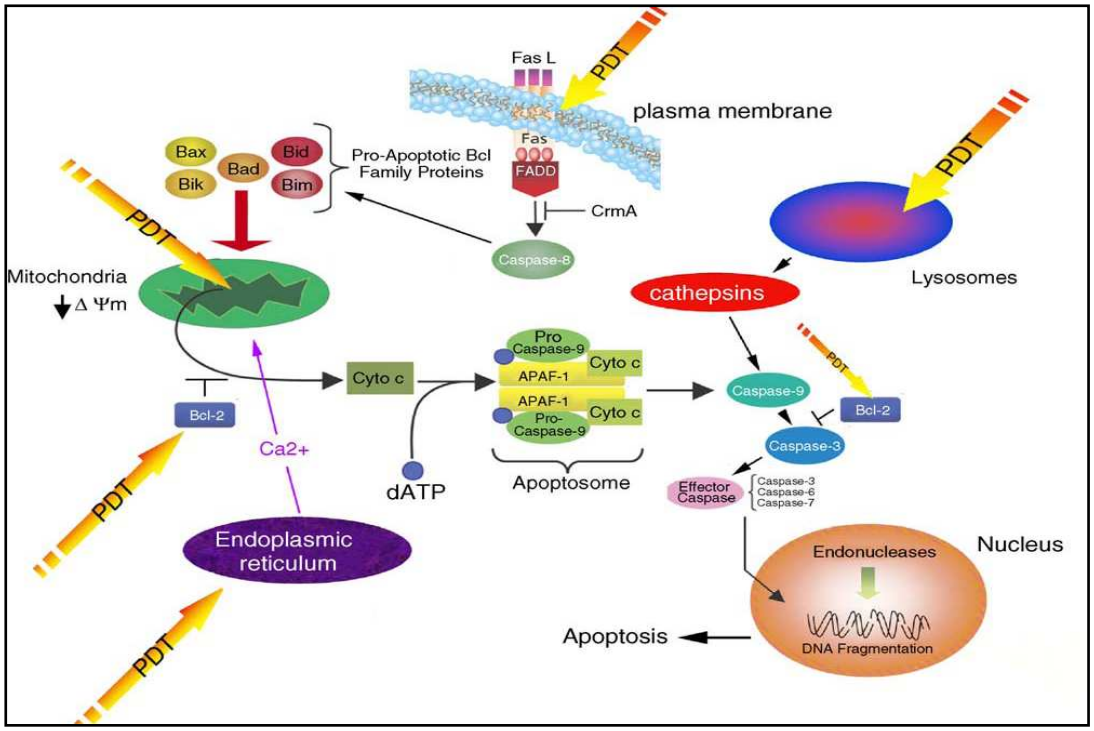

Figure 2.15 Cellular and molecular signalling pathways leading to apoptosis that have been found to occur in cells treated with PDT. The initial targets of PDT-generated ROS depend on the PS localization (Castano, Demidova and Hamblin, 2005a).

The mitochondria are also important initiators of cell death pathways resulting in the photodamage of other subcellular sites or organelles as illustrated in Figures 2.15 and Figure 2. 16 (Buytaert, Dewaele and Agostinis, 2007). PS located in the lysosomes release cathepsins upon PDT and this promotes Bid-mediated apoptosis. ER localized dyes initiate active cell death by releasing Ca^{2+} into the cytoplasm as depicted in Figure 2.15 and Figure 2.16 (Plaetzer *et al*., 2003).

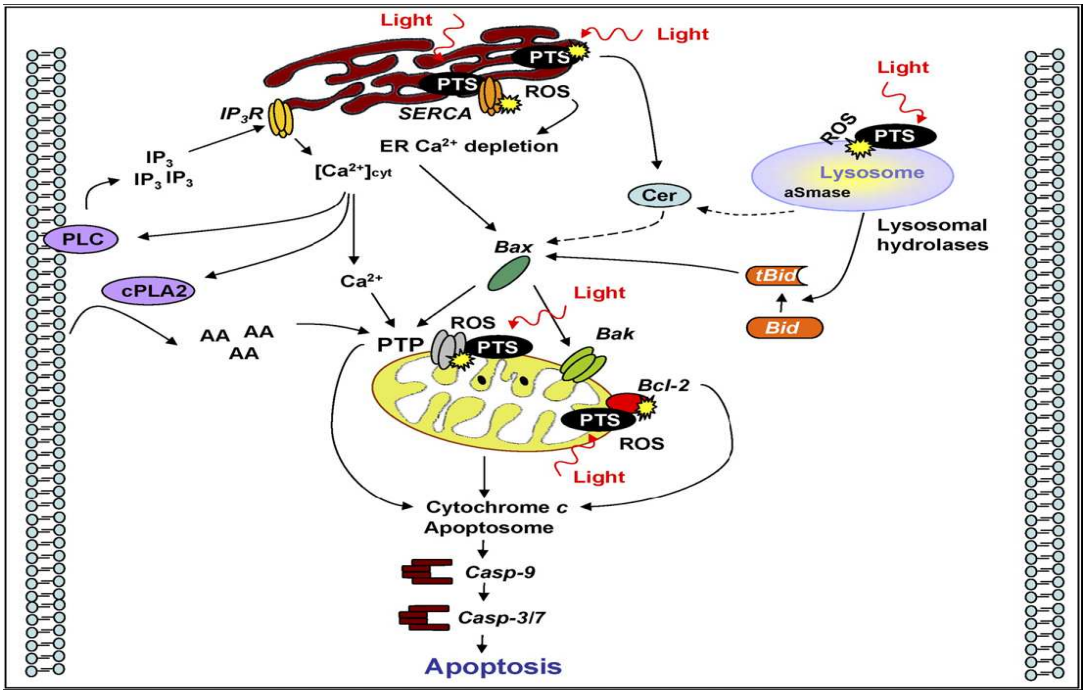

Figure 2.16 The interplay between the localization of the PS and different molecules for the activation of dependent mitochondrial apoptosis (Buytaert, Dewaele and Agostinis, 2007).

In PDT the production of ROS in the mitochondria or in the cytoplasm are the potent inducers of apoptosis (Figure 2.16). Several theories have indicated that links exist between PDT-produced ROS and mitochondrial pore opening which results in the release of the pro-apoptotic proteins for the induction of cell death (Almeida *et al.*, 2004; Buytaert, Dewaele and Agostinis, 2007; Plaetzer *et al*., 2003). Also, literature states that PDT leading to cell death of cancerous cells via apoptosis can be activated by the extrinsic pathway (Plaetzer *et al*., 2003).

2.7.3 Autophagy

The term autophagy means literally *self-eating* in Greek and often referred to macroautophagy. Autophagy contributes to the maintenance of intracellular homoeostasis and can signal cell death or survival. Under conditions of nutrient

starvation, this pathway will supply cells with metabolic substrates, and hence represents an important pro-survival mechanism (Galluzzi *et al*., 2008). However, autophagy is also associated with cell death though excessive self-digestion and degradation of essential cellular constituents. Electron microscopy studies revealed morphology changes like nuclear collapse, highly condensed nucleus, structures required for protein synthesis (e.g. polyribosomes, ER and golgi) disappearing , few clusters of intact mitochondria persist in close vicinity to autophagic vacuoles and the nuclear envelope that characterize autophagy (Bursch *et al*., 2008). This cellular pathway activates cell death though the absence of caspase-signaling or caspase inhibition (Buytaert, Dewaele and Agostinis, 2007).

The first step in autophagy is the formation of a double-membrane structure that sequesters cytoplasmic components as well as organelles. Also, it shapes the autophagic vacuoles or autophagosomes. These autophagosomes fuse with lysosome and their cytoplasmic material is degraded by lysosomal hydrolase. A family of autophagy-related genes (Atg) controls the formation of the autophagosomes and this includes Atg6/Beclin1 and Atg8/LC3. The molecular machinery of autophagy is regulated by class I and class II phosphatidylinositol 3 kinase (P13K) signaling pathway, which inhibit and stimulate the autophagy respectively. Literature suggests that several anti-cancer drugs can kill cancer cells by sending out stress responses to induce the autophagy cell death mechanism (Buytaert, Dewaele and Agostinis, 2007).

Recent studies have indicated that PDT may induce non-apoptotic cell death associated with the induction of autophagy cell death mechanism (Figure 2.17). In PDT, due to the large amounts of photogenerated ROS autophagy is initiated in an

attempt to eradicate oxidative damaged organelles or to degrade large aggregates of cross-linked proteins (produced by photochemical reactions). The induction of apoptosis in a PDT treated cell can be prevented if there is a deficiency in pro-apoptotic protein (Bax and Bak) which will result in the activation of another mode of cell death. Therefore, cell death by autophagy is induced as an alterative mode of cell death. Autophagy cell death can also be detected by biochemical and ultra structural changes in dying cell (Buytaert, Dewaele and Agostinis, 2007). Also, the down regulation of Bcl-2 can result in stimulation of autophagy by the release and hence the activation of the pro-autophagic protein Beclin from a Beclin: Bcl-2 complex. *In vitro* studies have shown that autophagy is another response to ER photodamage, perhaps serving to eradicate cells not initially removed by apoptosis or when apoptosis is blocked (Kessel, 2006).

More studies are required to identify the molecular mediators which may turn autophagy into a well defined cell death pathway. Also, to help researchers better understand the cross-talk between autophagy and the apoptotic machinery in PDT-induced autophagy. Defining the autophagy pathway will help in determining the PDT dose for the induction of autophagy and contribute to cancer cell death rather than survival. It is important to assess whether autophagy is an *in vivo* tumor response evoked by PDT and if the use of pharmacological modulators of this catabolic process in combination with PDT will prove beneficial to improve its therapeutic efficacy (Buytaert, Dewaele and Agostinis, 2007).

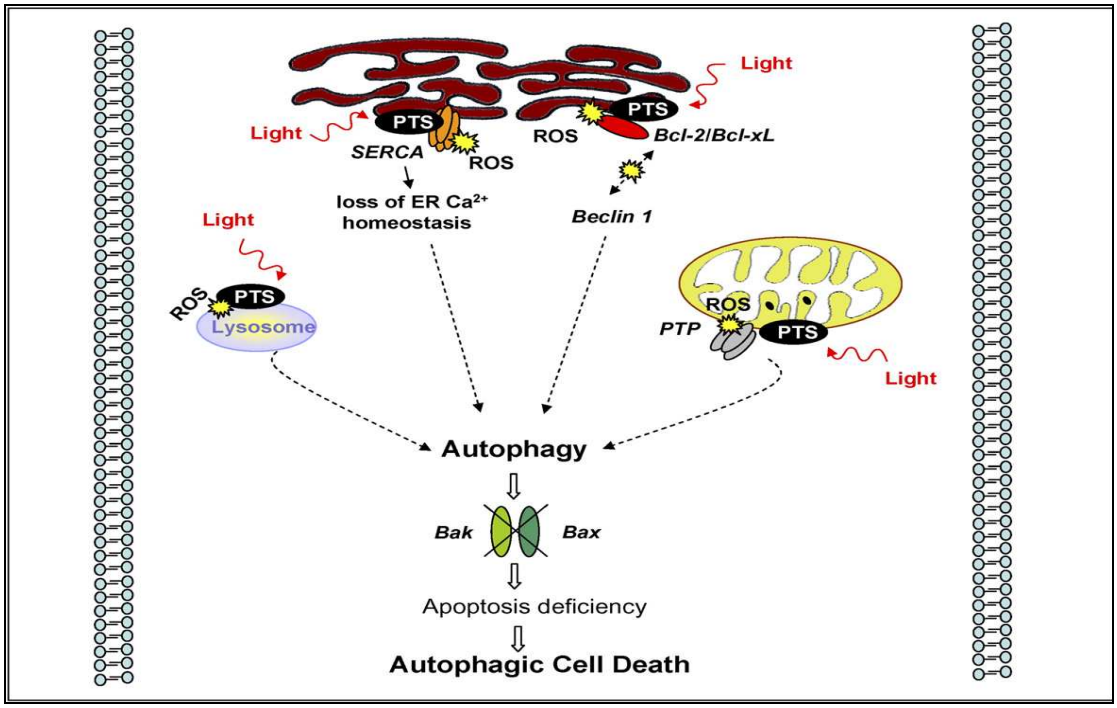

Figure 2.17 The autophagy cell death pathway is induced in PDT treated cells lacking the pro-apoptotic proteins. It is induced in PDT treated cells by photo-oxidative damage to intracellular organelles/targets. Photo-oxidative damage occurs specifically to the ER or anti-apoptotic Bcl-2/Bcl-xL proteins, which may alter Bcl-2/Bcl-xL interaction with Beclin 1 to favour the induction of autophagy (Buytaert, Dewaele and Agostinis, 2007).

2.8 Photodynamic Therapy (PDT) for Skin Cancer Treatment

Skin cancer incidence is increasing rapidly and poses a major health threat (Fuchs and Thiele, 1998). The major risk factor for skin cancer is exposure to the sun because in this generation the ozone layer in the atmosphere can offer very little protection against the harmful UV rays from the sun. Therefore, skin cancer is most likely to be seen on areas of the body that are most often exposed to the sun (Schuitmaker *et al.*, 1996). Malignancies of the skin can be primary or metastatic in nature and include many types of skin cancer as listed in Table 2.2. There are three forms of skin cancer that can occur, namely, basal cell carcinoma, squamous cell carcinoma, and melanoma (Schuitmaker *et al.*, 1996).

Table 2.2 The warning signs associated with the different types of skin cancers (Ferniany, 2008).

Name	Description
Basal cell carcinoma	Basal cell carcinoma accounts for approximately 75% of all skin cancers. This highly treatable cancer starts in the basal cell layer of the epidermis (the top layer of skin – Figure 2.18) and grows very slowly. It usually appears as a small, shiny bump or nodule on the skin (mainly those areas exposed to the sun, such as the head, neck, arms, hands, and face). This cancer commonly occurs among people with light-colour complexion.
Squamous cell carcinoma	Squamous cell carcinoma accounts for about 20% of all skin cancer cases. Although more aggressive than basal cell carcinoma, this cancer is highly treatable. It may appear as nodules or red, scaly patches of skin (found on the face, ears, lips, and mouth). However, squamous cell carcinoma can spread to other parts of the body. This type of skin cancer is usually found in fair-skin people.
Malignant melanoma	Malignant melanoma accounts for 4% of all skin cancers. It starts in the melanocytes cells (Figure 2.18). Melanocytes cells produce melanin (skin pigment) which is responsible for the variation in skin colours that occur. It usually begins as a mole that then turns cancerous (Figure 2.19). This cancer may spread quickly and all skin types may be affected, but fair-skin people are more susceptible.

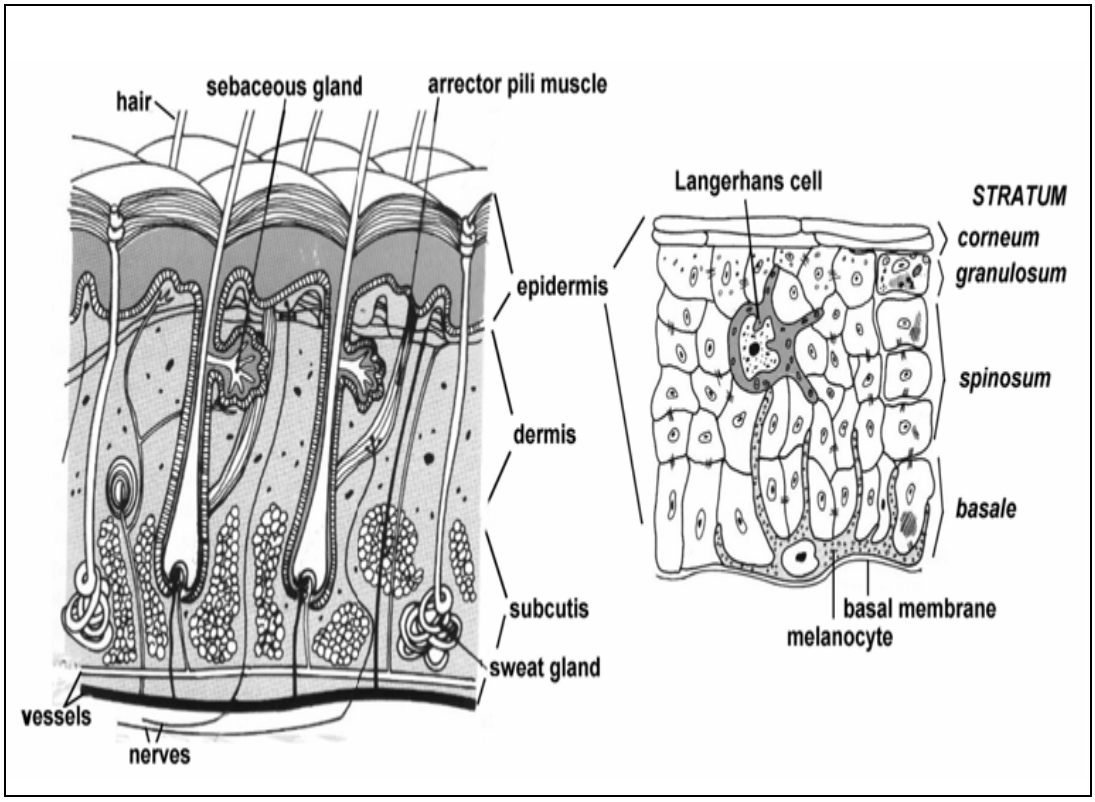

Figure 2.18 Different parts of an ordinary human skin model to understand the specific location of the different skin cancers (Holbrook, 1983).

Melanoma is the most lethal primary skin cancer as it has significant ability for local, regional and systemic spread (Allison *et al*., 2006). Melanoma sometimes known as cutaneous or malignant melanoma has a tendency to spread very quickly to other parts of the body via the body's lymphatic systems. This disease must be caught in the early stages, for full recovery. Melanoma can be prevented by regular skin examinations (screens at home or dermatologists) and becoming familiar with moles or other skin conditions. Moles that are present at birth, and atypical moles, have a greater chance of becoming malignant. Therefore by having regular skin examinations changes in moles can be detected by using the ABCD Chart. The ABCD chart is illustrated in Figure 2.19 and is crucial for detecting malignant melanoma at its earliest stage (Ferniany, 2008).

Normal Mole	Melanoma	Sign	Characteristic
		Asymmetry	when half of the mole does not match the other half
		Border	when the border (edges) of the mole is irregular
		Colour	when the colour of the mole varies throughout
		Diameter	when the mole diameter is larger than a pencil's eraser

Figure 2.19 The ABCD chart contains information on the warning signs commonly associated with melanoma cancer (Ferniany, 2008).

There are a variety of skin cancer treatments that exist (in order of decreasing efficacy) Moh's surgery, convectional surgical excision, radiation therapy, electrodesiccation and cryotherapy for skin cancer (Schuitmaker *et al*., 1996). These treatments have disadvantages in terms of healing, functional and cosmetic outcome, largely when the lesions are located on the face or in areas of poor vascularization (e.g. ankle or heel). Repeated treatment is impossible and multiple lesions are difficult to treat within reasonable time-span. Finally, treatment can be expensive (Schuitmaker *et al*., 1996).

Literature states that skin is a target organ for PDT treatment because it is easily accessible to light that is required for the photosensitizer (PS) activation and the PS can be applied to the affected area topical (Fuchs and Thiele, 1998). Therefore, melanoma lesions or skin cancer can be successfully treated with PDT as it is an

irreversible and single treatment. A major advance in PDT treatment for cancers is that damage to normal tissue can be minimized or the healing is usually excellent. Since healing of the subcutaneous collagen occurs by regeneration rather than scarring (Stewart, Baas and Star, 1998). Also, by topically applying the PS it will result in an increased penetration in abnormal skin where the stratum corneum or the outermost layer of the epidermis (Figure 2.18) is damaged as opposed to normal skin with an intact stratum corneum (Schuitmaker *et al*., 1996).

CHAPTER 3

METHODOLOGY

3.1 Description of cells

Three cell lines were used in these experiments. A human malignant (cancer) melanoma cell line (UACC-62) purchased from UACC (Lonza, Walkersville, MD, USA), a secondary keratinocyte cell line which was kindly donated by the University of Cape Town and a primary cell line (fibroblasts) which were isolated from human skin biopsies acquired from patients at University of Limpopo under ethical approval (MREC/M/63/2009: IR). Cells were not passaged more than 15 times.

3.1.1 Melanoma Cancer Cells

The melanoma cancer cells (UACC-62) used in this study was obtained from Bioscience, CSIR (Pretoria) which were purchased from UACC (Lonza, Walkersville, MD, USA). The melanoma cancer cells were grown in T-75 cell culture flask (Greiner Bio-One, Cellstar, Lasec, South Africa) containing 15 ml of RPMI-1640 medium without L-Glutamine (Lonza, Walkersville, USA) supplemented with 10% Foetal Bovine Serum (FBS; Gibco - Invitrogen), 1% Penicillin/ Streptomycin (Lonza, Walkersville, USA) and 1% Non-essential amino acids (NEAA; Sigma, St.Louis, USA). The cells were grown in a 5% CO_2 incubator (Galaxy, RS Biotech) with a humidified atmosphere at 37°C. Flasks were examined on a daily basis for turbidity and colour changes in the growth media. Cell growth or proliferation was monitored with an inverted microscope (Axiovert 40 Zeiss, Germany) and were either passaged or harvested when they reached 80% confluency (Decreau *et al*., 1999).

3.1.2 Epidermal Keratinocyte Cells

The keratinocyte cells were kindly provided from Department of Biology at the University of Cape Town. The primary keratinocyte cells were isolated from human biopsies and cultured *in vitro* using low calcium concentrations to attain an immortalized human keratinocyte cell line known as $HaCaT_3$ (Deyrieux and Van Wilson, 2007). This was to overcome two major drawbacks of primary keratinocyte, i.e. (i) the isolated primary keratinocyte cells require supplementary growth factors to survive *in vitro* and (ii) once induced for differentiation they rapidly die and isolated primary keratinocyte cells do not allow long-term usage as their cell passage numbers are limited (Deyrieux and Van Wilson, 2007).

Keratinocyte cells were grown in a T-75 cell culture flask containing Eagles Minimum Essential Media (EMEM - Lonza, Walkersville, USA) supplemented with 10% FBS and 1% Penicillin/ Streptomycin (Lonza, Walkersville, USA). The cells were stored and maintained as the melanoma cancer cells except that the medium used was EMEM (Radestock *et al*., 2007).

3.1.3 Dermal Fibroblast Cells

Dermal fibroblasts were obtained from skin using a punch biopsy procedure described by Van Den Bogaerdt *et al*. (2002).

Ethical approval for the use of human skin biopsies for the isolation of primary fibroblast cells was obtained from Medunsa Research & Ethics Committee, University of Limpopo (Medunsa Campus) in June 2009. The Ethics Clearance number for this study is MREC/M/63/2009: IR.

Skin biopsies were collected from volunteers at the Medunsa academic hospital by performing a 3 mm punch biopsy on the volunteers. Punch biopsies were placed in 50 ml centrifuge tubes (Lasec, South Africa) containing transport medium. The transport medium contained 96 ml of Hank's Balanced Salt Solution (HBSS; Sigma, St.Louis, USA), 2ml Penicillin/ Streptomycin and 2 ml Gentomycin (Lonza, Walkersville, USA).

Punch biopsies were transported on ice to the CSIR, Biphotonics laboratory. At the biophotonics laboratory the fat was removed before placing pieces of the skin biopsies in 6-well tissue culture plates (Greiner Bio-One, Cellstar, Lasec, South Africa) containing a 1:10 dispase solution (Refer to Appendix). The preparation of dispase solution involved adding 1 ml of dispase (BD Biosciences, USA) into 9 ml of HBSS. The dispase solution was used for the separation of the dermis from the epidermis. Tissue culture plates containing the punch biopsies in dispase solution were incubated overnight at 37ºC in a 5% CO_2 incubator.

The next morning the dermis (thick layer) was separated from the epidermal layer (thin layer) with a sterile tweezer. The dermis was placed in another 6-well tissue culture plate. Each of the dermal pieces was washed three times with HBSS and 2 ml of 0.25% of Trypsin-EDTA solution (Lonza, Walkersville, USA) was added to dissociate the cells from the tissue. The cells were incubated at 37ºC in a 5% CO_2 incubator for 15 min, which included manually shaking the plates at 5 min intervals for 5 min. Cell dissociation was monitored under an inverted microscope until a large number of single cells were visible in the media.

Thereafter, Fibroblast Basal Medium (FGM-2® Bullet kit®, Clonetics®, Lonza, USA) supplemented with insulin, rhFGF-B, GA-1000 and FBS (FGM-2® SingleQuots®, Clonetics®, Lonza, USA) was added to each well to stop the reaction. The cell suspension was centrifuged once at 1000 rpm for 10 min using centrifuge (Sigma 2-16K, Germany). The supernatant was discarded and the pellet was dissolved in 1 ml of culture media before transferring to a T-25 cell culture flask (Greiner Bio-One, Cellstar, Lasec, South Africa) containing 5 ml of Fibroblast Basal Medium. The cells were incubated at 37°C in 5% CO_2 incubator. Culture medium was changed every second day until flask was 80% confluent. The cells were then trypsinized and sub-cultured in a T-75 tissue culture flask. The distinct cell morphology of the isolated cells was assessed under an inverted microscope (Axiovert 40 Zeiss, Germany) to ensure only fibroblast cells were being isolated.

The isolated primary skin dermal fibroblast cells were maintained aseptically in T-75 cell culture flasks containing as for Basal cells except the culture media was made up of Fibroblast Basal Medium with FBS and growth factors (e.g. insulin, rhFGF-B and GA-1000). Cells were not passaged more than 15 times.

3.2 Sub–Culturing or Cell Harvesting

Cells were grown to 80% confluency for harvesting or sub-culturing. When cells were 80% confluent the media was removed and cells were washed twice with 5 ml of HBSS before adding 4 ml of 0.25% of Trypsin-EDTA solution (Lonza, Walkersville, USA) to detach the cells from the bottom of the flask. Flasks were incubated for 5 min in a 5% CO_2 incubator. The detachment of cells was viewed under the inverted

microscope (Axiovert 40 Zeiss, Germany) before 400 µl of FBS was added together with 10 ml of culture media to inactivate the trypsin. Cells were centrifuged at 1000 rpm for 10 min. Supernatant was discarded and the pellet was dissolved in 5 ml of culture media. Thereafter, a cell count was conducted using the Trypan Blue exclusion test in order to determine the number of live or viable cells. Following the cell count, cells were either sub-cultured into two new T-75 flasks or cell pellet was harvested for the use in PDT experiments.

3.3 Cell Storage

Cells were harvested and the cell pellet was resuspended in 400 µl of FBS and cooled on ice. A cryoprotective medium (Lonza, Walkersville, USA) which contains Basal Eagles Medium with Hank's BSS and 15% Dimethylsulfoxide without L-Glutamine was used as cryoprotecting agent and also placed on ice. Equal aliquots (0.5 ml) of the cell suspension and the cryoprotective agent were added to a cryotube (Nunc, Japan). The tubes were stored overnight at -20°C and subsequently stored in a biofreezer (Thermo Electron Corporation, Labotec) at -80°C. For long-term storage cells were stored in 35 L Dewar flask (Taylor-Wharton, Harsco) containing liquid nitrogen.

3.4 Cell Enumeration using the Trypan Blue Exclusion Test

Principle

The numbers of cells were enumerated using the Trypan Blue Exclusion Test which stains dead cells blue and viable cells appear colourless because of their intact membranes which exclude the dye.

Protocol

The cell pellet was resuspended in 5 ml of culture medium and 200 µl of this cell solution was transferred into a separate centrifuge tube before adding 200 µl of 0.4% Trypan Blue (Sigma, St. Louise, USA). 50 µl of the resulting solution was used to fill the chamber on the Haemocytometer (Merck, Darmstadt, Germany) and cells were counted under an inverted microscope (Axiovert 40 Zeiss, Germany). Cell counting was conducted in duplicate. The total cell count in 5 ml of culture media was calculated using this formula:

Total Cell Count = (Cells counted / Number of squares x Dilution factor x 10^4) x 5ml

3.5 Dark Toxicity Assay

To determine any inherent toxicity of PS AlTSPc and ZnTSPc on the cell viability of melanoma, fibroblast and keratinocyte cells a modified protocol outlined by Jiménez-Banzo *et al*. (2008) was followed in which the effects of the PS were studied without any irradiation – dark toxicity.

3.6 Toxicity screening of aluminum tetrasulfonatedphthalocyanine (AlTSPc) and zinc tetrasulfonatedphthalocyanine (ZnTSPc)

3.6.1 Cell Culturing System

In this experiment the 80% confluent melanoma, keratinocyte or fibroblast cells were harvested and the cell density was adjusted to 30 000 cells/ml. These were seeded in 24-well tissue culture plates (Greiner Bio-One, Cellstar, Lasec, South Africa) and the cells were allowed to attach overnight at 37°C in 5% CO_2 incubator.

3.6.2 Drug Preparation

The PS agents aluminum tetrasulfonatedphthalocyanine (AlTSPc) and zinc tetrasulfonatedphthalocyanine (ZnTSPc) used in this study were synthesized and kindly provided by Professor Tebello Nyokong from Rhodes University (Department of Chemistry). The photosensitizers were stored at room temperature and used under light-restricted conditions. Stock solutions of ZnTSPc or AlTSPc (100 μg/ml) were further diluted with either RPMI-1640 medium without L-Glutamine, Fibroblast Basal or EMEM medium for treating melanoma, fibroblast or keratinocyte cells respectively to give concentrations of the PS in range of 10 μg/ml – 100 μg/ml.

3.6.3 Photosensitization of Cells

After 24 h of cell growth the culture medium from each well was removed and the cells were washed twice with Phosphate Buffered Saline (PBS: Sigma, St. Louise, USA). The PS solutions (1 ml) of each dilution were added to the cells. A negative control with no PS (medium only) was also included. Each concentration was tested in triplicate. The plates were wrapped in aluminium foil and incubated at 37°C in 5% CO_2 incubator for 2 h.

Laser scanning microscopic studies on the subcellular co-localization of phthalocyanines have been conducted by a colleague and this unpublished work clearly shows the uptake of these photosensitizers by the different cell lines.

3.6.4 Laser Irradiation of Cells with Continuous Wave (CW) Laser

After the two hour incubation period, cells as monolayer cultures were irradiated with a diode laser (continuous wave laser; CW) emitting a wavelength at 672 nm. The laser

set-up is shown in Figure 3.1. The output power of laser varied for each experiment and the beam was measured using a power meter (Nova, Ophir) as shown in Figure 3.2 A for each experiment. The output power was between 20 – 30 mW and the irradiation time (s) was calculated (using the calculations below) to deliver a light dose of 4.5 J/cm^2. A beam of 1 cm in diameter was used to deliver a light dose of 4.5 J/cm^2 to the cells as shown in Figure 3.2 B.

$$\text{Area of Light Beam} = \pi r^2$$

$$\text{Power Density} = \frac{\text{Output Power Measured with the Power Meter (mW)}}{\text{Area of Light Beam (cm}^2\text{)}}$$

$$= \text{Answer} \times 10^{-3}\ \text{Wcm}^{-2}$$

$$\text{Irradiation Time (s)} = \frac{\text{Dose Required (J/cm}^2\text{)}}{\text{Power Density (W/cm}^2\text{)}}$$

After irradiation the plates were incubated at 37°C in 5% CO_2 for 24 h before cell viability was measured using the CellTiter Blue® Viability Assay. Cells treated with the laser but without PS and cells treated with PS and not irradiated served as controls.

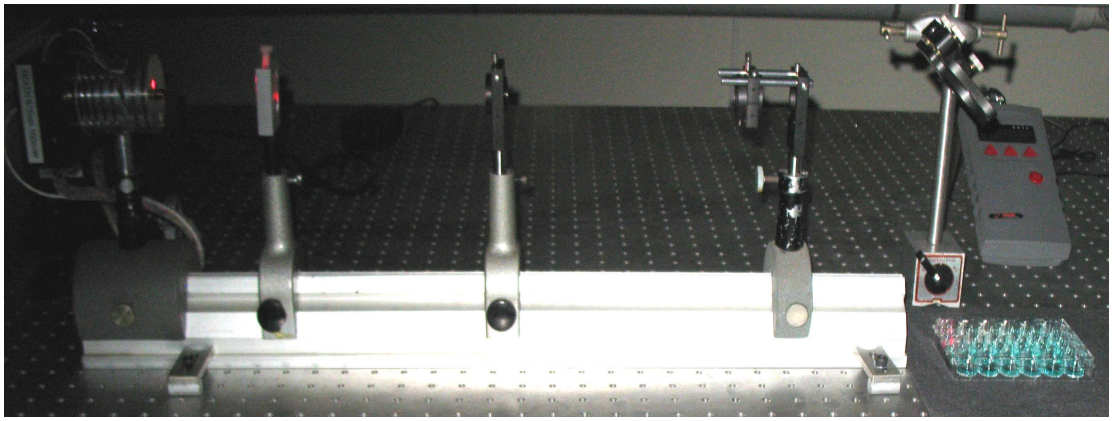

Figure 3.1 Set-up of the red light diode laser at a wavelength of 672 nm.

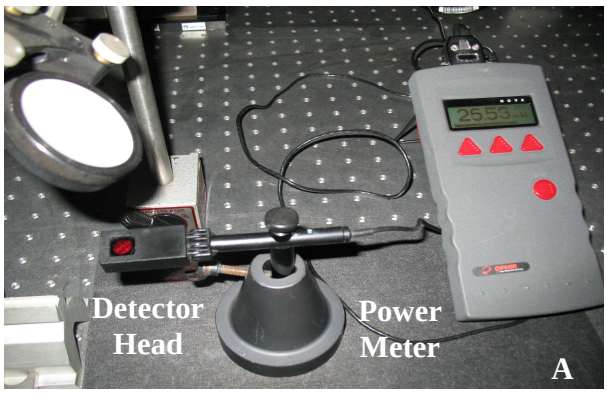

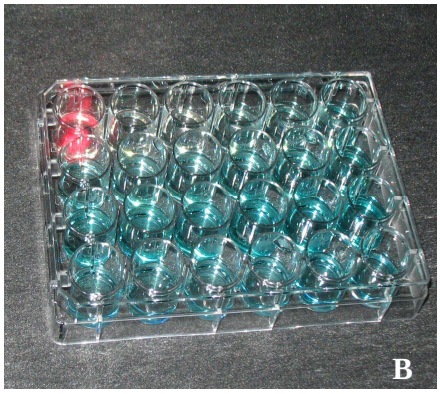

Figure 3.2 The detector head of the power meter measures the output power of a light beam with a diameter of 1 cm (A) which is used to deliver a light dose of 4.5 J/cm^2 to a monolayer of cells in each well and the diameter of each well is 1.57 cm (B).

3.7 Cell Viability Assay

Principle

The CellTiter-Blue is a fluorometric method for estimating the number of viable cells present in multiwall plates. It uses the indicator dye resazurin to measure the metabolic capacity of cells which is an indicator of cell viability. The metabolic active viable cells have the ability to reduce resazurin into resorufin. Resourfin is a fluorescent product. Non-viable cells rapidly lose metabolic capacity and cannot reduce the indicator dye thus do not generate a fluorescence signal. Resazurin is dark

blue in colour and has little fluorescence until reduced to resorufin. Resorufin is pink and highly fluorescence.

The procedure of this homogenous assay involves the direct addition of a single reagent known as CellTiter Blue® (Promega Corporation) to cells cultured in serum-supplemented medium. After an incubation period of 4 h, cell viability is measured using a fluorometer with appropriate emission and excitation filters. The fluorescence signal reading is proportional to the number of viable cells.

Protocol

The number of viable cells was measured using the CellTiter Blue® Reagent from Promega Corporation. 100 µl CellTiter Blue® reagent was added to each well containing 1 ml of fresh culture medium without FBS and plates were placed in 5% CO_2 for 4 h. Each plate was kept protected from the light by keeping each plate wrapped in aluminium foil. The fluorescence signal was measured using a plate reader (FLUOstar, Optima, BMG Labtech) with an excitation filter at 544 nm and an emission filter at 620 nm. The EC_{50} graph was constructed by calculating the cell viability (CV) percentage (%) using the equation below (Ketabchi *et al*., 1998; Jiménez-Banzo *et al*., 2008).

$$CV\ \% = \frac{(\text{Fluorescence Signal}_{\text{Sample}} - \text{Fluorescence Signal}_{\text{Media}})}{(\text{Fluorescence Signal}_{\text{Untreated Cells}} - \text{Fluorescence Signal}_{\text{Media}})} \times 100$$

The EC_{50} means the effective concentration and the subscript 50 means that the drug concentration was acutely lethal to kill 50% of the treated cells under controlled

laboratory conditions. This was used to determine the optimum active AlTSPc and ZnTSPc concentration that killed 50% or more of melanoma cancer cells.

The culture media without cells was used as a negative control and measured for each set of experiments for the detection of background fluorescence. The control of untreated cells was used for two main reasons. Firstly, the intended number of cells for each well was 30 000 cells/well. The inability to obtain a constant number of cells for all the experiments may result in inaccurate data. Therefore, control wells (untreated cells) were seeded out for every set of experiments performed. The control or untreated cells contain a concentration of 0 µg/ml of drug, which reveals the close consistency of cell numbers for every experiment. Secondly, it could be used to calculate the cell viability percentage as it offers an estimation of the amount cells present before treatment.

3.8 Determination of the Effective Light Dose

The EC_{50} concentrations of AlTSPc (40 µg/ml) or ZnTSPc (50 µg/ml) were prepared using RPMI-1640 medium, Fibroblast Basal or EMEM medium for treating melanoma, fibroblast or keratinocyte cells respectively. The optimum concentrations (AlTSPc: 40 µg/ml; ZnTSPc: 50 µg/ml) were extracted from the EC_{50} graph which was constructed using the phototoxicity experimental data. The cells were grown in 24-well plates and washed with PBS as described in section 3.6.3. After a 2 h exposure to the PS the cells (monolayer cultures) were irradiated with a diode laser emitting a wavelength of 672 nm. The output power of the continuous wave laser varied between 20 – 30 mW and the irradiation time was calculated to deliver light doses of 2.5 J/cm^2, 7.5 J/cm^2 or 10.5 J/cm^2. The output power of a beam of 1 cm in

diameter was measured using a power meter (Nova, Ophir). After irradiation the plates were placed at 37ºC in a 5% CO_2 incubator for 24 h before cell viability was measured using the CellTiter Blue® Viability Assay. The untreated cells with 0 µg/ml of the PS were not irradiated and another set of controls that were cells treated with the laser using the different light doses but without the PS.

3.9 Comparison of the Continuous Wave Laser and a Pulsed Laser

In these experiments the effect of the continuous wave (CW) laser (diode laser with a wavelength of 672 nm) was compared to the femtosecond laser (pulsed laser) on melanoma, fibroblast and keratinocyte cells. The cells were cultured in 24-well tissue culture plates and were exposed to AlTSPc (40 µg/ml) or ZnTSPc (50 µg/ml) for 2 h. After the two hour incubation, cells as monolayer cultures were irradiated with femtosecond laser (pulsed laser) emitting a wavelength of 672 nm. The output power of the pulsed laser varied between 2 – 12 mW and the irradiation time was calculated to deliver a light dose of 4.5 J/cm^2. The output power of a beam of 1 cm in diameter was measured using a power meter (Nova, Ophir)**.** After exposure to light the plates were incubated at 37°C in 5% CO_2 for 24 h before cell viability was measured using the CellTiter Blue® Viability Assay. The untreated cells with 0 µg/ml of the PS were not irradiated. Cells treated with the laser but without PS were used as another control. The untreated cells with 0 µg/ml of the PS were not irradiated and another set of controls that were cells treated with the pulsed laser using the treatment light dose of 4.5 J/cm^2 but without the PS.

3.10 Cytology of Melanoma Cells Exposed to AlTSPc and ZnTSPc

3.10.1 Light Microscopy

Light microscopic observations of the effect of the PS on melanoma cells were carried out using the inverted microscope (Axiovert 40 Zeiss, Germany).

In this study the 80% confluent melanoma cancer cells were harvested and counted with a haemocytometer using the methodology previously described in Section 3.3 and 3.4 respectively. Cells were seeded in 24-well cell culture plates at a density of approximately 20000 cells/ml per well. Cells were allowed to attach overnight at 37 ºC in a 5% CO_2 incubator.

Culture medium from each well was removed before washing twice with PBS. Cells in triplicate wells were photosensitized by adding 1ml of the stock solution of AlTSPc (40 μg/ml) or ZnTSPc (50 μg/ml). Untreated cells with 0 μg/ml of the PS was used as a control. Plates were wrapped in aluminium foil before incubating at 37ºC in a 5% CO_2 incubator for 2 h.

After the two hour incubation period, cells as monolayer cultures were irradiated with the diode laser emitting a wavelength of 672 nm. The measured output power of the laser was 16.20 mW and a light dose of 4.5 J/cm^2 was delivered in 3 min 38 sec to each well. After irradiation the plates were incubated at 37ºC in a 5% CO_2 incubator for 24 h. Changes in cell morphology were analysed by viewing plates under an inverted microscope and photographed (Ketabchi *et al*., 1998).

3.10.2 Ultrastructural Changes Using the Transmission Electron Microscopy (TEM)

The melanoma cancer cells were grown in T25 culture flask containing 5 ml of RPMI-1640 medium supplemented with 10% FBS, 1% Penicillin/ Streptomycin and 1% NEAA. The cells were grown at 37 ºC in a 5% CO_2 incubator. Cells were grown to 80% confluency in the flask before removal of culture media for the washing of cells with PBS. Cells were photosensitized by adding 5ml of the stock solution of AlTSPc (40 μg/ml) or ZnTSPc (50 μg/ml) into each flask accordingly. Untreated cells with 0 μg/ml of the PS were used as a control. Flasks were wrapped in aluminium foil before incubating at 37ºC in a 5% CO_2 incubator for 2 h.

After the two hour incubation period, cells as monolayer cultures were irradiated with diode laser emitting a wavelength of 672 nm. The output power of the continuous wave laser was 28.71 mW and the output power was measured using a power meter (Nova, Ophir). A beam of 1.5 cm in diameter was used to deliver light doses of 4.5 J/cm^2 in 4 min 38 sec. After irradiation the flasks were incubated at 37ºC in a 5% CO_2 incubator for 24 h.

Cells were processed for TEM and analysed at University of Pretoria in the laboratory for microscopy and microanalysis. Cells were detached from the flask with a cell scraper and centrifuged at 1000 rpm for 5 min. After centrifugation the supernatant was discarded.

Cellulose microcapillary tubes were placed in hexadecane before cutting it into small pieces with a blade and this was done under a microscope. A pipette was used to

transfer a drop of cells into the microcapillary tubes. Thereafter, the sides of each microcapillary tube were cut with a blunt blade to efficiently seal in the cells. For each sample the pieces of the microcapillary tubes were loaded onto gold coated chambers. Samples were immediately loaded on a high pressure freezing device (EMPACT 2, Leica). This device builds up pressure on the sample and then cools the sample by an independent mechanism. By introducing the sample into a small closed chamber which pressurized the sample to 210 MPa and then immediately cooling the specimen from the outside to -196ºC by using a double jet of liquid nitrogen (Studer, Humbel and Chiquet, 2008).

Samples were embedded in resin (Refer to Appendix for detailed a method) before thin sections were cut to be placed onto copper grids. The copper grids were stained with uranyl acetate for 10 min and after 10 min washed with double distilled water. Each copper grid was blotted onto paper before staining with lead citrate for 3 min following washing with double distilled water and blotting again. Post-stained copper grids were examined using a JEOL 2100F (200 kW) TEM and digital images were captured for examination (Ketabchi *et al*., 1998).

3.10.3 Apoptotic DNA Ladder Assay: Agarose Gel Electrophoresis

The melanoma cancer cells were grown in T25 cell culture flask containing 5 ml of RPMI-1640 medium supplemented with 10% FBS, 1% Penicillin/ Streptomycin and 1% NEAA. The cells were grown at 37ºC in a 5% CO_2 incubator. Cells were grown until 80% confluent before culture medium was removed from each flask for the washing of cells with PBS. Then cells were photosensitized by adding 5 ml of the stock solution of AlTSPc (40 μg/ml) or ZnTSPc (50 μg/ml) into each flask accordingly. Untreated cells with 0 μg/ml of the PS were used as a control. Flasks

were wrapped in aluminium foil before incubating at 37ºC in a 5% CO_2 incubator for 2 h.

After the two hour incubation, cells as monolayer cultures were irradiated with diode laser emitting a wavelength of 672 nm. The output power of the laser was 16.20 mW and measured using a power meter (Nova, Ophir). A beam of 1 cm in diameter was used to deliver light doses of 4.5 J/cm^2 in 3 min 38 sec. The flask was divided into sections and each section was given a light dose of 4.5 J/cm^2. This was done to ensure that majority of the cells in the flask were irradiated. After exposure to light the flasks were incubated at 37ºC in a 5% CO_2 incubator for 24 h.

The next day the DNA was isolated from the untreated and PDT treated samples using the Apoptotic DNA Ladder Kit (Roche Diagnostics, Germany). The kit contained one vial of lysis buffer, washing buffer, elution buffer, positive control and tubes. The kit also contained a detailed protocol which was followed.

Firstly, cells were prepared by removing the culture media from each flask. Thereafter, the adherent melanoma cells were washed in cold PBS before adding 4 ml of 0.25% of Trypsin-EDTA solution (Lonza, Walkersville, USA) for the detaching of the cells from the bottom of the flask. Flasks containing the trypsin were placed for 5 min in a 5% CO_2 incubator. Each flask was viewed under the inverted microscope to see if the cells had detached before adding 400 µl of FBS and 10 ml of culture media. Cells were centrifuged at 1200 rpm for 10 min at 10°C. The supernatant was discarded and the pellet was resuspended in 5 ml of cold PBS. Cells were centrifuged at 1200 rpm for 10 min at 10°C. The supernatant was discarded. The pellet from each

sample was resuspended in 200 µl of cold PBS. Then 200 µl of lysis buffer was added with mixing immediately. Samples were incubated for 10 min at room temperature. After incubation 100 µl of isopropanol was added to each of the samples and the positive control before shaking each sample with a vortex.

A filter tube and collection tube were combined. Samples and the positive control were pipetted into the upper reservoir before centrifugation with a Spectrafuge Mini Centrifuge Model C1301 (Labnet International Incorporation) for 1 min at 6000 rpm. The flowthrough in the collection tube was discarded and the filter tube with the used collection tube was combined. 500 µl washing buffer was added to the upper reservoir and samples were centrifuged for 1 min at 6000 rpm. This step was repeated to remove any existing residual wash buffer from the sample. The DNA from each sample was eluted by adding 200 µl of prewarmed elution buffer (70 ºC) and samples were centrifuged for 1 min at 6000 rpm. DNA was stored at – 20 ºC for analysis the next day.

The next day purified DNA samples were quantified using a Nanodrop ND – 1000 Spectrophotometer at Biosciences (CSIR, Pretoria). 15 µl of the purified DNA plus loading dye (6 x Orange Loading Dye ; Fermentas, UK) for each sample and the 15 µl of the positive control plus loading dye were loaded on a 1% agarose gel containing ethidium bromide (Refer to Appendix). Additionally, DNA Molecular Weight Marker (Gene Ruler^{TM} DNA, Mix Ready-To-Use; Fermentas, UK) was also loaded onto the gel. The gel was run in 1 x TBE (Tris – Borate EDTA, refer to Appendix) buffer at 75 V for 1.5 h (RT). After 1.5 h the gel was analysed under UV illumination for a visual

DNA laddering by placing the gel onto a UV box source. Gel was also photographed for further analysis.

3.11 Statistical Analysis

Data are presented as a mean ± standard deviation of at least three experiments. Statistical analysis was performed using ANOVA. A p-value less than 0.001 were considered statistically significant.

CHAPTER 4

RESULTS

4.1 Dark Toxicity Assay – Photosensitization of Cells with No Light Activation

The effect of the PS AlTSPc and ZnTSPc (10 µg/ml - 100 µg/ml) without light activation on the cell viability of melanoma cancer cells as well as healthy normal fibroblast and keratinocyte cells was measured by the fluorescence signal (544 nm/620 nm) and is presented in Figure 4.1 and Figure 4.2 respectively**.**

There is a significant difference between AlTSPc photosensitized melanoma cells and fibroblast cells, $p < 0.001$; melanoma cells and keratinocyte cells, $p < 0.001$. This is statistically the same for ZnTSPc photosensitized melanoma cells and fibroblast cells, $p < 0.001$; melanoma cells and keratinocyte cells, $p < 0.001$.

In melanoma cells a marked decrease in fluorescence signal was observed in the melanoma cells that were photosensitized with AlTSPc or ZnTSPc when compared to the fluorescence signal reading of the untreated melanoma cells (Figure 4.1 and Figure 4.2). This decrease in fluorescence signal indicates that there was a decrease in the cell viability. As the AlTSPc concentration increased the cell viability of melanoma cells proportionally decreased. A decrease in cell viability as the PS concentration increases is significantly larger in melanoma cells photosensitized with AlTSPc than ZnTSPc.

In both cases, negligible cytotoxicity was observed in fibroblast and keratinocyte cells photosensitized with either AlTSPc or ZnTSPc (Figure 4.1 and Figure 4.2).

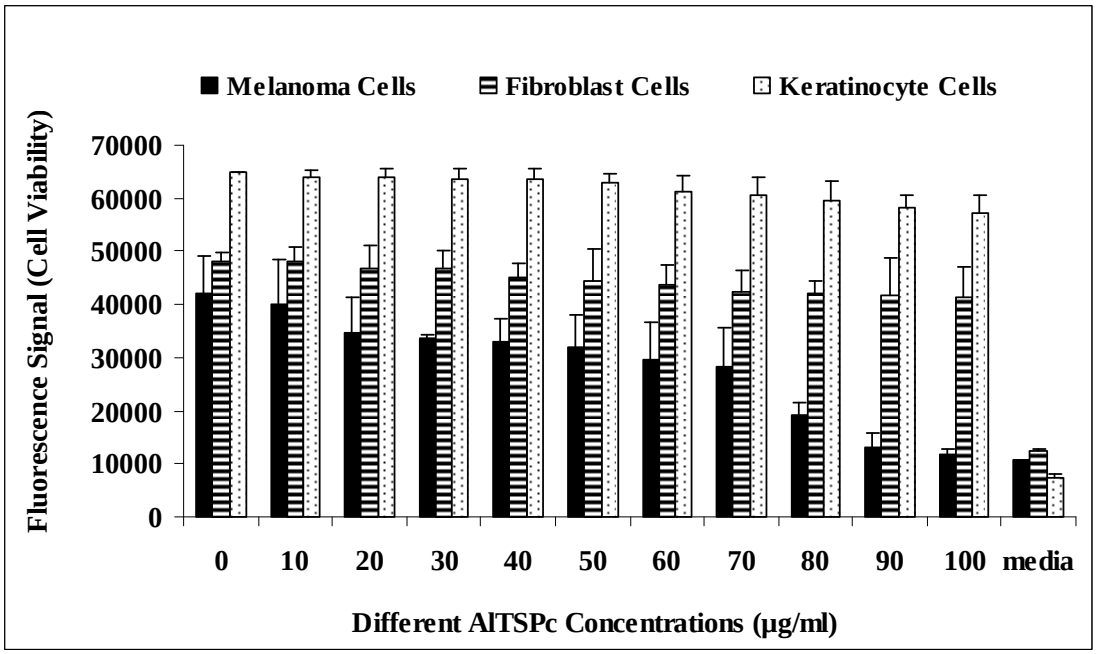

Figure 4.1 The effect of different AlTSPc concentrations in its inactive form on the cell viability of melanoma, fibroblast and keratinocyte cells were measured using the CellTiter-Blue® Viability Assay. 0 = untreated cells and fluorescence signal is proportional to the number of viable or live cells.

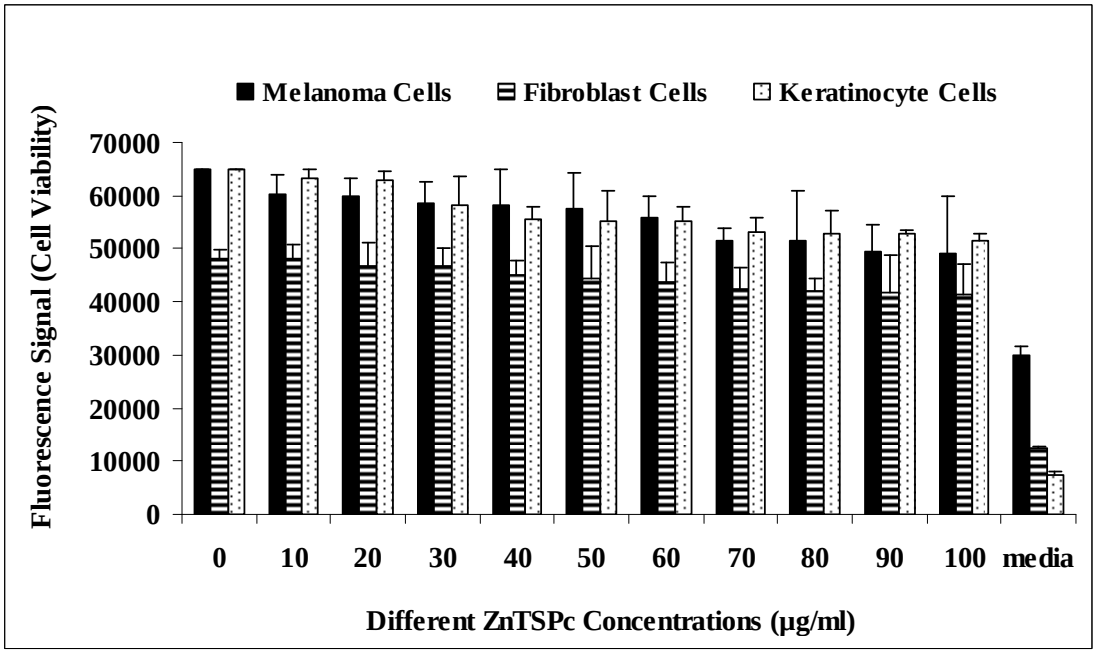

Figure 4.2 The effect of different ZnTSPc concentrations in its inactive form on the cell viability of melanoma, fibroblast and keratinocyte cells were measured using the CellTiter-Blue® Viability Assay. 0 = untreated cells and fluorescence signal is proportional to the number of viable or live cells.

In Figure 4.3 and Figure 4.4 the cell viability percentage for each cell line photosensitized with the different concentrations of AlTSPc and ZnTSPc was calculated using a negative control (media control containing no cells or PS) to determine background fluorescence that may be present in fluorescence signal readings and an untreated cell control.

Results indicated that melanoma cells photosensitized with an AlTSPc concentration of 100 µg/ml killed approximately 90% of the cells (Figure 4.3). Whereas, melanoma cells photosensitized with a ZnTSPc concentration of 100 µg/ml killed 50% of the cells (Figure 4.4). These results indicate that AlTSPc had significant cytotoxic effects on melanoma cancer cells, which were induced under experimental conditions in the absence of light activation.

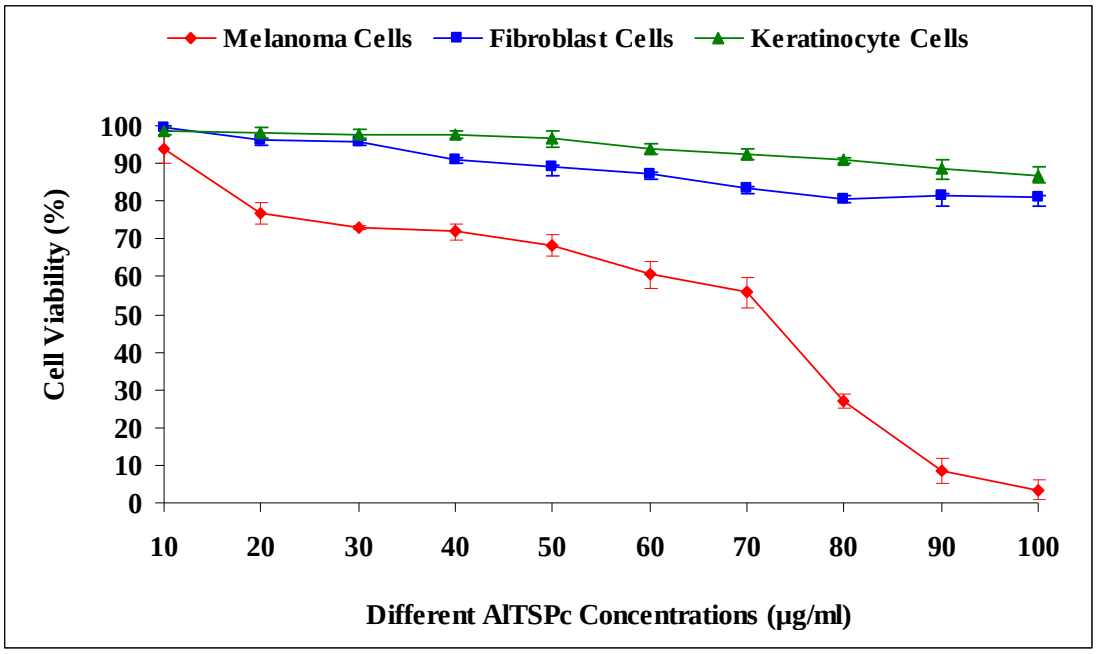

Figure 4.3 Changes in the cell viability (%) of melanoma, fibroblast and keratinocyte cells photosensitized with different concentrations of AlTSPc in the absence of laser activation. Cell viability was measured using the CellTiter-Blue® Viability Assay and original viability is expressed as a percentage of the untreated cells.

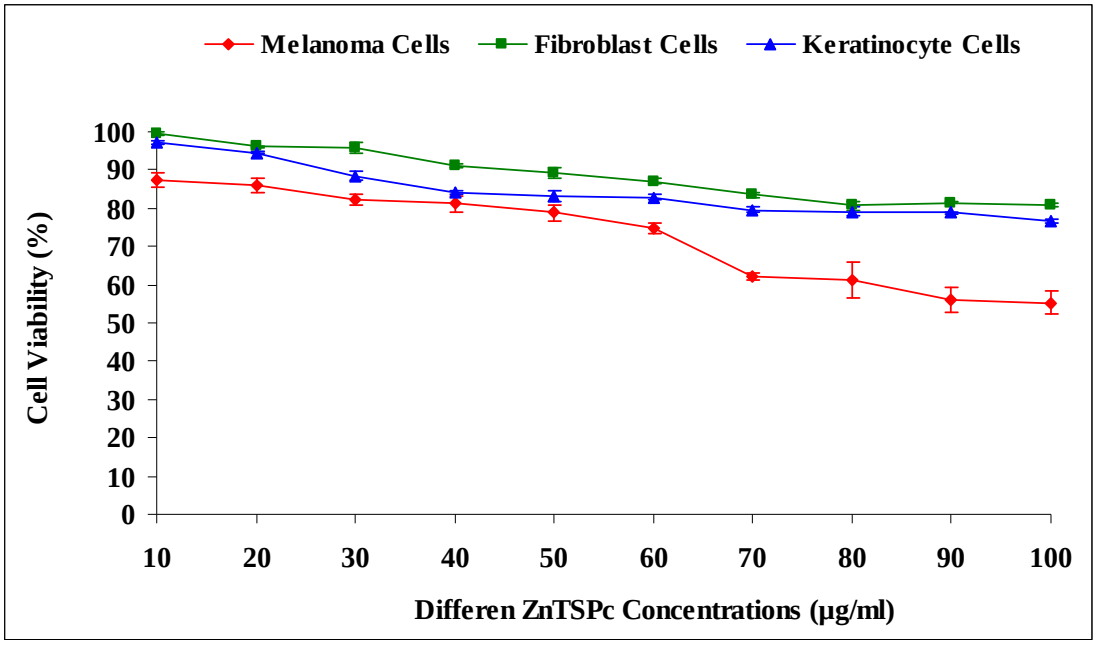

Figure 4.4 Changes in the cell viability (%) of melanoma, fibroblast and keratinocyte cells photosensitized with different concentrations of ZnTSPc in the absence of laser activation. Cell viability was measured using the CellTiter-Blue® Viability Assay and original viability is expressed as a percentage of the untreated cells.

Statistically, data on each cell line were grouped for each of the PS and the significance difference between AlTSPC and ZnTSPc is $p < 0.001$. AlTSPc is killing 25% more cells than ZnTSPc.

4.2 Toxicity Screening of AlTSPc and ZnTSPc

Each cell line (melanoma, fibroblast and keratinocyte cells) was photosensitized with different concentrations AlTSPc and ZnTSPc before irradiation with continuous wave laser (CW, diode laser) at a wavelength of 672 nm. Post-irradiated cells were incubated for 24 h before cell viability was measured. Results show that for each post-irradiated cell line, treated with different concentrations of AlTSPc and ZnTSPc there is a decrease in cell viability as the PS concentration increased. This decrease in cell

viability for each of the cell lines indicated that the laser was able to activate AlTSPc and ZnTSPc as illustrated in Figure 4.5 and Figure 4.6.

The cell viability of AlTSPc or ZnTSPc photosensitized melanoma cells after laser irradiated was significantly reduced when compared to the untreated melanoma cells (control). Cells (in the absence of photosensitizer) exposed to the laser are compared to untreated cells to rule out the possibility that the laser in the absence of the PS is responsible for the destruction of cells.

Results in this experiment indicate that AlTSPc or ZnTSPc with the laser can effectively kill melanoma cancer cells. It was observed that post-irradiated melanoma cells photosensitized with AlTSPc was more effective in decreasing the number of viable melanoma cells in comparison to ZnTSPc. A decrease in cell viability of healthy normal fibroblast and keratinocyte cells was also detected. This decrease in cell viability of melanoma, fibroblast and keratinocyte cells were concentration dependent because the cytotoxic effect of PDT increased as the concentrations of AlTSPc or ZnTSPc increased.

There is a significant differences between photoactivated AlTSPc melanoma cells and fibroblast cells, $p < 0.001$; melanoma cells and keratinocyte cells, $p < 0.001$. This is statistically the same for photoactivated ZnTSPc melanoma cells and fibroblast cells, $p < 0.001$; melanoma cells and keratinocyte cells, $p < 0.001$.

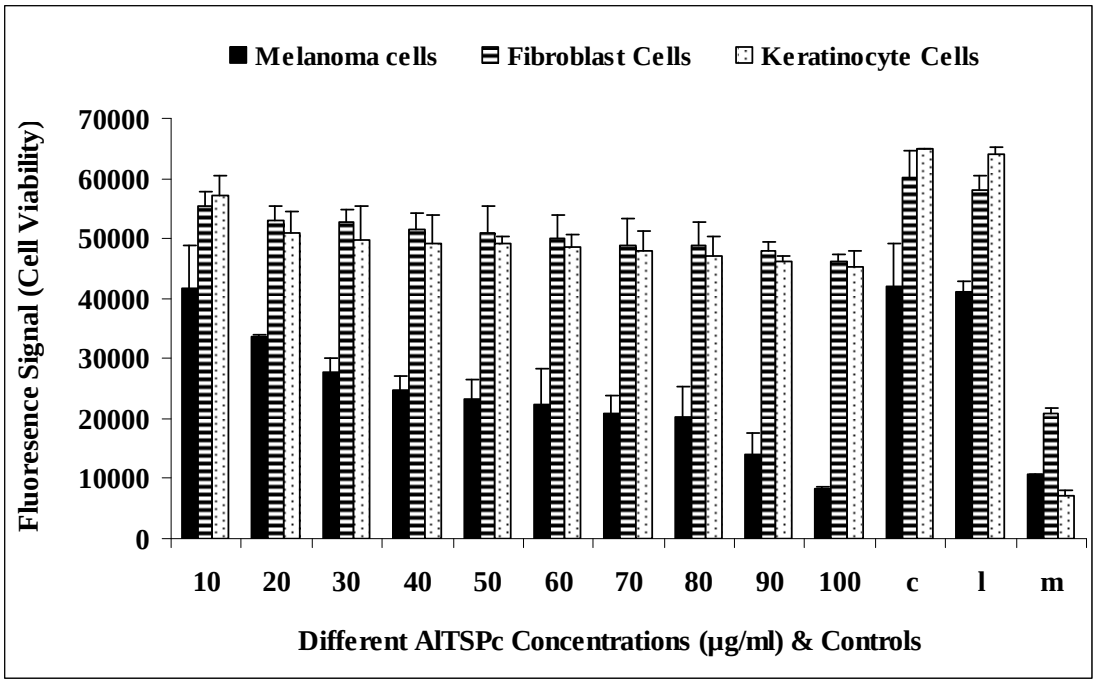

Figure 4.5 The effect of different AlTSPc concentrations activated with CW laser on the cell viability of different cell lines were measured using the CellTiter-Blue® viability Assay. c = untreated cells, l = laser irradiated cells without AlTSPc, m = culture media.

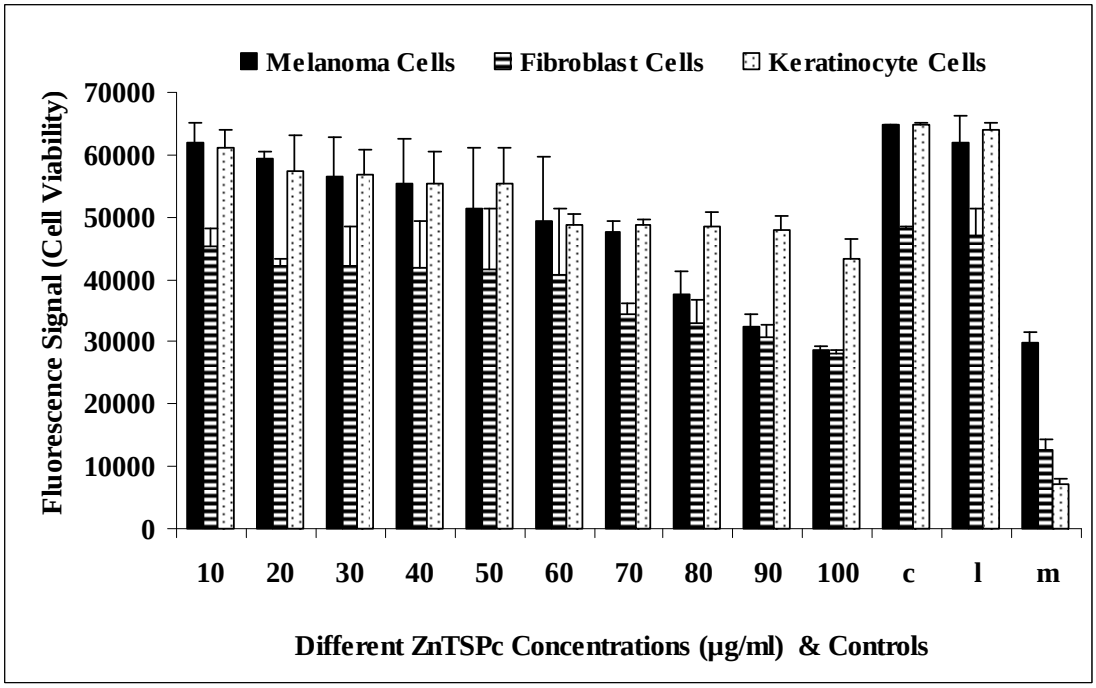

Figure 4.6 The effect of different ZnTSPc concentrations activated with CW laser on the cell viability of different cell lines were measured using the CellTiter-Blue® Viability Assay. c = untreated cells, l = laser irradiated cells without ZnTSPc, m = culture media.

The relationship between the different PS concentrations and the magnitude of measured change in cell viability is shown in Figure 4.7 and Figure 4.8. These also show the effective AlTSPc and ZnTSPc concentration that are acutely lethal to kill 50% of the treated cells under controlled laboratory conditions.

The graphs indicate there was higher survival rate for the healthy normal fibroblast and keratinocyte than melanoma cells for every drug concentration. At the AlTSPc concentrations of 30 µg/ml, 40 µg/ml and 100 µg/mlthere was respectively a 54.91%, 45.37% and -7.21% cell viability for the melanoma cells. This means that there are no surviving melanoma cancer cells at an AlTSPc concentration of 100 µg/ml. The corresponding viabilities for fibroblast cells treated with AlTSPc concentrations of 30 µg/ml, 40 µg/ml and 100 µg/ml were 80.79%, 78.17% and 64.15% respectively. The resulting cell viability for keratinocyte cells treated with 30 µg/ml, 40 µg/ml and 100 µg/ml were 73.24%, 72.89% and 66.14% accordingly. Therefore the EC_{50} value for AlTSPc was between 30 µg/ml and 40 µg/ml.

Using ZnTSPc at concentrations of 50 µg/ml, 60 µg/ml, 70 µg/ml and 100 µg/ml there was accordingly a 61.4%, 55.29%, 50.45% and 3.34% cell viability for melanoma cells. In the case of fibroblast treated with ZnTSPc concentrations of 50 µg/ml, 60 µg/ml, 70 µg/ml and 100 µg/ml there was accordingly a 81.32%, 79.32%, 61.57% and 43.46% cell viability. For keratinocyte cells treated with ZnTSPc at concentrations of 50 µg/ml, 60 µg/ml, 70 µg/ml and 100 µg/ml the cell viability was 83.32%, 72.23%, 72.05% and 62.68% respectively. The EC_{50} value for ZnTSPc was between 50 µg/ml and 60 µg/ml.

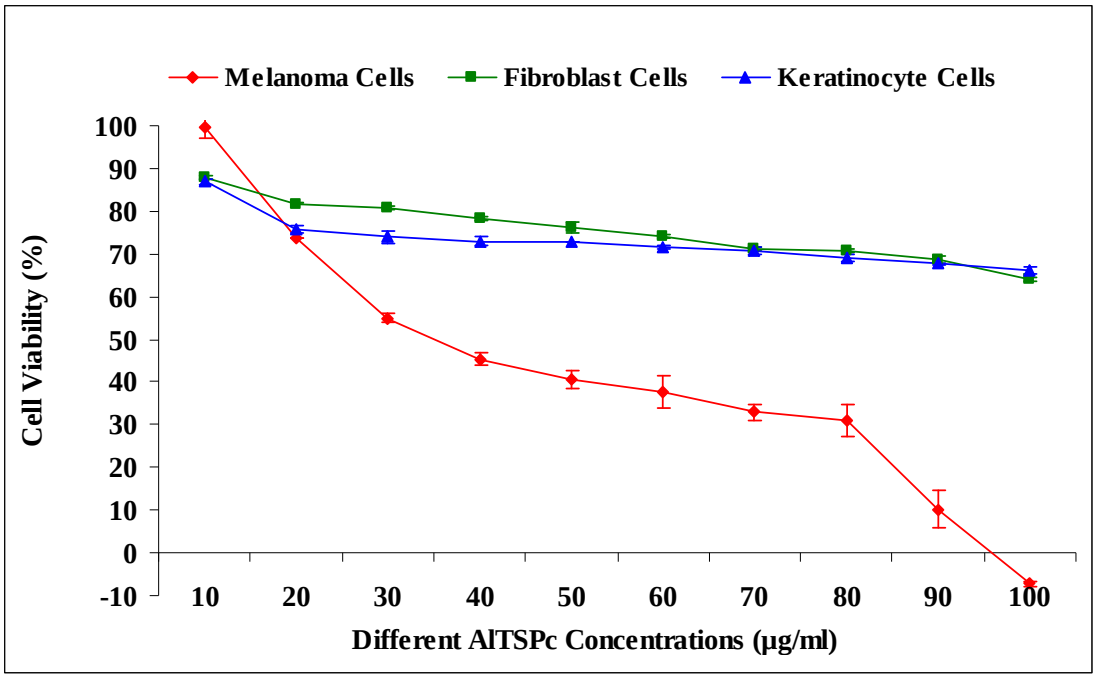

Figure 4.7 The dose-dependent effect of the different AlTSPc concentrations photoactivated with a light dose of 4.5 J/cm^2 from a CW laser on the cell viability of melanoma, fibroblast and keratinocyte cells.

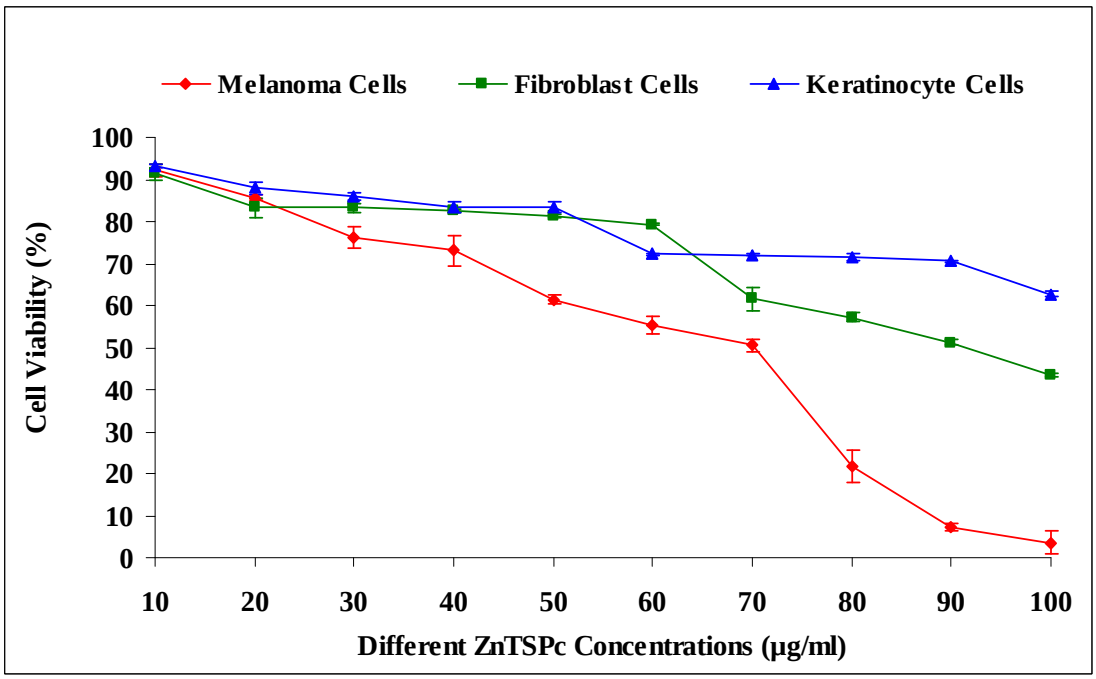

Figure 4.8 The dose-dependent effect of the different ZnTSPc concentrations photoactivated with a light dose of 4.5 J/cm^2 from a CW laser on the cell viability of melanoma, fibroblast and keratinocyte cells.

Statistically, when the data for each of the concentrations were grouped (area under the curve) significant differences ($p < 0.001$) were found between the viability of the melanoma cells, fibroblast cells and keratinocyte cells.

4.3 Light Dose Study

In Figure 4.9 and Figure 4.10 the effect of different light doses (2.5 J/cm^2, 4.5 J/cm^2, 7.5 J/cm^2 and 10.5 J/cm^2) delivered from a CW laser at a wavelength of 672 nm on the cell viability of melanoma cells photosensitized with AlTSPc and ZnTSPc respectively are shown. The greatest reduction in cell viability of melanoma cells was achieved by exposure of photosensitized melanoma cells to a light dose of 4.5 J/cm^2.

It was observed in Figure 4.11 and Figure 4.12 that the photoactivation of fibroblast cells treated with 40 µg/ml of AlTSPc and 50 µg/ml of ZnTSPc respectively, with a treatment dose of 2.5 J/cm^2 killed less healthy normal fibroblast cells in comparison to a light dose of 4.5 J/cm^2. Thereafter, the cell viability of fibroblast cells decreased as the treatment light dose increased. The cell viability of the post–irradiated keratinocyte cells indicated that a treatment light dose of 2.5 J/cm^2 killed more keratinocyte cells in comparison to a treatment light dose of 4.5 J/cm^2 as illustrated in Figure 4.13. A further decrease in cell viability with a treatment light dose of 7.5 J/cm^2 was observed. There was a slight increase in cell viability with a treatment light dose of 10.5 J/cm^2 in comparison to treatment light doses of 4.5 J/cm^2 and 7.5 J/cm^2.

In Figure 4.14 results demonstrated that keratinocyte photosensitized with 50 µg/ml of ZnTSPc and irradiated with a light dose of 4.5 J/cm^2 had the highest cell viability in comparison to treatment light doses of 2.5 J/cm^2, 7.5 J/cm^2 and 10.5 J/cm^2.

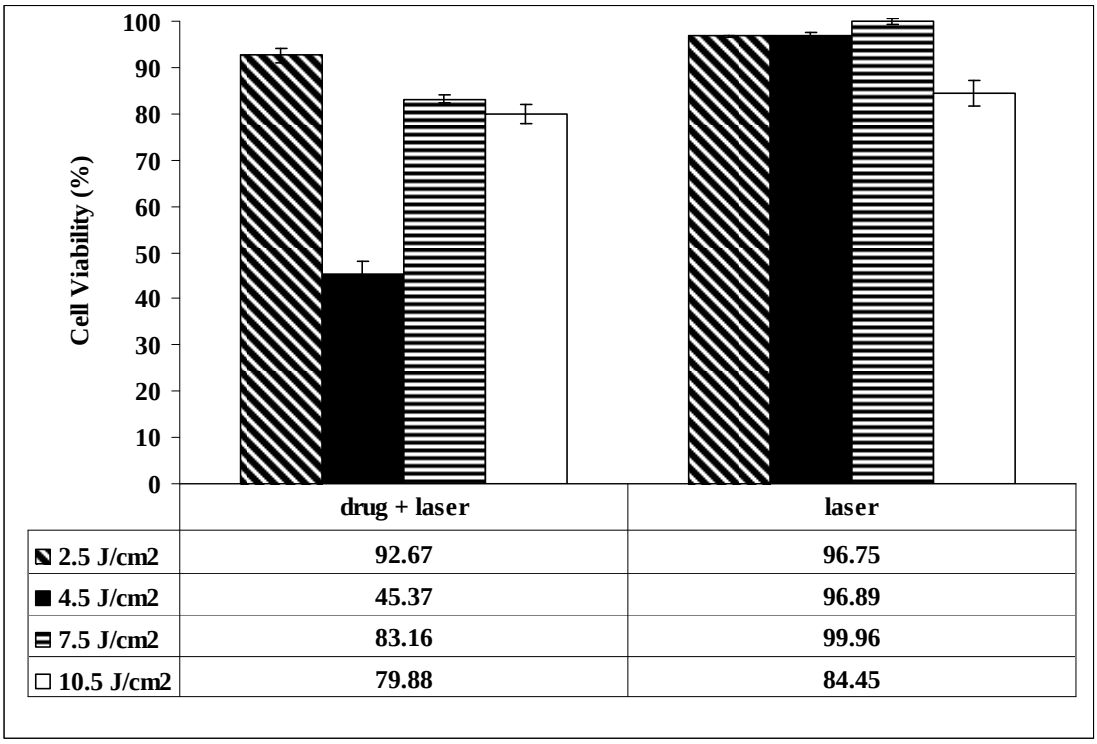

	drug + laser	laser
2.5 J/cm2	92.67	96.75
4.5 J/cm2	45.37	96.89
7.5 J/cm2	83.16	99.96
10.5 J/cm2	79.88	84.45

Figure 4.9 The effect of varying treatment light doses (J/cm^2) on the cell viability (%) of melanoma cells photosensitized with AlTSPc concentration of 40 µg/ml.

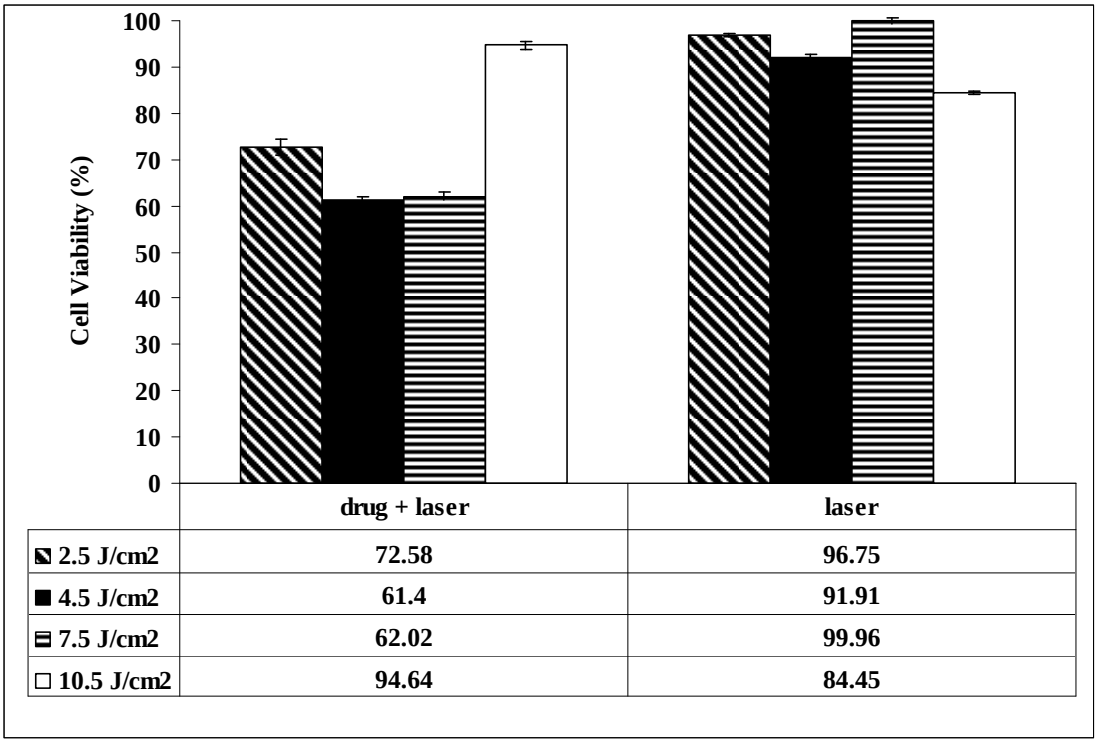

	drug + laser	laser
2.5 J/cm2	72.58	96.75
4.5 J/cm2	61.4	91.91
7.5 J/cm2	62.02	99.96
10.5 J/cm2	94.64	84.45

Figure 4.10 The effect of varying treatment light doses (J/cm^2) on the cell viability (%) of melanoma cells photosensitized with ZnTSPc concentration of 50 µg/ml.

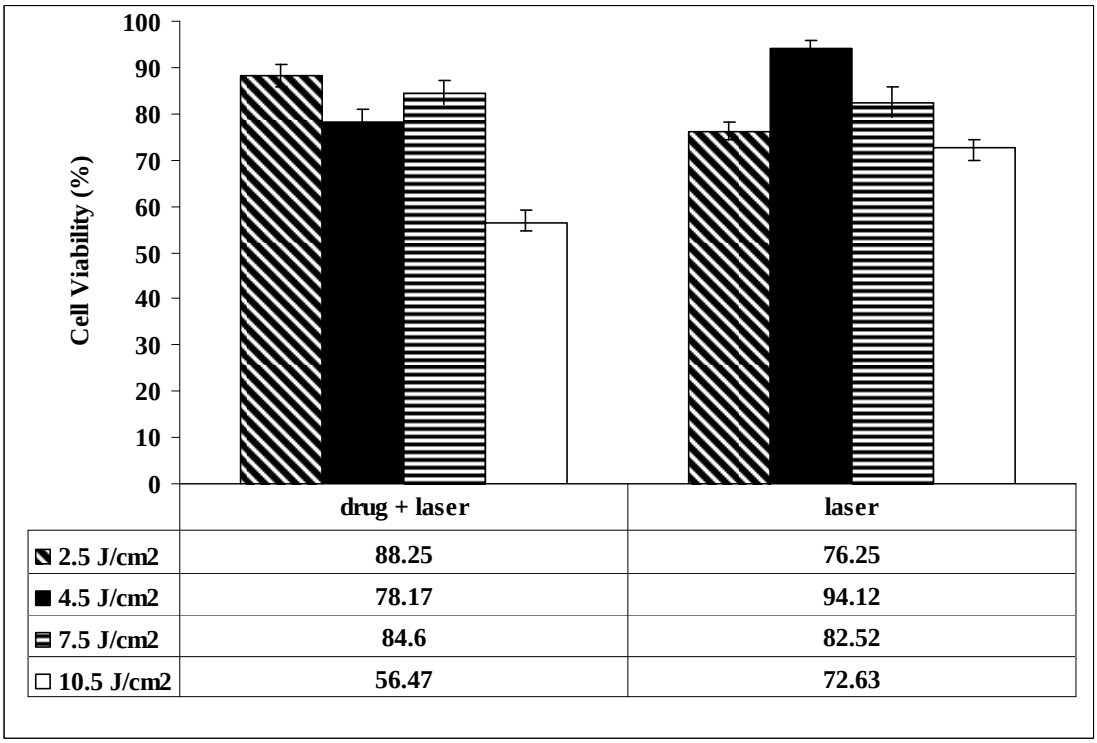

	drug + laser	laser
2.5 J/cm2	88.25	76.25
4.5 J/cm2	78.17	94.12
7.5 J/cm2	84.6	82.52
10.5 J/cm2	56.47	72.63

Figure 4.11 The effect of varying treatment light doses (J/cm^2) on the cell viability (%) of fibroblast cells photosensitized with AlTSPc concentration of 40 µg/ml.

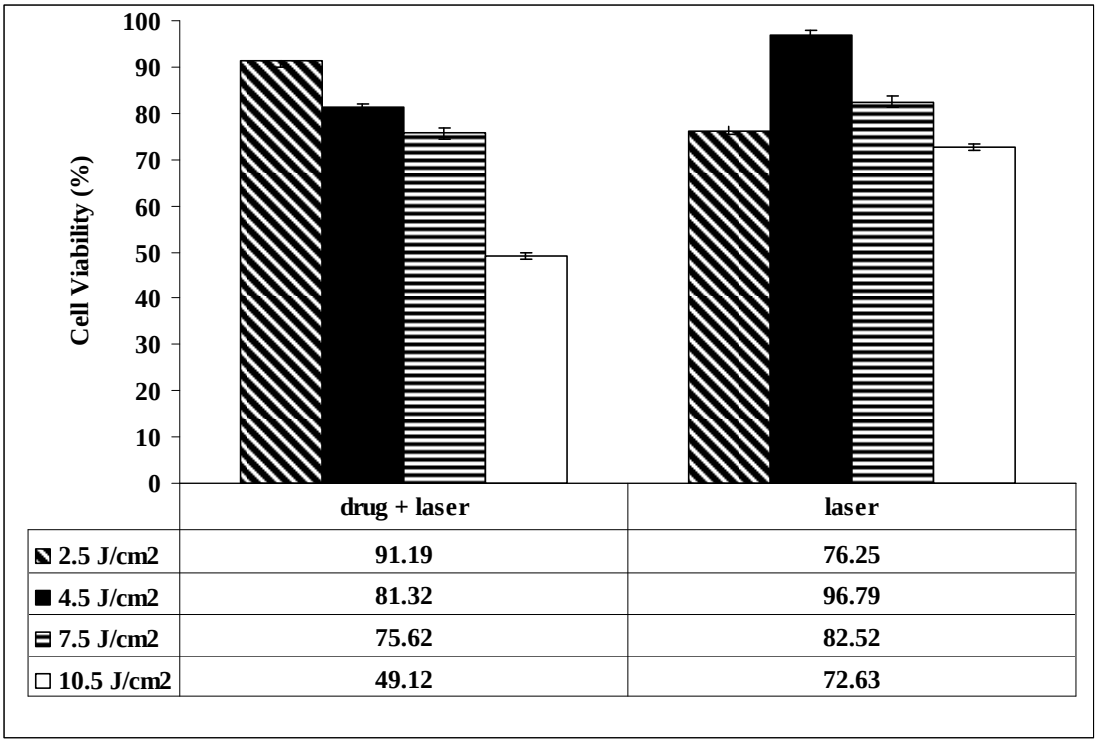

	drug + laser	laser
2.5 J/cm2	91.19	76.25
4.5 J/cm2	81.32	96.79
7.5 J/cm2	75.62	82.52
10.5 J/cm2	49.12	72.63

Figure 4.12 The effect of varying treatment light doses (J/cm^2) on the cell viability (%) of fibroblast cells photosensitized with ZnTSPc concentration of 50 µg/ml.

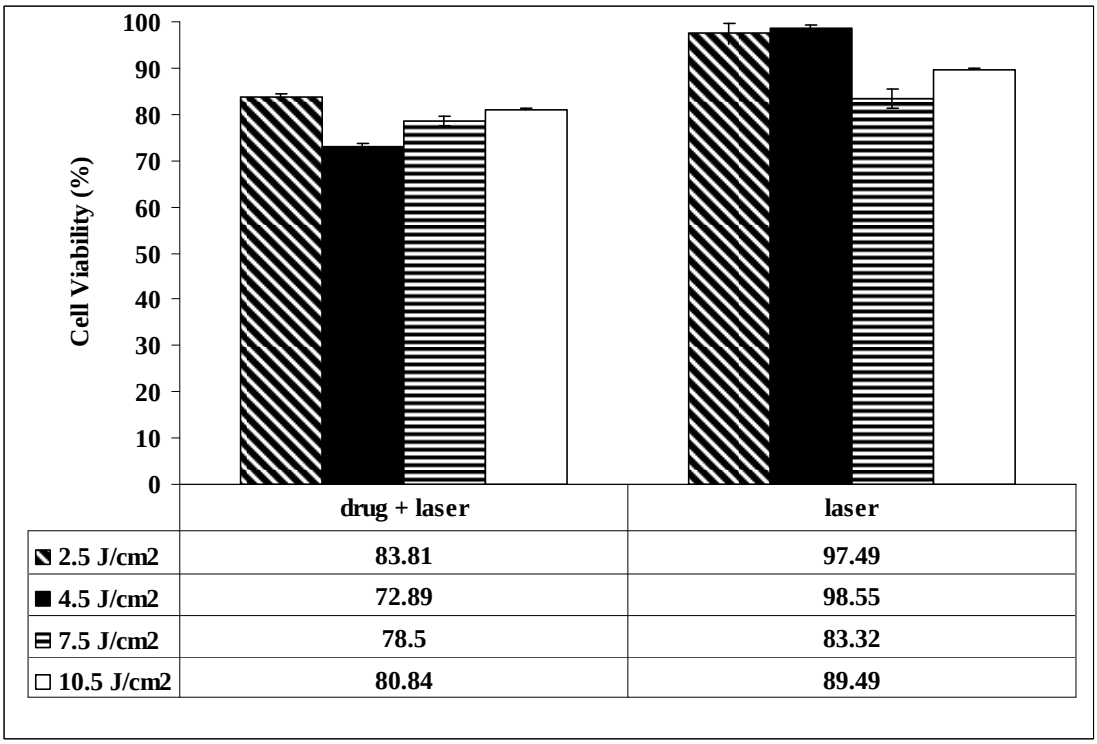

	drug + laser	laser
2.5 J/cm2	83.81	97.49
4.5 J/cm2	72.89	98.55
7.5 J/cm2	78.5	83.32
10.5 J/cm2	80.84	89.49

Figure 4.13 The effect of varying treatment light doses (J/cm^2) on the cell viability (%) of keratinocyte cells photosensitized with AlTSPc concentration of 40 µg/ml.

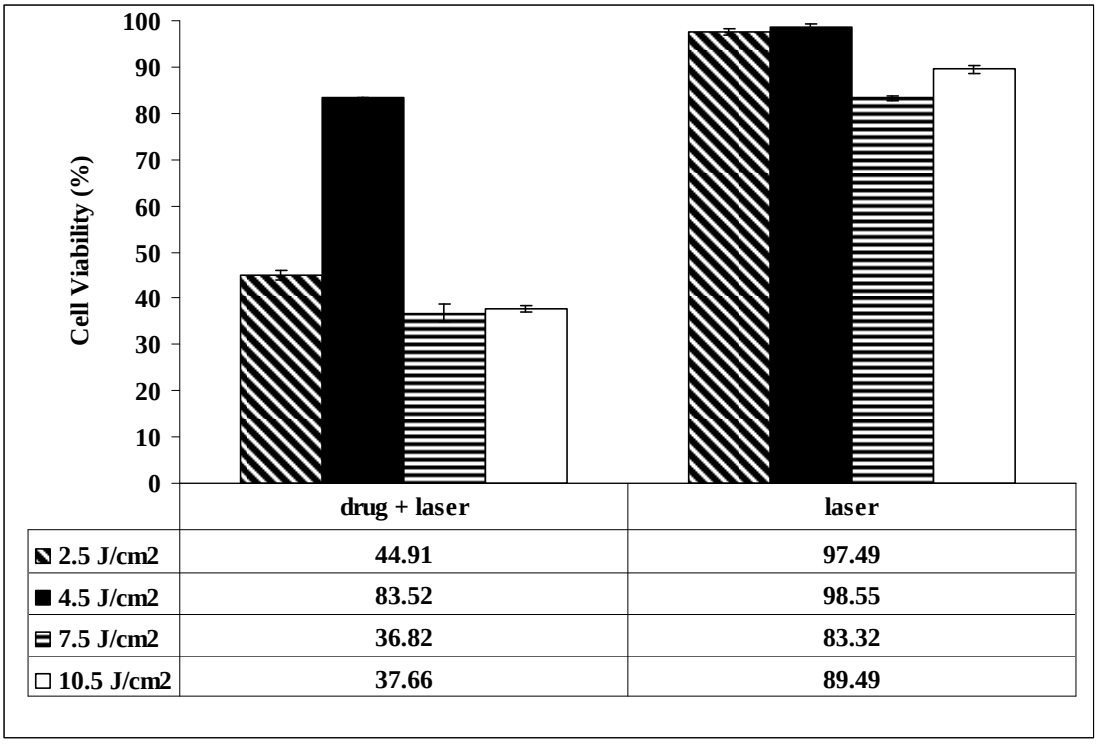

	drug + laser	laser
2.5 J/cm2	44.91	97.49
4.5 J/cm2	83.52	98.55
7.5 J/cm2	36.82	83.32
10.5 J/cm2	37.66	89.49

Figure 4.14 The effect of varying treatment light doses (J/cm^2) on the cell viability (%) of keratinocyte cells photosensitized with ZnTSPc concentration of 50 µg/ml.

Therefore, cell viability studies above have shown that the optimum cytotoxic effect observed in melanoma cancer cells was obtained in the presence of laser light dose of 4.5 J/cm^2 and at the AlTSPc concentration of 40 µg/ml, and ZnTSPc at the concentration of 50 µg/ml. These combinations of photosensitizer concentrations and the related light dose of 4.5 J/cm^2 is not lethal for the healthy normal fibroblast and keratinocyte cells.

4.4 Light Treatment with a Pulsed Laser

Figure 4.15 and Figure 4.16 compares the use of the continuous wave (CW) laser source (Diode laser) and pulsed laser (Femtosecond laser) source for the killing of melanoma cancer cells photosensitized with AlTSPc and ZnTSPc respectively. Also, the influence of the laser sources (CW and pulsed) on the cytotoxic effects of healthy normal fibroblast and keratinocyte were investigated and results are presented in

Figure 4.15 and Figure 4.16. The post-irradiated cells were incubated for 24 h before cell viability was measured by CellTiter-Blue® Cell Viability Assay, and the results were used to calculate the percentage cell viability for each of the different cell lines.

The percentage cell viability values of melanoma cells indicated that irradiation by CW laser was more effective in killing the melanoma cancer cells than the pulsed laser for both photosensitizers. The viability of healthy normal fibroblast and keratinocyte cells irradiated with the pulsed laser was also significantly reduced for both photosensitizers. Indeed, the cytotoxic efficacy of the CW laser for this study was better than that of the pulsed laser in killing the melanoma cancer cells at a light dose of 4.5 J/cm^2.

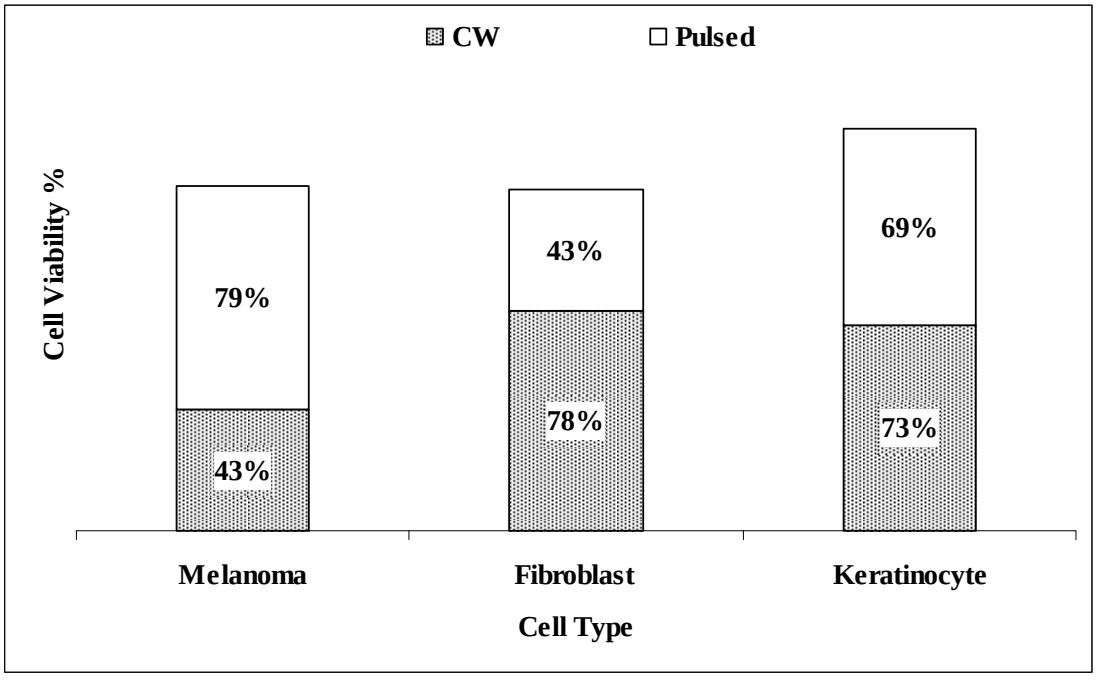

Figure 4.15 The cell viability of melanoma, fibroblast and keratinocyte cells after photosensitization with 40 µg/ml of AlTSPc and photoactivation with a light dose of 4.5 J/cm^2 from a CW or a pulsed laser source.

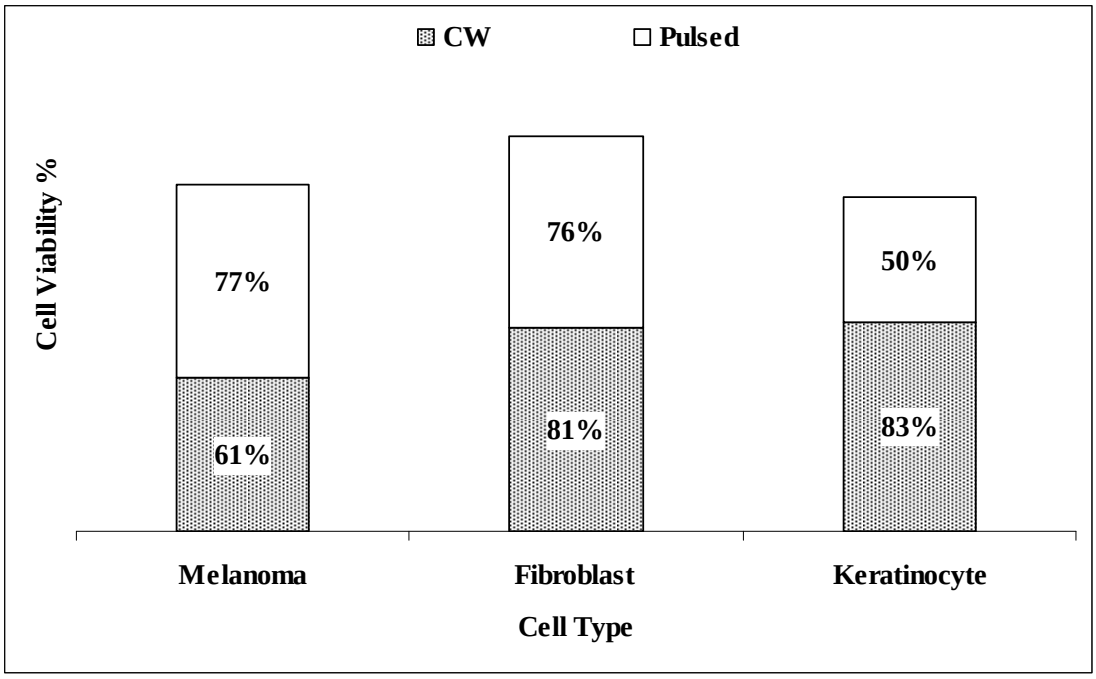

Figure 4.16 The cell viability of melanoma, fibroblast and keratinocyte cells after photosensitization with 50 µg/ml of ZnTSPc and photoactivation with a light dose of 4.5 J/cm^2 from a CW or a pulsed laser source.

4.5 Cell Death Mechanism

4.5.1 Inverted Microscopy

The change in cell morphology as a result of PDT mediated cell death was observed using an inverted microscope and is shown in Figure 17 – 19. There were observable morphological changes between untreated melanoma cells and treated melanoma cells. The treated cells showed features of apoptosis which was not prominent in untreated melanoma cells. Apoptosis features like the occurrence of scattered single cells indicate that treated melanoma cells lost contact with and detached from neighbouring cells due to cell shrinkage as visible in Figure 4.18A and Figure 4.19A. In Figure 4.18B and Figure 4.19B blebbing of melanoma cells photosensitized with higher concentration of PS is noticed. Also, the blebbing continued until finally cells entered the condensation stage which is characterized by the formation of apoptotic bodies. Thus, the evidence of cell shrinkage, blebbing and formation of apoptotic

bodies confirms that PDT mediated by photosensitization of AlTSPc and ZnTSPc can effectively kill melanoma cells via the apoptosis mechanism.

Figure 4.17 Untreated melanoma cancer cells (Magnification = 20 x 0.30 Phase 1).

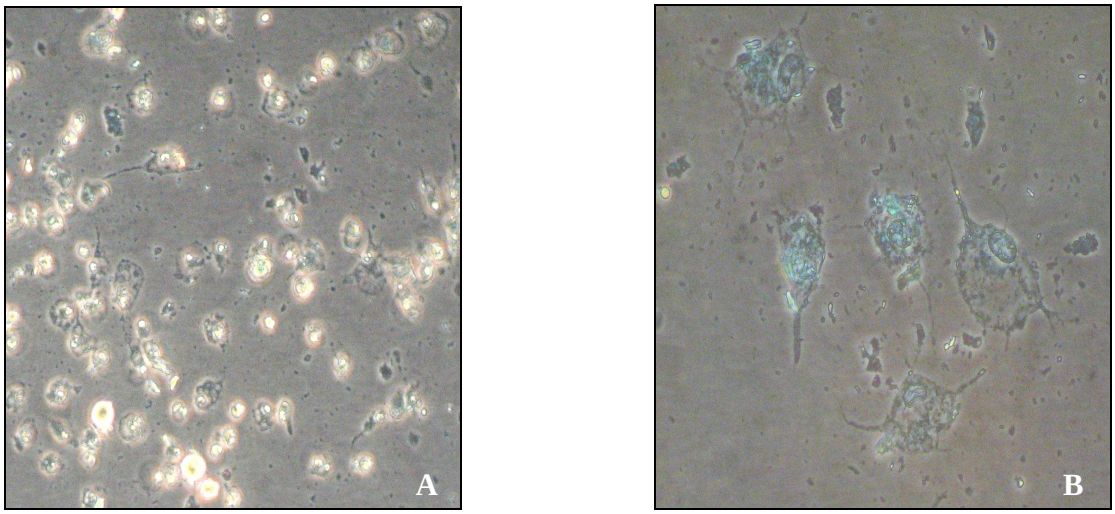

Figure 4.18 Micrographs showing the cell morphology of post–irradiated melanoma cancer cells treated with 40 µg/ml of AlTSPc (A) and 100 µg/ml of AlTSPc (B); (Magnification = 20 x 0.30 Phase 1).

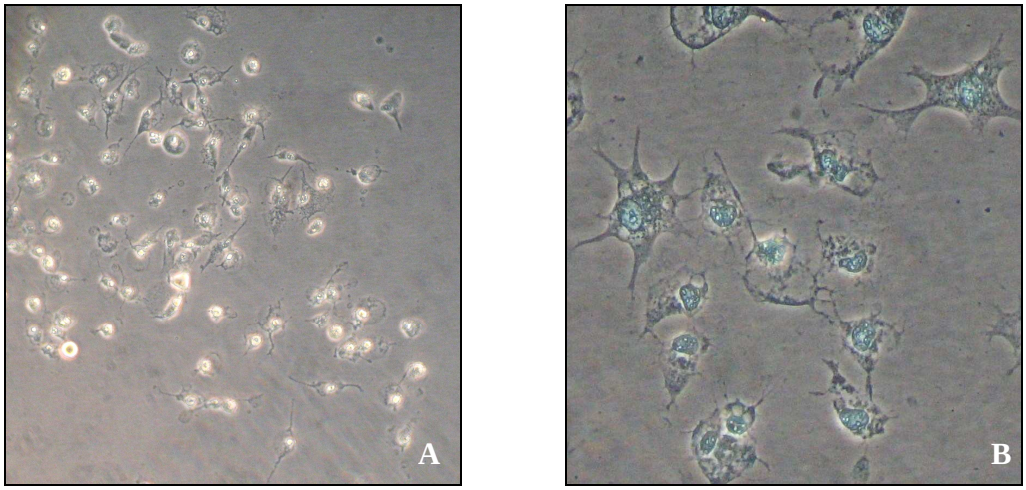

Figure 4.19 Micrographs showing the cell morphology of post-irradiated melanoma cancer cells treated with 50 µg/ml of ZnTSPc (A) and 100 µg/ml of ZnTSPc (B); (Magnification = 20 x 0.30 Phase 1).

4.5.2 Transmission Electron Microscopy (TEM)

The control cell or untreated melanoma cell in Figure 4.20 presents an intact plasma membrane and nucleus. An increased nuclear:cytoplasmic ratio was observed on melanoma cells that were phototreated with AlTSPc as illustrated in Figure 4.21 and Figure 4.22 in comparison to untreated melanoma cells. Specific morphological changes such as cell shrinkage, surface blebbing (protrusions from the plasma membrane), cytoplasm vacuoles containing digested materials, leakage of the nuclear chromatin and condensation of the chromatin (electron-dense black parts in the nucleus and at the nuclear periphery) were also seen in Figure 4.21. Also, Figure 4.21 illustrates the process of pyknosis which is the irreversible condensation of chromatin in the nucleus of a cell undergoing apoptosis. It is followed by karyorrhexis or DNA fragmentation of the nucleus as observed in Figure 4.22. After karyorrhexis the nucleus usually dissolves into apoptotic bodies with complete dissolution of the chromatin matter of the dying cell as seen in Figure 4.23.

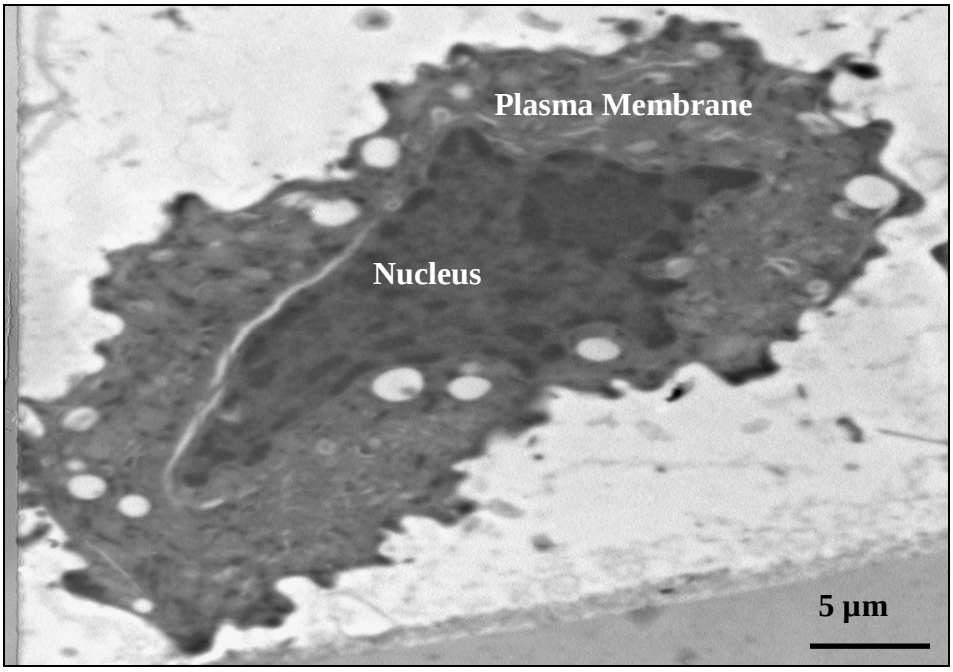

Figure 4.20 A TEM micrograph showing the normal morphology of a melanoma cell (untreated) at 12 000X magnification. Melanoma cell is intact with an intact nucleus bounded by a nuclear membrane and intact plasma membrane.

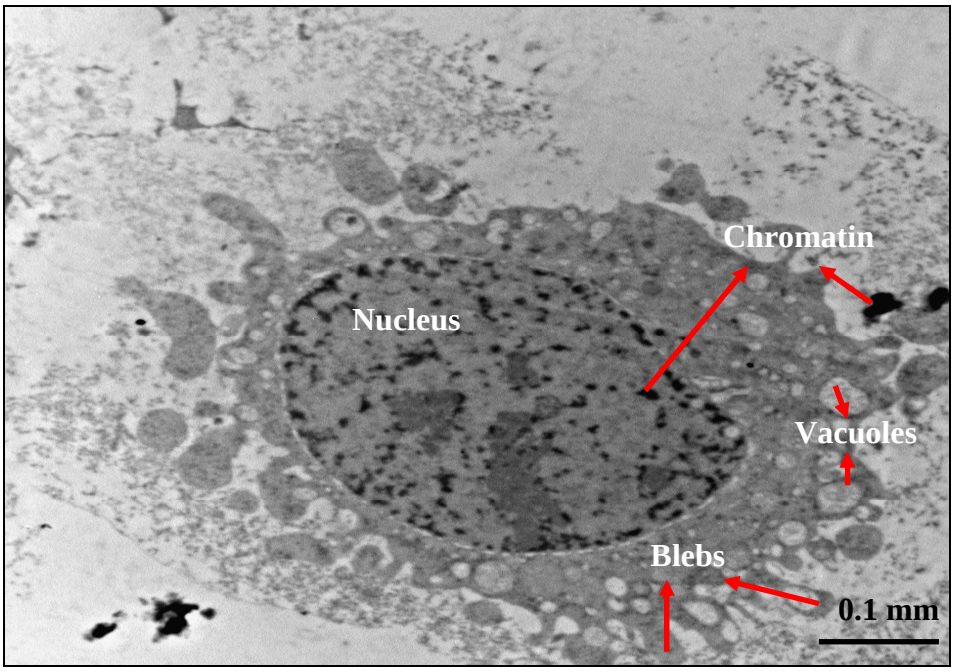

Figure 4.21 A TEM micrograph of a melanoma cell exposed to photoactivated AlTSPc (40 µg/ml) showing the apoptotic features of a dying cell such as cell shrinkage, blebbing and nucleus condensation (pyknosis) at 6 000X magnification.

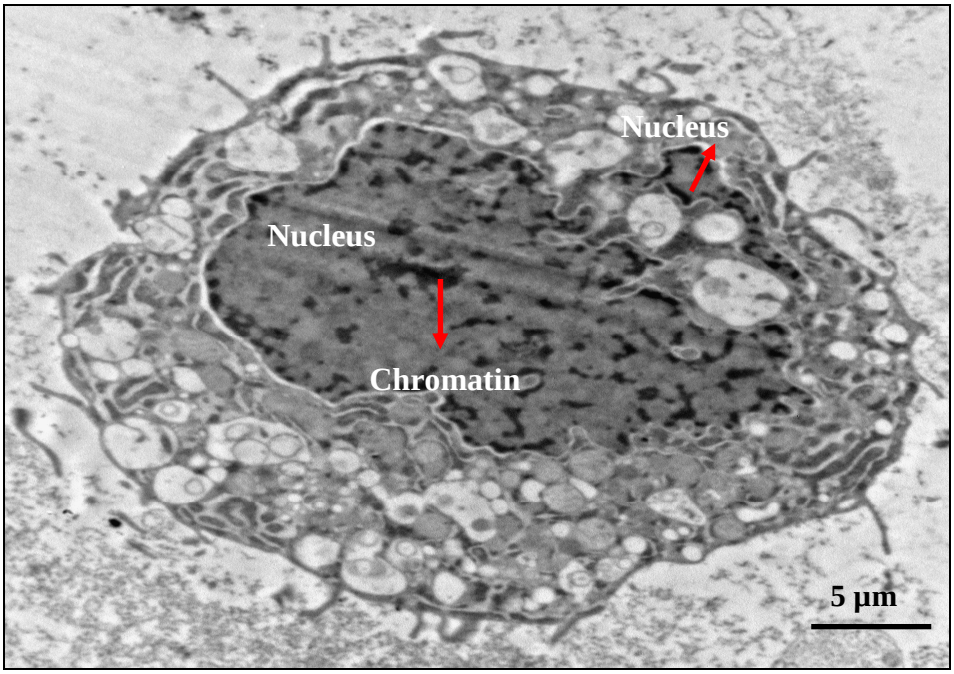

Figure 4.22 A TEM micrograph of a melanoma cell exposed to photoactivated AlTSPc (40 µg/ml) showing nuclear fragmentation, commonly known as karyorrhexis at 8 000X magnification.

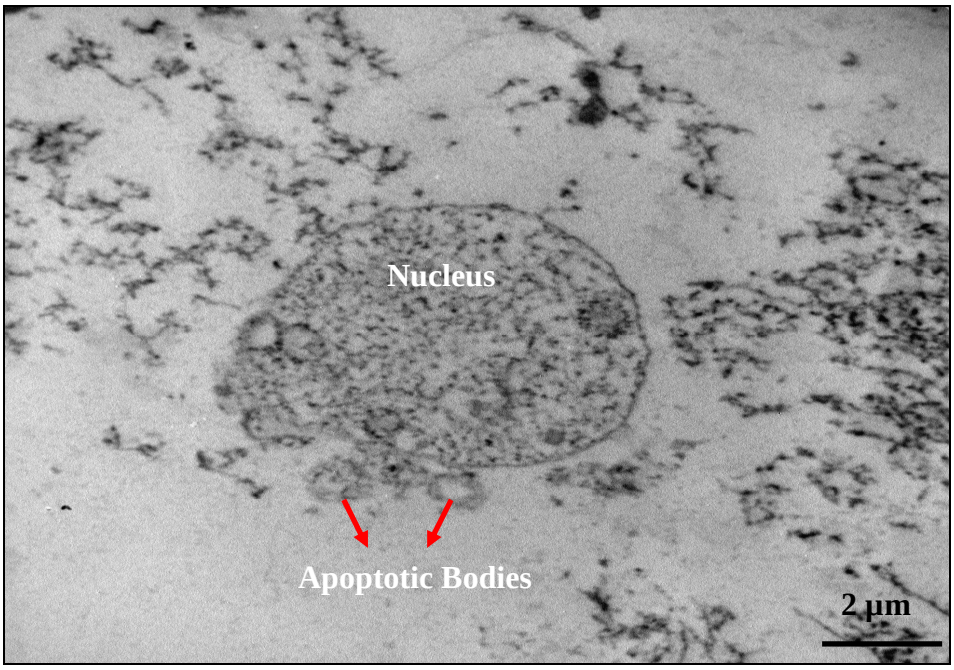

Figure 4.23 A TEM micrograph of a melanoma cell exposed to photoactivated AlTSPc (40 µg/ml) showing the splitting of an apoptotic nucleus into several apoptotic bodies and at the same time a residual nucleus can be seen without chromatin at 25 000X magnification.

In Figure 4.24 the super aggregation and condensation of a nucleus is shown of an apoptotic melanoma cell that was treated with ZnTSPc and laser. Also, at this stage of apoptosis the lack of a nuclear envelope is detected. Figure 4.25 shows lumpy, incomplete chromatin condensation.

The ultrastructural changes of a dying cell by the induction of apoptosis are evident in the melanoma cancer cells treated with AlTSPc or ZnTSPc followed by laser irradiation. Also, the treated melanoma cells with AlTSPc and ZnTSPc depicted the various stages of apoptosis.

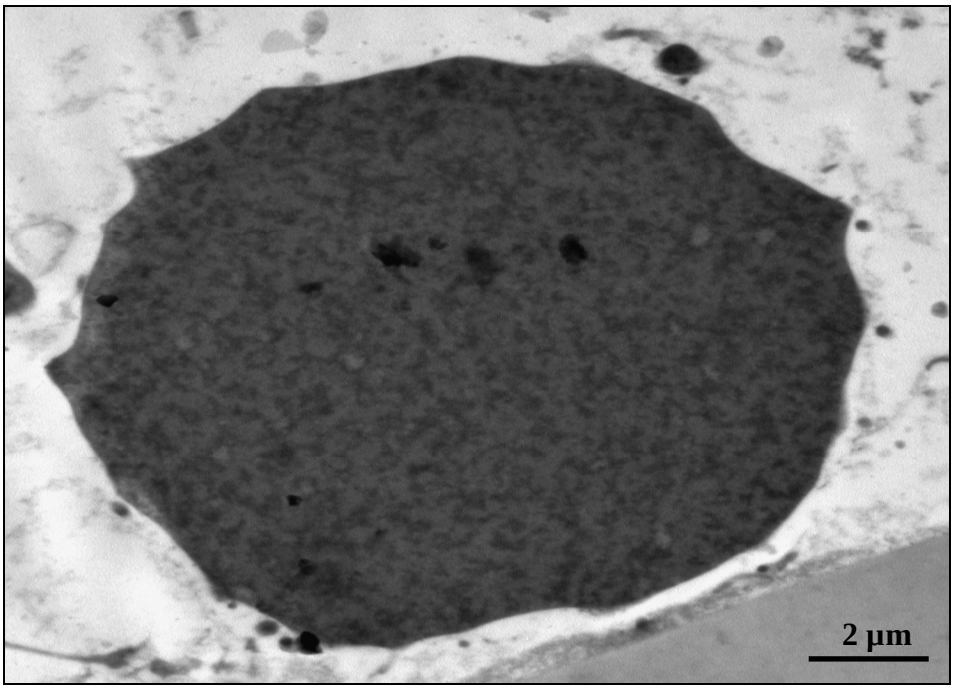

Figure 4.24 A TEM micrograph of a melanoma cell exposed to photoactivated ZnTSPc (50 µg/ml) showing chromatin aggregation at 20 000X magnification.

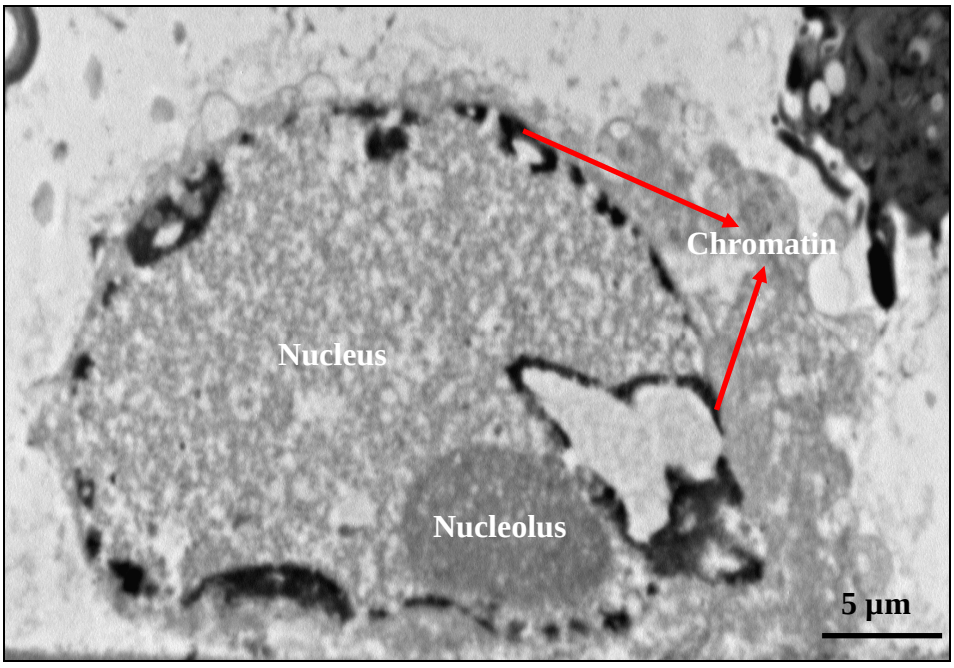

Figure 4.25 A TEM micrograph of a melanoma cell exposed to photoactivated ZnTSPc (50 µg/ml) showing chromatin and nucleus condensation at 10 000X magnification.

4.5.3 Apoptotic DNA Ladder Assay: Agarose Gel Electrophoresis

Results of a gel electrophoresis of AlTSPc and ZnTSPc photosensitized melanoma cells after irradiation showed degradation of the chromatin DNA (Figure 4.26). It is noteworthy that instead of a ladder pattern formation which is the hallmark of apoptosis (Figure 4.26 – Lane 3) a sequential band pattern representing DNA degradation was seen. Bands were produced at 1500 bp (base pairs) and 700 bp and each band contained about 209.1 µg of DNA.

Additionally, various cell lines will display differential apoptotic phenotypes. Therefore, morphology and ultrastructural studies were necessary to ascertain whether apoptosis or necrosis has occurred. Both the morphology and ultrastructural studies together with the DNA fragmentation assay have clearly confirmed that

photoactivated AlTSPc and ZnTSPc with continuous wave laser effectively induces apoptosis in melanoma cancer cells.

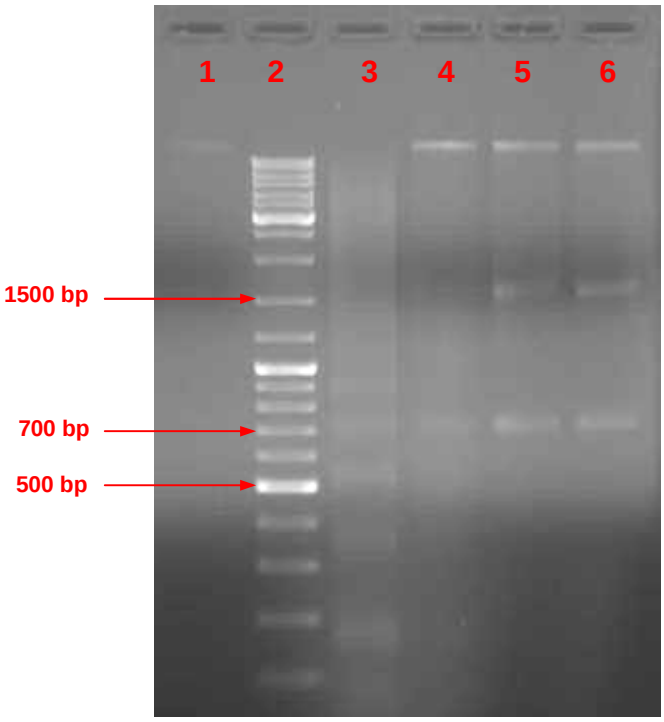

Figure 4.26 Agarose gel electrophoresis of DNA from treated melanoma cells after PDT and untreated melanoma cells. Lane 5: Treated melanoma cells using 40 µg/ml of AlTSPc and 4.5 J/cm^2 of laser irradiation. Lane 6: Treated melanoma cells using 50 µg/ml of ZnTSPc and 4.5 J/cm^2 of CW laser irradiation.

CHAPTER 5

DISCUSSION

5.1 Dark Toxicity Assay – Photosensitization of Cells with No Light Activation

Dark toxicity studies were performed to determine the cytotoxicity effects of AlTSPc and ZnTSPc in its inactive state on the melanoma cancer cells, as well as normal healthy fibroblast and keratinocyte cells. The data in Figure 4.1 – 4.4 indicated that high concentrations of AlTSPc and ZnTSPc ranging from 60 µg/ml – 100 µg/ml when compared to the untreated melanoma cells exhibit cytotoxic effects on melanoma cancer cells without laser light activation. In the case of fibroblast and keratinocyte cells photosensitized with either AlTSPc or ZnTSPc revealed an insignificant decrease in cell viability when compared with the control (untreated cell).

Both AlTSPc and ZnTSPc (tetrasubstituted phthalocyanines) are cationic PS that is probably the reason for dark toxicity. It is stated in literature that cationic PS are associated with dark toxicity (Morgan and Oseroff, 2001; Pashkovskaya *et al*., 2009). The dark toxicity effects on melanoma cancer cells is probably a response to tetrasubstituted cationic aluminium and zinc phthalocyanines displaying a significantly higher affinity for melanoma cancer cells than fibroblast or keratinocyte cells. This resulting in a greater accumulation of the PS in the melanoma cancer cells than fibroblast and keratinocyte cells, and the higher concentrations of both photosensitizers having the ability to cause destruction of the melanoma cancer cells without light activation.

The use of low PS concentrations can be the solution to minimize or eradicate any dark toxicity that can be caused by the PS in its inactive state before light activation to

cancerous and healthy surrounding tissues (Castano, Demidova and Hamblin, 2005b). Also, the incubation time with the PS before light activation or irradiation was 2 h in this experiment and this incubation time can be decreased to minimize the effect of dark toxicity on cells (Decreau *et al*., 1999).

5.2 Toxicity Screening of AlTSPc and ZnTSPc

The exposure of photosensitized melanoma, fibroblast and keratinocyte cells to red light from continuous wave laser (diode laser) at a wavelength of 672 nm resulted in a decrease in cell viability (Figure 4.5 and Figure 4.6). Results demonstrated that as the AlTSPc and ZnTSPc concentrations increased the cell viability of each cell line proportionally decreased. The viability studies have shown that the use of 40 µg/ml of AlTSPc and 50 µg/ml of ZnTSPc in combination with a laser light dose of 4.5 J/cm^2 at a wavelength of 672 nm are the optimum conditions in this *in vitro* study for the effective killing of melanoma cancer cells (Figure 4.7 and Figure 4.8).

The dark toxicity and the adverse killing effects of healthy normal fibroblast and keratinocyte cells were taken into consideration for each of the PS concentrations mentioned above. This was done before regarding EC_{50} value for AlTSPc and ZnTSPc would be 40 µg/ml and 50 µg/ml respectively. These concentrations were used for the investigation of the efficacy of continuous wave laser which was measured against a pulsed laser. Also, the effect of different light doses in comparison to 4.5 J/cm^2 was assessed. Lastly, the cell death mechanism induced by AlTSPc and ZnTSPc was investigated in this study.

In PDT the destruction of cancerous tissue can only occur if the cancerous tissue is exposed to the both the PS and light. Because these PS are considered inert until photoexicited by laser radiation at the correct wavelength and light dose it is important that the optimal laser parameters are used. Metal phthalocyanines complexes like Zn^{2+} and Al^{3+} are well known red light PS due to their high absorption in the red region of visible light (Seotsanyana-Mokhosi *et al*., 2006). A wavelength of 672 nm was used to activate the PS as the optimal absorption of the PS should correspond to the therapeutic or optical window between 650 nm and 850 nm. Also, tissue penetration is high and the energy of the triplet state is sufficient for singlet oxygen production at this wavelength range (Plaetzer *et al*., 2009).

The diode laser at a wavelength of 672 nm with a beam of 1 cm in diameter was used in this study to irradiate the photosensitized cells. The laser power or fluence rate varied between 20 – 30 mW and the irradiation time was calculated to deliver a light dose of 4.5 J/cm^2. Therefore, irradiation time will be between 1 to 3 min. Thus, the prolonged irradiation time which attributes to photodegradation of the PS can be avoided (Cubeddu *et al*., 2001; Plaetzer *et al*., 2009). Photodegradation is the chemical destruction of a PS molecule that results in the splitting of the PS into small fragments, which do not absorb in the visible spectral region or cannot be activated by laser light. As a consequence, photodegraded PS molecules lose their function within PDT (Plaetzer *et al*., 2009).

A laser power between the range 20 – 30 mW was used during this study to avoid oxygen depletion. Oxygen depletion can arise during PDT by the photochemical reaction consuming oxygen at a faster rate than it can be replenished. This is more

likely to happen for high fluence rates in combination with high PS concentrations (Stewart, Baas and Star, 1998).

Literature states that fluence rates or laser power between 50 -150 mW/cm^2 significantly diminished tumor oxygen levels during initial light delivery in majority of carcinomas. On the other hand, a fluence rate of 30 mW/cm^2 increases tumor oxygenation in majority of carcinomas. The higher fluence rate generated significant regions of hypoxia even near to tumor blood vessels and a parallel decrease in tumor perfusion which is not seen with the lower fluence rates (Castano, Demidova and Hamblin, 2005b; Stewart, Baas and Star, 1998). Also, *in vitro* studies have demonstrated that low fluence rates less than 5 mW/cm^2 can decrease the efficacy of PDT. Healthy normal tissue seems to be less susceptible to fluence rate effects, as they have better vascular supply with smaller intercapillary distances than tumors. Therefore, the magnitude of the fluence rate effect probably depends on tumor perfusion and intercapillary distances (Stewart, Baas and Star, 1998).

The laser parameters used for the light activation of AlTSPc and ZnTSPc in melanoma cells was selected to produce results on these PS that would indicate their capability for PDT as treatment for skin cancer. Both AlTSPc and ZnTSPc can effectively kill melanoma cancer cells and the process is clearly dose-dependent. However, the killing of healthy normal cells like fibroblast and keratinocyte cells can be minimized further by decreasing the incubation time of the cells with the PS before irradiation together with the use of low PS concentrations.

In this study there is a significant difference in the cell viability between absence of light activation and light activation for each cell line photosensitized with AlTSPc or ZnTSPc, ($p < 0.0001$) and adjusted for all variables. More likely fibroblast and keratinocyte cells would be killed with light exposure than without light exposure ($p < 0.0001$). More likely melanoma cells would be killed with light exposure than without light exposure ($p = 0.0016$).

5.3 Light Dose Study

The PDT effect at the tumor site depends on the PS concentration and the radiant energy density at the site which together determines the energy absorbed per unit volume at the target site. Knowledge of light dose and PS concentrations is therefore essential for the safe and effective treatment. Therefore, the influence of different light doses on the cell viability of melanoma, fibroblast and keratinocyte cells photosensitized with the optimum AlTSPc or ZnTSPc concentrations were evaluated during the light dose study (Figure 4.9 – Figure 4.14).

In this dose study a laser irradiation at the wavelength of 672 nm was used with light doses of 2.5 J/cm^2, 7.5 J/cm^2, 10.5 J/cm^2 and 4.5 J/cm^2. It was noted that the optimum AlTSPc (40 µg/ml) or ZnTSPc (50 µg/ml) concentrations and the light dose of 4.5 J/cm^2 was the most lethal for the melanoma cancer cells in comparison to the other light doses (2.5 J/cm^2, 7.5 J/cm^2 and 10.5 J/cm^2). The cell viability of healthy normal fibroblast cells photosensitized with AlTSPc (40 µg/ml) and ZnTPc (50 µg/ml) decreased with the increase in light dose. On the other hand, keratinocyte photosensitized with AlTSPc (40 µg/ml) showed the highest cell viability with the light doses of 4.5 J/cm^2 and 10 J/cm^2. Keratinocyte cells photosensitized with ZnTSPc

(50 µg/ml) showed the highest cell viability with the light dose of 2.5 J/cm^2 and 4.5 J/cm^2.

This indicates that the low light doses of 2.5 J/cm^2 and 4.5 J/cm^2 using the output power between 20 - 30 mW would be a better combination with the optimum PS concentrations than 7.5 and 10.5 J/cm^2 for the killing of melanoma cancer cells. The use of light doses 7.5 J/cm^2 and 10.5 J/cm^2 with the output power between 20 - 30 mW required irradiation times in range of 3 – 7 min. The possibility of PS photodegradation with these irradiation times associated with light doses 7.5 J/cm^2 and 10.5 J/cm^2 could be the reason for the ineffective killing of the melanoma cancer cells. Apparently, studies have shown that second-generation photosensitizers (e.g. Foscan®) can be more readily bleached than first-generation photosensitizers (e.g. Photofrin). Patients treated with Foscan® demonstrated that 75% of the photosensitizer in the tumor is bleached at the end of an irradiation light dose treatment with only 10 J/cm^2. Photobleaching has its advantages of theoretically helping to increase the therapeutic effects of PDT providing that the photosensitizer levels are higher in the tumors than surrounding healthy tissue (Macdonald and Dougherty, 2001; Plaetzer *et al*., 2009; Stewart, Baas and Star, 1998).

Unfortunately, healthy normal fibroblast and keratinocyte cells were not affected by PS degradation by the long irradiation times because as the light dose increased cell viability decreased in most cases. Thus, there are still several questions on the detailed effects of photobleaching that still needs to be answered in order to understand its role in photodynamic therapy.

Lastly, for this *in vitro* study the best suited light dose would be 4.5 J/cm^2 for the killing of most of the melanoma cancer cells while sparing most of the healthy normal fibroblast and keratinocyte cells.

5.4 Light Treatment with a Pulsed Laser

Recently, the use of pulsed lasers in PDT is becoming common but its cytotoxic effect is still not clear (Kawauchi *et al*., 2004). Results in Figure 4.15 and Figure 4.16 indicated the cytotoxic effect of PDT on melanoma cancer cells using a pulsed light was significantly less than that using the CW light under identical experimental conditions with a treatment light dose of 4.5 J/cm^2, wavelength of 672 nm and photosensitization with either AlTSPc (40 µg/ml) or ZnTSPc (50 µg/ml). Unfortunately, the cytotoxic efficacy of the pulsed laser was higher than that of the CW laser for the killing of healthy normal fibroblast and keratinocyte cells. Therefore, CW laser was more effective in killing more melanoma cancer cells and less healthy normal cells. Untreated cells exposed to femtosecond laser remained viable this helped to exclude the possibility that in the absence of PS the ultra-short pulses are responsible for the destruction of the cells.

The output power varied between 2 – 12 mW for fetmosecond laser experiments therefore irradiation time (s) were longer than CW irradiation time (s) to deliver the treatment light dose 4.5 J/ cm^2. Pilot studies were conducted with the CW laser using the output power between 2 – 12 mW to deliver a light dose of 4.5 J/ cm^2. Results demonstrated that 2 - 12 mW or 30 mW is acceptable if the irradiation time is calculated to deliver a light dose of 4.5 J/ cm^2 with a beam diameter of 1 cm at a wavelength of 672 nm. Several investigations have reported in literature that the use

of a pulsed laser of low power offers the same penetration to those of CW laser (Miyamoto, Umebayashi and Nishisaka, 1999).

A further study is required to understand the mechanistic particulars of the decreased effect of PDT using a pulsed laser.

5.5 Cell Death Mechanism

5.5.1 Inverted Microscopy

A cell dying via programmed death or apoptosis is characterized by nuclear and cytoplasmic condensation which leads to cell shrinkage. Cell shrinkage is followed by loss of the nuclear membrane, fragmentation of the nuclear chromatin, afterwards formation of multiple fragments of condensed nuclear material and cytoplasm. Necrosis is characterized by cell swelling rather than cell shrinkage because of the cell-membrane damage (Miyamoto, Umebayashi and Nishisaka, 1999).

Under inverted microscopy theses morphological changes of cell shrinkage and cell swelling are easily recognised in samples. The micrographs in Figure 4.17 – 4.19 showed that under experimental conditions the PDT treated melanoma cancer cells endured changes in morphology. Morphology changes like a reduction in cell volume, condensation of the nucleus and cell fragmentation giving rise to apoptotic bodies that were phagocytised by neighbouring cells, which are characteristics of predominantly apoptosis.

5.5.2 Transmission Electron Microscopy (TEM)

In addition to changes seen by the inverted microscopy, ultrastructural changes to the PDT treated melanoma cancer cells have been described by transmission electron microscopy (Figure 4. 20 – 4. 25).

Apoptotic cells possess distinct nuclear changes which can be detected with electron microscopy (Häcker, 2000). At a late stage of apoptosis the observable changes using an electron microscopy were nucleus condensation or pyknosis, chromatin condensation and fragmentation of the nucleus into several particles. When the cell disintegrates these particles are packaged into apoptotic bodies and taken up by phagocytes, and neighbouring cells. The early stage of apoptosis is detected by the appearance of the nuclear chromatin into more densely packed material along the nuclear membrane and is known as the electron-dense matter under the electron microscope (Häcker, 2000; Doonan and Cotter, 2008). Literature states that during apoptosis a number of specific apoptosis-related biochemical events occur at the same time and play in a role in the implementation of the cellular morphological changes. The condensation and fragmentation of the nucleus could be caspase-mediated (Häcker, 2000; Allen RT, Hunter III and Agrawal, 1997). Caspase-dependent apoptosis induces strong chromatin compaction in crescent shaped masses at the nuclear periphery, while caspase-independent apoptosis often results in lumpy incomplete chromatin condensation (Doonan and Cotter, 2008).

The changes to shape and structure of a cell undergoing apoptosis are visible by light and electron microscopy. The most common is the protrusions from the dying cell which are known as blebs. This continues for varying times in the apoptosis process

(Häcker, 2000; Allen RT, Hunter III and Agrawal, 1997). Also, the appearance of cytosolic vacuoles can be observed and suggested to be caused by the caspase-mediated cleavage of Rabaptin5. Rabaptin5 disturbs the membrane turnover in an apoptotic cell (Häcker, 2000).

Majority of these apoptosis characteristics and stages were noted in the melanoma cells photosensitized with AlTSPc and within 24 h post-irradiation (Figure 4. 21 – 4. 23). On the other hand, melanoma cancer cells treated with ZnTSPc and within 24 h post-irradiation only displayed caspase-independent apoptosis characteristics (lumpy, incomplete chromatin condensation) as illustrated in Figure 4.25. However, pyknotic, fragmented nucleus and chromatin condensation are not seen in cells dying via necrosis (Ziegler and Groscurth, 2004).

5.5.3 Apoptotic DNA Ladder Assay: Agarose Gel Electrophoresis

An agarose gel electrophoresis of DNA depicting a typical ladder formation due to endonucleosomal breakage or DNA fragmentation is generally considered as a reference or hallmark of apoptosis (Bortner, Oldenburg and Cidlowski, 1995; Fournel *et al*., 1995). In some cases, there is an absence of nuclear fragmentation which occurs in apoptotic cells displaying large DNA fragments (Fournel *et al*., 1995). It is currently unclear which type of DNA fragmentation (internucleosomal or large DNA fragmentation) is the best marker of apoptosis but some form of genomic degradation occurs in all apoptotic cells (Bortner, Oldenburg and Cidlowski, 1995).

A band pattern depicting DNA degradation was noted in melanoma cancer cells receiving PDT with the optimum AlTSPc and ZnTSPc concentrations (Figure 4.26).

Literature states that not all apoptotic cells will display the typical ladder formation (Van Cruchten and Van Den Broeck, 2002). This could occur due to various reasons such as not all cultured cells *in vitro* may accurately reflect the processes occurring *in vivo*. For example, cells grown *in vitro* may be prevented from exhibiting certain apoptotic characteristics through the loss of signal transduction pathways or metabolic components. Also, several features of apoptosis such as morphological characteristics or internucleosomal DNA cleavage may be inhibited (Bortner, Oldenburg and Cidlowski, 1995).

Therefore, DNA degradation remains a good indicator of apoptosis, particularly when ascertained with morphological characterization (Bortner, Oldenburg and Cidlowski, 1995).

CHAPTER 6

CONCLUSION

There has been a rapid increase in the number of incidence of malignant melanoma in the last decades. Its high mortality rate and pronounced therapy resistance pose a huge challenge. Therapy resistance occurs mainly in terms of defects in apoptosis (programmed cell death) signaling resulting in the proliferation of the cancer cells. Defects in apoptosis may result from the inactivation of pro-apoptotic effectors, activation of anti-apoptotic factors or from reinforcement of survival pathways (Eberle *et al*., 2007). Therefore, the design of a treatment like PDT has great potential in offering an efficient treatment for skin cancer. PDT is a treatment that combines drug (photosensitizer) and light (laser) to destroy cancer cells by inducing cell death (Katrin, 2002). The use of PS in cancer treatment has many benefits like different administrative routes, selectively taken-up by cancer cells, a wide selection of photosensitizers are available and treatment concentration of the photosensitizer can be minimized accordingly. Thus, similar to standard chemotherapeutic agents, there is an urgent need to improve on the current generation of photosensitizers to enhance therapeutic efficacy (Wojtyk *et al*., 2006).

In this *in vitro* toxicity study, the cytotoxic effect of different concentrations of two third-generation photosensitizers (AlTSPc: Aluminum tetrasulfonatedphthalocyanine; ZnTSPc: Zinc tetrasulfophthalocyanine) on melanoma cancer cells, healthy normal skin dermal fibroblast and epidermal keratinocyte cells were investigated. The efficacy of two different laser sources (continuous wave and femtosecond) and different light doses to activate both the photosensitizers for the destruction of the melanoma cancer cells was further investigated. Most importantly, the mode of cell

death induced in melanoma cancer cells by each of these photosensitizers was determined.

Results indicated that both AlTSPc and ZnTSPc exhibit dark toxicity at high concentrations between 60 µg/ml – 100 µg/ml in melanoma cancer cells. Phthalocyanines with the incorporation of a substituent group (such as sulfo) are capable of covalently binding to a suitable carrier e.g. lipoproteins, which directs the photosensitizer to the tumor without affecting the normal surrounding tissue (Chidawanyika and Nyokong, 2009). This was clearly observed when the cell viability of melanoma cancer cells were significantly decreased with high concentrations of both the photosensitizers, and the normal healthy fibroblast and keratinocyte cells showed an insignificant decrease in cell viability excluding light activation with a laser. Therefore, in the dark the accumulation of both the PS in melanoma cancer cells were higher than in healthy normal fibroblast and keratinocyte cells. Thus, high concentrations of both the PS in its inactive state were able to kill the melanoma cancer cells without laser activation.

The cytotoxic effect of AlTSPc and ZnTSPc on melanoma cancer cells were enhanced with the laser light activation at a wavelength of 672 nm. A continuous wave laser (diode laser) was used to deliver a light dose of 4.5 J/cm^2. This experiment concluded that PDT is a dose-dependent treatment. The concentrations of the active AlTSPc and ZnTSPc which reduced cell viability of melanoma cancer cells to approximately 50% (EC_{50}) while remaining non-toxic in their inactive state, and would be considered to cause minimal damage to normal healthy cells were regarded to be the optimal concentrations in this study. The optimal concentration for AlTSPc was 40 µg/ml and

ZnTSPc was 50 µg/ml. These concentrations were used in further experiments to determine the efficacy of the light dose of 4.5 J/cm^2 with other light doses, the efficacy of the continuous wave laser with a femtosecond laser and cell death mechanism induced by each of the PS.

The light dose of 4.5 J/cm^2 delivered by the continuous wave laser in combination with the optimal PS concentrations were the most effective in killing the melanoma cancer cells while causing minimal destruction to fibroblast and keratinocyte cells, in comparison to light doses of 2.5 J/cm^2, 7.5 J/cm^2 and 10.5 J/cm^2.

An interesting finding during this study was that the light dose of 4.5 J/cm^2 delivered by a pulsed laser (femtosecond laser) in combination with the optimal PS concentrations proved to be more effective in killing the healthy normal fibroblast and keratinocyte cells than the melanoma cancer cells in comparison to the continuous wave laser.

The mode of cell death induced by AlTSPc and ZnTSPc under optimal conditions in melanoma cancer cells was apoptosis. The DNA degradation accompanied by microscopy photos of morphology and ultrastructural changes in melanoma cancer cells after PDT clearly showed characteristics of programmed cell death or apoptosis.

It is therefore possible that AlTSPc and ZnTSPc can be used as potential photosensitizers in PDT for the treatment of malignant melanoma cancer. By using lower concentrations of both these PS the possibility of any dark toxicity is eliminated and the amount of PS in healthy normal tissue is reduced. Thus, injury to healthy

normal surrounding tissue is minimised. Also, the choice of light source and light dose in combination with the optimum or ideal PS concentration is essential for the effective killing of melanoma cancer cells in PDT.

CHAPTER 7

REFERENCES

Alexiades-Armenakas, M 2006, Laser-mediated photodynamic therapy, *Clinics in Dermatology* **(24)**: 16-25.

Allen, CM, Sharman, WM and Van Lier, JE 2001, Current status of phthalocynanines in the photodynamic therapy of cancer, *Journal of Porphyrins and Phthalocyanines* **(5)**: 161-169.

Allen, RT, Hunter III, WJ and Agrawal, DK 1997, Morphological and biochemical characterization and analysis of apoptosis, *Journal of Pharmacological and Toxicological Methods* **(37)**: 215-228.

Allison, RR, Sibata, CH, Dowie, GH and Cuenca, RE 2006, A clinical review of PDT for cutaneous malignancies, *Photodiagnosis and Photodynamic Therapy* **(3)**: 214-226.

Almeida, RD, Manadas, BJ, Carvalho, AP and Duarte, CB 2004, Intracellular signaling mechanisms in photodynamic therapy, *Biochimica et Biophysica Acta (BBA)* **1704(2)**: 59-86.

Ashkenazi, A 2002, Targeting death and decoy receptors of the tumor-necrosis super family, *Nature Reviews Cancer* **(2)**: 420-430.

Banfi, S, Caruso, E, Buccafurni, L, Ravizza, R, Gariboldi, M and Monti, E 2007, Zinc phthalocyanines-mediated photodynamic therapy induces cell death in adenocarcinoma cells, *Journal of Organometallic Chemistry* **(692)**: 1269-1276.

Blom, WM 2000. Cell death in rat hepatocytes: Apoptosis-inducing and protective mechanisms, http://www.imm.ki.se/sft/text/enews4.htm [Accessed 14/03/2006].

Bortner, CD, Oldenburg, NBE and Cidlowski, JA 1995, The role of DNA fragmentation in apoptosis, *Trends in Cell Biology* **(5)**: 21-26.

Brancaleon, L and Moseley H 2002, Laser and non-laser light sources for photodynamic therapy, *Lasers in Medical Science* **(17)**: 173-186.

Bursch, W, Karwan, A, Mayer, M, Dornetshuber, J, Fröhwein, U, Schulte-Hermann, R, Fazi, B, Sano, FD, Piredda, L, Piacentini, M, Petrovski, G, Fésüs, L and Gerner, C 2008, Cell death and autophagy: Cytokines drugs, and nutritional factors, *Toxicology* **(254)**: 147-157.

Buytaert, E, Dewaele, M and Agostinis 2007, Molecular effectors of multiple cell death pathways initiated by photodynamic therapy, *Biochimica et Biophysica Acta (BBA) – Reviews on cancer* **1776 (1)**: 86-107.

Calin, MA and Parasca, SV 2006, Photodynamic therapy in oncology, *Journal of optoelectronics and advanced materials* **8(3)**: 1173-1179.

Castano, AP, Demidova, TN and Hamblin, MR 2004, Mechanisms in photodynamic therapy: Part one – Photosensitizers, photochemistry and cellular localization, *Photodiagnosis and Photodynamic Therapy* **(1)**: 279-293.

Castano, AP, Demidova, TN and Hamblin, MR 2005a, Mechanisms in photodynamic therapy: Part two – Cellular signalling, cell metabolism and modes of cell death, *Photodiagnosis and Photodynamic Therapy* **(2)**: 1-23.

Castano, AP, Demidova, TN and Hamblin, MR 2005b, Mechanisms in photodynamic therapy: Part three – Photosensitizer pharmacokinetics, biodistribution, tumor localization and modes of tumor destruction, *Photodiagnosis and Photodynamic Therapy* **(2)**: 91-106.

Chen, G and Goeddel, DV 2002, TNF-R1 signaling: a beautiful pathway, *Science* **(296)**: 163-165.

Chidawanyika, W and Nyokong, T 2009, The synthesis and photophysicochemical properties of low-symmetry zinc phthalocyanine analogues, *Journal of Photochemistry and Photobiology A: Chemistry* **(206)**: 169-176.

Cubeddu, R, Canti, G, D'Andrea, C, Pifferi, A, Taroni, P, Torricelli, A and Valentini, G 2001, Effects of photodynamic therapy on the absorption properties of disulphonated aluminium phthalocyanine in tumor-bearing mice, *Journal of Photochemistry and Photobiology B: Biology* **(60)**: 73-78.

Decreau, R, Richard, MJ, Verrando, P, Chanon, M and Julliard, M 1999, Photodynamic activities of silicon phthalocyanines against achromic M6 melanoma cells and healthy human melanocytes and keratinocyte, *Journal of Photochemistry and Photobiology B: Biology* **(48)**: 48-56.

Denault, JB and Salvesen, GS 2002, Caspases: Keys in the ignition of cell death, *Chemistry Review* **102(12)**: 4489-4500.

DeRosa, MC and Crutchley 2002, Photosensitized singlet oxygen and its applications, *Coordination Chemistry Reviews* **233(234)**: 351-371.

Doonan, F and Cotter, TG 2008, Morphological assessment of apoptosis, *Methods* **(44)**: 200-204.

Deyrieux, AF and Van Wilson, G 2007, In vitro culture conditions to study keratinocyte differentiation using HaCaT cell line, *Cytotechnology* **(54)**: 77-83.

Dolmans, DE, Fukumura, D and Jain, RK 2003, Photodynamic therapy for cancer, *Nature Reviews: Cancer* **3(5)**: 380-387.

Eberle, E, Kurbanov, BM, Hossini, AM, Trefzer, U and Fecker, LF 2007, Overcoming apoptosis deficiency of melanoma – Hope for new therapeutic approaches, *Drug Resistance Updates* **(10)**: 218-234.

Fabris, C, Soncin, M, Miotto, G, Fantetti, L, Chiti, G, Dei, D, Roncucci, G and Jori, G 2006, Zn (II)-phthalocyanines as phototherapeutic agents for cutaneous diseases. Photosensitization of fibroblasts and keratinocyte, *Journal of Photochemistry and Photobiology B: Biology* **(83)**: 48-54.

Ferniany, W 2008, UBA Medicine: Skin cancer, www.health.uab.edu/15103/ [Accessed on 11/09/2009].

Fournel, S, Genestier, L, Rouault, JP, Lizard, G, Flacher, M, Assossou, O and Revillard, JP 1995, Apoptosis without decrease of cell DNA content, *FEBS Letters*, **(367)**: 188-192.

Fuchs, J and Thiele, J 1998 The role of oxygen in cutaneous photodynamic therapy, *Free Radical Biology and Medicine*, 24**(5)**: 835-847.

Galluzzi, L, Morselli, E, Vicencio, JM, Kepp, O, Joza, N, Tajedddine, N and Kroemer, G 2008, Life, death and burial: multifaceted impact of autophagy, *Biochemical Society Transaction* 36**(5)**: 786-790.

Häcker, G 2000, The morphology of apoptosis, *Cell Tissue Res*. **(301)**: 5-17.

Hausmann, W 1911, Die sensiblisierende wirkung des Hematoporphyrins, Biochem. Zeitung **(30)** 276-316.

Holbrook, KA 1983, Structure and function of the developing human skin, *Biochemistry and Physiology of the Skin Edition*, Oxford University Press 64-101.

Hopper, C 2000, Photodynamic therapy: a clinical reality in the treatment of cancer, *The Lancet Oncology* 1**(4)**: 212-219.

Jiménez-Banzo, A, Sagristà, ML, Mora, M and Nonell, S 2008, Kinetics of singlet oxygen photosensitization in human skin fibroblasts, *Free Radical Biology and Medicine* **(44)**: 1926-1934.

Johnson, AL 2009, Ovarian dynamics and follicle differentiation; Granulosa cell tumors, www.nd.edu/johnson.shtml [Accessed on 08/12/2009].

Jones, AZ 2008, Electromagnetic spectrum of light, http://physics.about.com [Accessed on 16/04/2010].

Josefsen, LE and Boyle RW 2008, Photodynamic therapy and the development of metal-based photosensitisers, *Metal-Based Drugs* 1-24.

Katrin, A and Salva, MD 2002, Photodynamic therapy: Unapproved, uses, dosages, or indications, *Clinics in Dermatology* **(20)**: 571-581.

Kawauchi, S, Morimoto, Y, Sato, S, Arai, T, Seguchi, K, Asanuma, H and Kikuchi, M 2004, Differences between cytotoxicity in photodynamic therapy using a pulsed

laser and a continuous wave laser: study of oxygen consumption and photobleaching, *Lasers in Medicine Science* **(18)**: 179-183.

Kerr, JF, Wyllie, AH and Currie, AR 1972, Apoptosis: a basic biological phenomenon with wide-ranging implications in tissue kinetics, *British Journal of Cancer* **(24)**: 239-257.

Kessel, D 2006, Death pathways associated with photodynamic therapy, *Medical Laser Applications* **(21)**: 219-224.

Ketabchi, A, MacRobert, A, Speight, PM and Bennet, JH 1998, Induction of apoptotic cell death by photodynamic therapy in human keratinocyte, *Archives of Oral Biology* **(43)** 143-149.

Kolarova, H, Lenobel, R, Kolar, P and Strnad, M 2007, Sensitivity of different cell lines to phototoxic effect of disulfonated chloroaluminium phthalocyanine, *Toxicology in Vitro* **(2)**: 1304-1306.

Kömerik, N 2002, A novel approach to cancer treatment: Photodynamic therapy, *Turkish Journal of Cancer* 32**(3)**: 83-91.

Lukšienė, Z 2003, Photodynamic therapy: mechanism of action and ways to improve the efficiency of treatment, *Medicina* 39**(12)**: 1137-1150.

MacDonald, IJ and Dougherty, TJ 2001, Basic principles of photodynamic therapy, *Journal of Porphyrins and Phthalocyanines* **(5)**: 105-129.

Mang, TS 2004, Lasers and light sources for PDT: past, present and future, *Photodiagnosis and Photodynamic Therapy* **(1)**: 43-48.

McLeod, H 2009, The impact of cancer on the future NHI, www.imsa.org.za/files/Library/NHI/policy [Accessed on 01/12/2009].

Mitton, D and Ackroyd, MD 2008, A brief overview of photodynamic therapy in Europe, *Photodiagnosis and Photodynamic Therapy* **(196)**: 1-9.

Miyamoto, Y, Umebayashi, Y and Nishisaka 1999, Comparison of phototoxicity mechanism between pulsed and continuous wave laser irradiation in photodynamic therapy, *Journal of Photochemistry and Photobiology B: Biology* **(53)**: 53-59.

Moor, ACE 2000, Signaling pathways in cell death and survival after photodynamic therapy, *Journal of Photochemistry and Photobiology B: Biology* **(57)**: 1-13.

Morgan, J and Oseroff, AR 2001, Mitochondria-based photodynamic anti-cancer therapy, *Advanced Drug Delivery Reviews* **(49)**: 71-86.

Nyokong, T 2007, Effects of substituents on the photochemical and photophysical properties of main group metal phthalocyanines, *Coordination Chemistry Reviews* **(251)**: 707-1722.

Ochsner, M 1997, Photophysical and photobiological processes in the photodynamic therapy of tumor, *Journal of Photochemistry and Photobiology B: Biology* **(39)**: 1-18.

Paschotta, R 2008, Lasers, *Encyclopaedia of Lasers Physics and Technology*.

Pashkovskaya, AA, Perevoshchikova, IV, Maizlish, VE, Shaposhnikov, GP, Kotova, EA and Antonenko, YN 2009, Interaction of tetrasubstituted cationic aluminium phthalocyanine with artificial and natural membranes, *Biochemistry (Moscow)* 74**(9)**: 1021-1026.

Plaetzer, K, Kiesslich, T Verwanger, T and Krammer, B 2003, The modes of cell death induced by PDT: An overview, *Medical Laser Application* **(18)**: 7-18.

Plaetzer, K, Krammer, B, Berlanda, J, Berr, F and Kiesslich, T 2009, Photophysics and photochemistry of photodynamic therapy: fundamental aspects, *Laser Medical Science* **(24)**: 259-268.

Radestock, A, Elsner, P, Gitter, B and Hipler, UC 2007, Induction of apoptosis in HaCaT cells by photodynamic therapy with chlorin e6 or pheophorbide a, *Skin Pharmacology and Physiology* **(203)**: 3-9.

Robertson, CA, Evans, DH and Abrahamse, H 2009, Photodynamic therapy: A short review on cellular mechanisms and cancer research applications for PDT, *Journal of Photochemistry and Photobiology B: Biology* **(96)** 1-8.

Rosenthal, I and Ben-Hur, E 1995, Role of oxygen in the phototoxicity of phthalocyanines, *International Journal of Radiation Biology* 67**(1)**: 85-91.

Satino, JL and Markou, M 2003, Hair regrowth and increased hair tensile strength using the HairMax LaserComb for low-level laser therapy, *International Journal Cosmetic Aesthetic Dermatology* **(5)**: 113-117.

Schuitmaker, JJ, Baas, P, Van Leengoed, HLLM, Van der Meulen, Star, WM and Van Zandwijk, N 1996, Photodynamic therapy: a promising new modality for the treatment of cancer, *Journal of Photochemistry and Photobiology B: Biology* **(34)**: 3-12.

Seotsanyana-Mokhosi, I, Kresfelder, T, Abrahamse, H and Nyokong, T 2006, The effect of Ge, Si and Sn phthalocyanine photosensitizers on cell proliferation and viability of human oesophageal carcinoma cells, *Journal of Photochemistry and Photobiology B: Biology* **(83)**: 55-62.

Sharman, WM, Allen, CM and Van Lier, JE 1999, Photodynamic therapeutics: basic principles and clinical applications, *DDT* 4**(11)**: 507-517.

Stewart, F Baas, P and Star, W 1998, What does photodynamic therapy have to offer radiation oncologists (or their cancer patients)?, *Radiotherapy and Oncology* **(48)**: 233-248.

Steiner, R 2006, New laser technology and future application, *Medical Laser Applications* **(21)**: 131-140.

Studer, D, Humbel, BM and Chiquet, M 2008, Electron microscopy of high pressure frozen samples: bridging the gap between cellular ultrastructure and atomic resolution, *Histochemistry and Cell Biology* 130**(5)**: 877-889.

Triesscheijn, M, Baas, P, Schellens, JHM and Stewart, FA 2006, Photodynamic therapy in oncology, *The Oncologist* 11**(9)**: 1034-1044.

Van Cruchten, S and Van Den Broeck, W 2002, Morphological and biochemical aspects of apoptosis, oncosis and necrosis, *Anat. Histol. Embryol*. **(31)**: 214-223.

Van Den Bogaerdt, AJ, Van Zuijlen, PM, Van Galen, M, Lamme, EN and Middelkoop, E 2002, The suitability of cells from different tissues for the use in tissue-engineered skin substitutes, *Arch Dermatol Res*. **(294)**: 135-142.

Wojtyk, JTC, Goyan, R, Gudgin-Dickson, E and Pottier, R 2006, Exploiting tumor biology to develop novel drug delivery strategies for PDT, *Medical Laser Applications* **(21)**: 225-238.

Wyld, L, Reed, MWR and Brown NJ 2001 Differential cell death response to photodynamic therapy is dependent on dose and cell type, *British Journal of Cancer*, 84**(10)**: 1384-1386.

Ziegler, U and Groscurth, P 2004, Morphological features of cell death, *News Physiol Science* **(19)**: 124-128.

APPENDIX

Equipment

5% CO_2 incubator (Galaxy, RS Biotech) with a humidified atmosphere at 37°C

Inverted microscope (Axiovert 40 Zeiss, Germany)

Centrifuge (Sigma 2-16K, Germany)

Haemocytometer (Merck, Darmstadt, Germany)

Power meter (Nova, Ophir)

Plate reader (FLUOstar, Optima, BMG Labtech)

High pressure freezing device (EMPACT 2, Leica)

JEOL 2100F (200 kW) Transmission Electron Microscopy

Spectrafuge Mini Centrifuge Model C1301 (Labnet International Incorporation)

Gel Tank (Bio-Rad, Laboratories Incorporation)

Nanodrop ND-1000 Spectrophotometer

Consumables

T-25 cell culture flask (Greiner Bio-One, Cellstar, Lasec, South Africa)

T-75 cell culture flask (Greiner Bio-One, Cellstar, Lasec, South Africa)

50 ml centrifuge tubes (Lasec, South Africa)

6-well tissue culture plates (Greiner Bio-One, Cellstar, Lasec, South Africa)

24-well tissue culture plates (Greiner Bio-One, Cellstar, Lasec, South Africa)

RPMI-1640 medium without L-Glutamine (Lonza, Walkersville, USA)

Foetal Bovine Serum (FBS; Gibco - Invitrogen)

Penicillin/ Streptomycin (Lonza, Walkersville, USA)

Non-essential amino acids (NEAA; Sigma, St.Louis, USA)

Eagles Minimum Essential Media (EMEM - Lonza, Walkersville, USA)

Hank's Balanced Salt Solution (HBSS; Sigma, St.Louis, USA)

0.25% of Trypsin-EDTA solution (Lonza, Walkersville, USA)

0.4% Trypan Blue (Sigma, St. Louise, USA)

Dulbecco's Phosphate Buffered Saline (PBS: Sigma, St. Louise, USA)

CellTiter Blue® Reagent (Promega Corporation)

Seakem® LE Agarose (Lonza, Walkersville, USA)

6 x Orange Loading Dye (Fermentas, UK)

Gene Ruler™ DNA, Mix Ready-To-Use (Fermentas, UK)

Fibroblast Basal Medium (FGM-2® Bullet kit®, Clonetics®, Lonza, USA) supplemented with insulin, rhFGF-B, GA-1000 and FBS (FGM-2® SingleQuots®, Clonetics®, Lonza, USA)

Drugs or Photosensitizers

Aluminum tetrasulfonatedphthalocyanine (AlTSPc)

Zinc tetrasulfophthalocyanine (ZnTSPc)

Light Source: Lasers

Diode Laser (λ = 672 nm) – continuous wave laser (CW)

Femtosecond Laser (λ = 672 nm) pulsed laser

Preparation of transport medium

96 ml of HBSS

2 ml of Pen/Strep and 2ml of gentomycin

Preparation of dispase solution

1 ml of dispase into 9 ml of HBSS

Preparation of 1% Agarose-DNA gel

Fill 1g Agarose in an Erlenmeyer-flask and add 100 ml TBE-buffer. Place the flask into a microwave oven and heat at maximum energy level. Observe the solution (do not over heat).Microwave until agarose is completely dissolved. Cool solution and add 5µl of ethidium bromide.

Preparation of TBE buffer

Dissolve 5.4 g Tris, 2.8 g boric acid in 800 ml distilled water and add 2 ml of 0.5 M EDTA solution. Stir until dissolved, final pH 8.0. Make up to mark (1 liter) with distilled water.

Preparation of samples for Transmission Electron Microscopy: Embedding

- Fix in 2,5% glutaraldehyde in 0,075 M phosphate buffer(pH 7,4) for 1 to 2 h at room temperature
- Rinse each sample in 0,075 M phosphate buffer for 10 min (3 times)
- Fix in 0,5% aqueous osmium tetroxide (work under fume hood) for 1 – 2 h
- Rinse in distilled water (3 times)
- Dehydrate in ethanol (30%, 50%, 70%, 90%, 100%, 100%, 100%) for 10 min
- Material may be stored in 100% ethanol for a few days
- Infiltrate with 30% Quetol in ethanol for 1 h
- Infiltrate with 60% Quetol in ethanol for 1 h
- Infiltrate with pure Quetol for 4 h or longer.

- Infiltration and embedding must be done in one day
- Polymerise @ 60°C for 39 h
- Cut ultrathin sections, pick up on copper grids
- Stain for 10 min in 4% aqueous uranyl acetate, rinse in water
- Stain for 2 min in Reynolds' lead citrate, rinse in water
- Cut 0,5 µm monitor sections
- Stain in Toluidine blue
- Mount in immersion oil